A METHODOLOGY FOR DEVELOPING PERFORMANCE-RELATED SPECIFICATIONS FOR PAVEMENT PRESERVATION TREATMENTS

A Dissertation

by

LITAO LIU

Submitted to the Office of Graduate and Professional Studies of
Texas A&M University
in partial fulfillment of the requirements for the degree of

DOCTOR OF PHILOSOPHY

Chair of Committee,	Nasir G. Gharaibeh
Committee Members,	Jon A. Epps
	Dan G. Zollinger
	Jeffrey D. Hart
Head of Department,	Robin Autenrieth

December 2013

Major Subject: Civil Engineering

ABSTRACT

Current materials and construction specifications for pavement preservation treatments are predominantly prescriptive and they have little or no methodical linkage between initial treatment quality and future performance. There is an imperative need for performance-related specifications (PRS) that link the initial quality of pavement preservation treatments to their long-term performance and life-cycle costs so that rational pay adjustment and acceptance decisions can be made. However, the current literature lacks a methodology for developing PRS for pavement preservation treatments. The aim of this research is to fill this gap in the literature, with focus on thin HMA overlays.

In this dissertation, a novel approach was devised for developing performance prediction models for pavements that received preservation treatments. In this approach, the model consists of two tightly-coupled components: the first component is responsible for predicting the performance (e.g., IRI) of the existing pavement if no treatment was applied. The second component is responsible for predicting the reduction in pavement deterioration due to the application of the treatment. Inputs to the first component include material and construction properties of the existing pavement layers, climatic conditions, and traffic factors. Inputs to the second component include the treatment's acceptance quality characteristics (AQCs), climatic conditions, and traffic factors. The artificial neural networks (ANNs) and the Bayesian regression methods were used for developing the two model components. Using this approach, a model was

developed for predicting the International Roughness Index (IRI) of flexible pavement treated with thin HMA overlay. The data used for developing and testing this model was obtained from the Long-Term Pavement Performance (LTPP) database. Artificial neural networks (ANNs) and Bayesian regression techniques were employed for developing the first and second components of this model, respectively.

A PRS methodology was developed for quantifying the difference between the initial quality levels of as-constructed and as-designed treatments. This methodology consists of a novel approach for determining the probability distributions of service life and present-worth value (PWV). This approach allows for transforming the probabilistic distribution of future IRI (predicted by the Bayesian model) into probability distributions for service life and PWV. Pay factors are then estimated based on the difference between the as-constructed and target PWVs. Finally, this dissertation provides insights into the relationships between initial quality (measured in terms of both mean and standard deviation of key acceptance quality characteristics) and expected pay factors through analysis of real world case studies of asphalt pavements treated with thin HMA overlays.

This work is dedicated to my wife, Hong Shan,

my lovely daughters, Catherine and Sophia, my parents, and my brothers

for their love, understanding, and support.

ACKNOWLEDGEMENTS

I sincerely thank my advisor, Dr. Nasir G. Gharaibeh, for his constant support and guidance on this research. Dr. Gharaibeh is always helpful, and he is the most organized person that I have ever seen. I am also very grateful for his support and understanding while I was applying for a job and for his help at difficult times.

I would like to thank Dr. Jon A. Epps, Dr. Dan G. Zollinger, and Dr. Jeffery D. Hart, for serving as my doctoral advisory committee members. I am very grateful to Dr. Hart for his valuable advices and instructions on Bayesian regression. Many thanks to Dr. Zollinger for his support in my research and when I first applied to the Civil Engineering program at Texas A&M University. I wish to express my special gratitude to Dr. Epps for his help on my research and job search. Many thanks are also conveyed to the persons who have worked and helped on this research.

I also acknowledge the financial support from the National Cooperative Highway Research Program (NCHRP) and the Southwest Region University Transportation Center (SWUTC) that makes this research possible.

NOMENCLATURE

AADTT	Average annual daily truck traffic
AQC	Acceptance quality characteristics
ESAL	Equivalent single axle load
FDOT	Florida Department of Transportation
FHWA	Federal Highway Administration
FI	Freezing index
GPS	General Pavement Studies
HMA	Hot-mix asphalt
HPD	Highest posterior density
IRI	International Roughness Index
LHS	Latin Hypercube Sampling
LCC	Life-cycle cost
LTPP	Long-Term Pavement Performance
MEPDG	Mechanistic-Empirical Pavement Design Guide
NAPA	National Asphalt Pavement Association
PCC	Portland cement concrete
PWV	Present-worth value
QC	Quality control
QA	Quality assurance
SAS	Statistical Analysis System
SHRP	Strategic Highway Research Program
SMA	Stone matrix asphalt
SPS	Specific Pavement Studies
TCMA	Two-Component Modeling Approach
TRB	Transportation Research Board
TxDOT	Texas Department of Transportation
WIM	Weight-in-motion

TABLE OF CONTENTS

Page

LIST OF FIGURES

Page

LIST OF TABLES

Page

CHAPTER I

INTRODUCTION

PROBLEM STATEMENT

Major financial resources are invested in preserving and maintaining the nation's roadway infrastructure every year. For example, the Federal Highway Administration SAFETEA-LU program has authorized $25.2 billion for preserving just the interstate highway system during the period of 2005-2009. Figure 1 shows that highway preservation and maintenance investment in the U.S. has been steadily rising since 1945, reaching approximately $50 billion per year in 2009-2010 (FHWA, 2010).

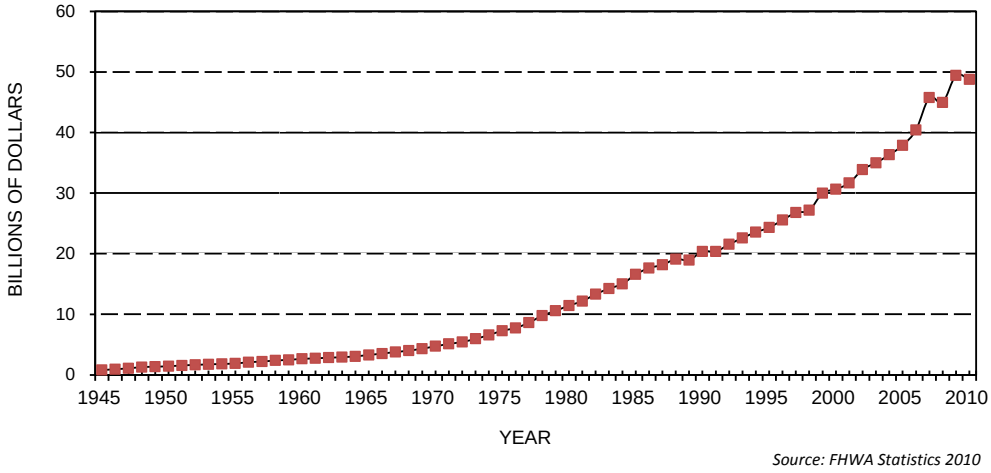

Figure 1 Highway preservation and maintenance disbursements in the U.S. during 1945-2010.

Preservation treatments applied to hot-mix asphalt (HMA) pavement include crack sealing, slurry seals, chip seals, microsurfacing, cape seals, fog seals, hot in-place recycling, cold in-place recycling, and thin HMA overlays. Preservation treatments applied to Portland cement concrete (PCC) pavement include joint resealing, crack

sealing, diamond grinding, dowel bar retrofitting, partial-depth repair, slab stabilization (undersealing), and full-depth repair. Generally, these preservation treatments are applied to extend pavement service life, enhance its performance, delay costly rehabilitation and reconstruction, and ultimately, reduce the pavement total life-cycle cost.

Considering the major investment in pavement preservation and the impact that preservation treatments have on extending the longevity of roadway infrastructure, it is imperative that the initial quality and long-term performance of these treatments be assured in the best possible way. However, current materials and construction specifications for these treatments are predominantly prescriptive and have little or no linkage between initial quality of preservation treatments and their future performance. For example, the Texas Department of Transportation's (TxDOT) 2004 Specifications for thin HMA overlays assign a pay increase when the absolute deviation from the target laboratory-molded density is less than 1% and assign a pay decrease when the deviation is greater than 1% (TxDOT 2004). This pay adjustment method greatly depends on subjective judgments of the relationships between the treatment initial quality and its future performance.

As a result of this situation, highway agencies have very limited capacity to capture the performance lost or gained due to differences between the as-designed treatment and as-constructed treatment; and the contractors' ability to be innovative by focusing on quality characteristics that affect the treatment's in-service performance is also restricted. To account for these limitations, performance-related specifications (PRS)

that relate the treatment's initial materials and construction quality to its future performance are needed.

PRS specify the desired levels of key materials and construction acceptance quality characteristics (AQCs) (e.g., air voids of hot-mix asphalt) that correlate with future performance and are amenable to acceptant testing at the time of construction. Additionally, PRS employ quantitative models for predicting pavement performance as a function of AQCs and other site factors. These models provide the basis for rational pay adjustment decisions. Over the past two decades, significant progress has been made in developing and implementing PRS for new pavements (both HMA and PCC) (Hoerner et al. 2000; Fugro and ASU 2011). However, the literature is lacking a methodology for developing PRS for pavement preservation treatments. This dissertation presents a research endeavor to fill this gap in the literature, with focus on thin HMA overlay.

RESEARCH SCOPE AND HYPOTHESES

Although the pavement community is making great efforts to develop PRS methodologies, little progress has been made with respect to pavement preservation treatments. Based on the aforementioned observations, the following specific research questions are addressed in this dissertation:

- How do we model the post-treatment performance of pavements so that the treatment acceptance quality characteristics can be linked to its future performance?
- How do we quantify the economic loss or gain due to the deviation of the as-constructed treatment from the target (as-designed) quality level?

To address these questions, the following hypotheses are made:

Hypothesis #1: Pavement post-treatment performance is affected by three categories of factors: treatment quality, condition and design of existing pavement, and site conditions (e.g., traffic and climatic factors).

Hypothesis #2: The economic loss or gain due to deviation from as-designed (i.e., target) quality level can be quantified through life-cycle cost analysis in terms of the difference between present-worth values of the as-constructed and the as-designed treatments.

While this research focuses on thin HMA overlays, the modeling approach and the PRS methodology developed and presented in this dissertation can potentially be applied to other pavement preservation treatments.

RESEARCH OBJECTIVES AND PERFORMED TASKS

The aim of this research is to find answers to the questions raised in Section 1.2, and to develop a PRS methodology for pavement preservation treatments, with application to thin HMA overlay. This entails the following specific objectives and corresponding tasks to achieve each objective:

Objective #1: Develop a performance prediction modeling approach for pavement preservation treatments and apply it to thin HMA overlays

Task 1. Develop a conceptual approach for predicting preservation treatment performance

The performance of preservation treatments is affected by a large number of factors. These factors include key material and construction properties of the

treatment, the condition of the existing (original) pavement, the design of the existing pavement, and other site factors such as traffic and climate. The modeling approaches and model forms used in new pavement studies may not work for pavement preservation treatments. Additionally, available pavement preservation performance data tend to be incomplete and highly variable (i.e., without clear patterns). A "Two-Component Modeling Approach" was developed based on a perspective analysis of the distress mechanism in a pavement before and after preservation treatment is applied.

Task 2. Develop pavement prediction models for thin HMA overlays

Preservation treatment and performance data were obtained from the Long-Term Pavement Performance (LTPP) Standard Data Release (SDR) 26. The LTPP dataset was carefully evaluated and processed to form a high-quality dataset for developing performance prediction models for flexible pavements treated with think HMA overlays. The final dataset included 88 flexible pavement sections that were treated with thin HMA overlay, located throughout the U.S. and some Canadian Provinces and overlaid between 1989 and 2003. Artificial neural networks and Bayesian regression techniques were employed for developing these performance prediction models. The predictive power of the developed prediction models was checked by using them to predict the performance of LTPP test sections that have received thin HMA overlay treatments.

Objective #2: Develop a PRS methodology for pavement preservation treatments

To accomplish this objective, the following task was carried out:

Task 3. Develop a simulation-based methodology for pavement preservation treatments

In this task, a PRS methodology was developed to allow for determining pay adjustment based on the economic value of performance lost or gained due the differences between the treatment's as-designed (i.e., target) and as-constructed levels of quality. This economic value is quantified by estimating the difference in the present-worth values (PWVs) of the as-designed and as-constructed treatments, and is ultimately converted to pay adjustment factors.

Objective #3: Apply the developed PRS methodology to thin HMA overlays to investigate the impact of treatment initial quality on long-term performance and pay adjustment

To accomplish this objective, the following tasks were carried out:

Task 4. Apply the developed PRS methodology to case studies of flexible pavements treated with thin HMA overlays

In this task, the developed PRS methodology was applied to case studies that consist of LTPP test sections with various combinations of mean and standard deviation of initial quality levels, climate, traffic volume, and existing pavement designs and conditions.

Task 5. Investigate the impact of initial quality characteristics on pay adjustment

The following quality scenarios were simulated for Task 4 case studies: 1) on-target quality, in which the initial quality characteristics of the as-constructed treatment have mean and standard deviation values equal to the target values; 2)

high quality, in which the initial quality characteristics of the as-constructed treatment have mean and standard deviation values superior to the target values; and 3) poor quality, in which the initial quality characteristics of the as-constructed treatment have mean and standard deviation values inferior to the target values.

CHAPTER II

LITERATURE REVIEW

OVERVIEW

This chapter presents a review of the literature in pavement construction and materials specifications, preservation treatments, and performance prediction models. An introduction about the artificial neural networks modeling technique, which is used in this research, is also provided in this chapter.

HIGHWAY CONSTRUCTION SPECIFICATIONS

In highway constructions, specifications are used for measuring compliance of as-constructed products to what is specified in the contract. They are also used as a basis for competitive bidding for the delivery of products (Chamberlin 1995). Highway construction specifications can be classified into different categories based on different criteria (TRB, 2009). For example, based on who is responsible for the quality of construction, it can be classified into 1) materials and methods specifications (0% contractor responsibility), 2) quality assurance (QA) specifications, and 3) end results specifications (100% contractor responsibility). Based on the type of sampling, highway construction specifications can also be classified into 1) representative sampling specifications (little information), 2) statistical specifications, and 3) 100% sampling specifications (much information).

Based on the relation to performance, highway construction classifications can be classified into four categories: 1) intuitive specifications, 2) performance-related

specifications, 3) performance-based specifications, and 4) performance specifications. For highways, performance is typically described in terms of changes in physical conditions of the surface and its response to load. Figure 2 shows a diagram that helps distinguish between the different levels of construction specifications taking pavement performance into consideration (TRB, 2009).

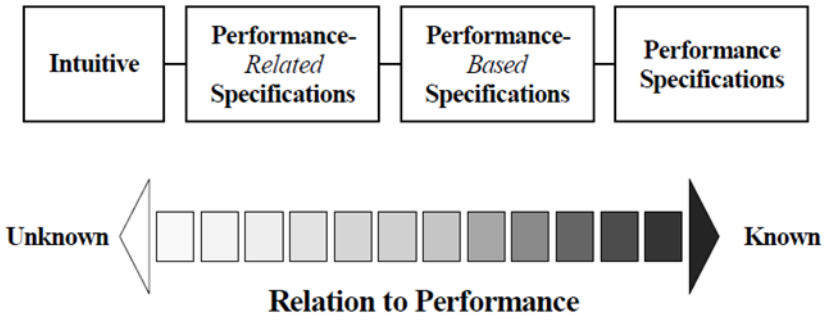

Figure 2 Classification of highway construction specifications according to relation to performance.

Among the different types of specifications shown in Figure 2, performance-related specifications (PRS) are the focus of this study. The other three types of specifications, based on relation to performance, are briefly introduced in the following sections, while more details will be provided about PRS.

Intuitive Specifications

Intuitive specifications provide the least relation to pavement long-term performance. In intuitive specifications, materials and construction quality characteristics are used to control quality and tied to performance through intuition, engineering judgment, or both (Epps et al. 2002). For example, minimum density is

used as an acceptance quality characteristic (AQC) in an intuitive specification where the connection to better performance is intuitive, that is, higher densities generally mean better performance.

Most construction specifications used by state highway agencies can be classified into this category based on their features in specifying the intuitive specification limits and pay adjustment schedules. There is a consequence to the contractor for not satisfying the specification, which usually results in the removal and replacement of defective pavement, or a reduced payment.

Performance-Based Specifications

Performance-based specifications (PBS) describe the desired levels of fundamental engineering properties (e.g., resilient modulus, creep properties, and fatigue properties) that are predictors of performance. These properties appear in primary prediction relationships (or models) that are used to predict pavement stress, distress, or performance from combinations of predictors that represent traffic, environmental, roadbed, and structural conditions. For most part, these fundamental properties are not amenable to timely acceptance testing (Chamberlin 1995).

In PBS, the selection of a particular AQC by itself does not make the specification performance-based. Instead, there must be the connection to performance through some valid empirical or mechanistic prediction model that accounts for the effect of deviations of the as-constructed AQC level from the as-designed AQC level (Epps et al. 2002). The difference in predicted performance between the as-designed and as-constructed product is then used as a basis for pay adjustment.

Because most fundamental engineering properties associated with pavements are currently not amenable to timely acceptance testing, performance-based specifications have not found applications in highway construction (TRB 2009).

Performance Specifications

Performance specifications represent the level of most known relation of AQCs to performance. It includes the specifications that describe how the finished product should perform over time (TRB, 2009). For example, the specifications can require that "no cracking after 5 years," "permanent deformation less than 0.4 inch after 10 years," and "IRI no greater than 150 in/mile after 20 years."

Performance specifications are not widely used for highway pavement construction because they involve time (e.g., 10 years) as a factor and there have not been suitable non-destructive tests to measure long-term performance immediately after construction (TRB 2009). The ones that have been used typically from the form of warranty or guarantee specifications, under which the contractor agrees to build and maintain the pavement for specified period of time (Epps 2002).

Performance-Related Specifications

Performance-related specifications (PRS) are quality assurance specifications that describe the desired levels of key materials and construction quality characteristics that have been found to correlate with the long-term performance of the finished product, thus providing the basis for rational acceptance and price adjustments (TRB 2009; Hoerner and Darter 1999). These quality characteristics (for example, air voids in HMA

pavement) should be amendable to acceptance testing at the time of construction. Generally, a systematically complete and scientifically sound PRS should include the following elements (Chamberlin 1995; Hoerner and Darter 1999; Weed 2006):

- Acceptance quality characteristics (AQCs) that correlate with the performance (or longevity) of the pavement
- Pavement performance indicators that are affected by the defined AQCs
- Statistical acceptance sampling and testing plan, including definition of lots, sublots, and sample size
- Pay adjustment factors
- Operating characteristic (OC) curves to evaluate the agency's and contractor's risks

AQCs and performance indicators are core elements in PRS. The essence of PRS is that these two elements can be linked through mathematical relationships. AQCs that are amendable to PRS can be described as follows:

- Measurable at the time of construction
- Can be controlled by the contractor or material supplier
- Affect the future performance of the finished product

Efforts to develop PRS for highway construction were dated back to as early as the late 1940s. Weed (1989) provided a prototype PRS which used total life-cycle cost (LCC) as an overall measure of pavement quality. This approach was modified and adopted in a series of FHWA-sponsored research studies that resulted in guidelines for

developing PRS for new PCC pavements and the *PaveSpec* PRS software (Hoerner and Darter 1999). A follow-up research was sponsored by the FHWA to improve the performance prediction models used in the PRS methodology for PCC pavement and to revise the *PaveSpec* software (Hoerner et al. 2000), which represents the current PRS methodology and guidelines for new PCC pavement at the national level.

Initial efforts to develop PRS for new HMA pavements began under the NCHRP Project 10-26 "Performance-related specifications for hot-mix asphaltic concrete", where Anderson et al. (1990) identified relationships between materials and construction properties and performance of HMA pavements. During 1998 to 2000, the NCHRP Project 09-20 "Performance-related specifications for hot-mix asphalt construction" was carried out to develop PRS for HMA pavements based on field data from the WesTrack accelerated pavement test sections by examining how deviations in materials and construction properties affected pavement performance (Seed et al. 1997; Epps et al. 2002). The PRS software, namely *HMA Spec*, was developed under this project but not publicly distributed because it has been superseded by another PRS developed in the NCHRP Project 09-22. Conducted during 2000 to 2011, the NCHRP Project 09-22 "Beta testing and validation of HMA PRS" developed a new PRS methodology for new HMA pavements and incorporated closed-form solutions (CFS) of AASHTO's mechanistic-empirical models for predicting HMA pavement performance which was indicated by three major distresses – rutting, fatigue cracking, and thermal cracking (Fugro and ASU 2011). The PRS methodology and accompanying Quality-Related Specification Software (QRSS) was documented in NCHRP Report 704, which

represents the current PRS methodology and guidelines for new HMA pavement at the national level.

Table 1 compares key aspects of current PRS methodologies for new PCC and HMA pavements. While the general PRS framework is similar, the two pavement types have different acceptance quality characteristics and distress types. The two methodologies also differ in terms of the basis for computing pay adjustment factors. The HMA PRS methodology determines pay factors based on the difference in expected life between as-designed and as-constructed pavements; whereas, the PCC PRS methodology determines pay factors based on the difference in total life-cycle costs (LCC) between as-designed and as-constructed pavements. Finally, the PCC PRS methodology considers initial IRI as an AQC and is equipped with models to predict future IRI as a performance indicator; whereas, the HMA PRS methodology considers pavement smoothness through user-defined pay adjustment factors for various values of initial IRI (three different payment schedules are provided in QRSS for users to adjust penalty/bonus values based on initial IRI).

Currently, most materials and construction specifications for pavement preservation treatments provide little or no linkage between their initial quality (material properties, construction quality, and design) and future performance (short and long-term). For example, the Texas DOT (TxDOT) 2004 Specifications for thin HMA overlays assign a reward (i.e., pay factor > 1.0) when the absolute deviation from target laboratory-molded density is less than 1% and assign a penalty (i.e., pay factor < 1.0) when the deviation is greater than 1% (TxDOT 2004). The Michigan DOT (MDOT)

2012 Specifications for chip seals specify a tolerance (e.g., ±1 pound per square yard of the required aggregate application rate) for the quality characteristics. No pay adjustment is made if the acceptance testing is within the tolerance; otherwise, the agency makes a pay adjustment if the test result is outside of the tolerance (MDOT 2012).

Table 1 Comparison of Current PRS for PCC and HMA Pavements

PRS Components	New PCC Pavement	New HMA Pavement
AQCs	• PCC strength (compressive or flexural) • Slab thickness • Air content • Initial smoothness • Consolidation around dowel bars	• Asphalt concrete (AC) layer thickness • Gradation: ¾ in., ⅜ in., #4, and #200 • Asphalt content (%) • Air voids (%) • Max. theoretical specific gravity of mix
Performance Indicators	• Transverse cracking • Joint faulting • Joint spalling • International Roughness Index (IRI)	• Bottom-up fatigue cracking • Top-down (longitudinal) fatigue cracking • Permanent deformation (rutting) • Thermal (transverse) cracking
Pavement Smoothness	• Initial smoothness considered as an AQC • Future IRI considered as a performance indicator	User-defined pay factors based on initial IRI (at the time of construction)
Performance Prediction Models	Empirical and Mechanistic-empirical models	Rapid closed-form of AASHTO's mechanistic-empirical models
Basis for Pay Factor	Difference in life-cycle costs between as-designed and as-constructed pavements	Difference in expected lives between as-designed and as-constructed pavements
Composite Pay Factor	• Individual pay factors combined using multiple options (multiplication, average, weighted average, etc.) • Overall pay factor computed based on LCC	Summation of individual pay factors

This pay adjustment method is greatly based on subjective judgment of the relationships between the AQC of the treatment and its future performance (e.g., the

longest service life). The performance of a pavement section, especially after preservation, is affected by many factors including site conditions, climatic conditions, and materials and construction quality (Epps et al. 2002). The current standard specifications for pavement preservation treatments lack objective relationships between the AQCs and the long-term performance of the pavement after preservation. A pay adjustment derived from subjective deviation of some AQCs from a certain tolerance may not appropriately reflect the true life-cycle cost of the as-constructed product and consequently of the payment it deserves.

PRS specify the desired levels of key AQCs that correlate with future performance. In addition, PRS employ quantitative relationships containing the characteristics to predict long-term pavement performance. They thus provide the basis for rational pay adjustment decisions and work as an alternative approach to address the limitations described previously.

However, it was found that the literature lacks a methodology for developing performance models for pavement preservation treatments that can be used in PRS. Another key component in PRS that is missing is a rational method for determining pay adjustment factors. In PRS, pay adjustment decisions are made based on the knowledge of life expectancy or life-cycle cost (LLC) of the as-designed and as-constructed products. The PRS methodology for PCC pavement, documented in FHWA reports RD-98-155, -156, -171, and RD-99-059, specified the use of differentiation in LLCs of the as-designed and as-constructed pavement as the basis for estimating pay adjustment factors (FHWA 1998). In contrast, the pay adjustment for new HMA pavement is based

on the loss or gain in the service life predicted through close-form pavement prediction models (Fugro and ASU 2011). How these pay adjustment methods can be adapted into the PRS for pavement preservation treatments (thin HMA overlay in this dissertation) has not been understood.

This dissertation presents a research endeavor aiming to fill this gap in the literature, with focus on thin HMA overlays.

PAVEMENT PRESERVATION TREATMENTS

The concept of "pavement preservation" has emerged as a cost-effective alternative to reactive maintenance. Generally, preservation treatments are applied to extend pavement service life, enhance its performance, and reduce its life-cycle cost (FHWA 1999; Smith 2002; Zhang et al. 2010). Applications of preservation pavements are used to postpone costly rehabilitation and reconstruction and consequently reduce the life-cycle cost of the pavement. Figure 3 depicts the effect of preservation treatments on pavement performance and service life.

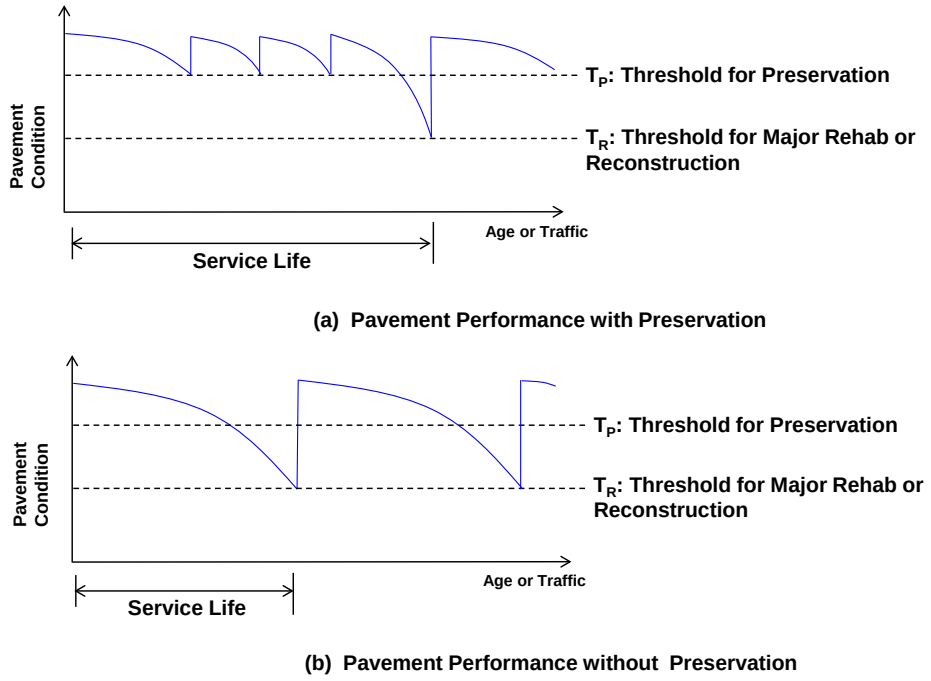

Figure 3 Effect of preservation treatments on pavement service life.

A questionnaire survey by Morian (2011) found that thin HMA overlay, microsurfacing, crack sealing, and chip seal techniques are the most frequently used treatments for HMA pavement. The same survey also indicated that thin HMA overlays are used for all the traffic levels. Another questionnaire survey of 50 highway agencies by Peshkin et al. (2011) concluded that crack sealing, crack filling, cold milling, and thin HMA overlays are the treatments most extensively used on both rural and urban high volume HMA-surfaced roadways.

Cuelho et al. (2006) conducted a web-based emailing survey that was distributed to all the 50 U.S. states, Washington, D.C., and 11 Canadian provinces. Responses from 34 U.S. states and five Canadian provinces indicated that crack sealing, thin HMA

overlays, chip seal, maintenance of drainage features, and microsurfacing are the most frequently used treatments for HMA-surfaced pavements.

This dissertation defines pavement preservation treatments as "treatments applied to preserve an existing roadway, slow future deterioration, and maintain and improve its functional condition (without substantially increasing structural capacity)." This definition is consistent with the FHWA definition of pavement preservation, which includes preventive maintenance, minor rehabilitation (non-structural), and some routine maintenance activities (FHWA 2005). The developed PRS methodology has been applied to thin HMA overlays to investigate its applicability. Furthermore, the developed concepts and methodology can potentially be applied to other pavement preservation treatments, such as slurry seals, microsurfacing, and chip seals.

THIN HMA OVERLAYS AND SPECIFICATIONS

Thin HMA Overlays

Thin HMA overlays are composed of asphalt binder and aggregate combined in a central mixing plant and place with a paving machine. They are typically placed in thin lifts of 0.5 to 1.5 inches thick, occasionally up to 2.0 inches (Liu et al. 2010; Peshkin et al. 2011). Based on aggregate gradation, thin HMA overlays can be distinguished into dense-graded, open-graded, and stone matrix asphalt (SMA). Dense graded thin overlays, which are relatively impermeable mix, are intended for general use. Due to the thin thickness, small nominal maximum aggregate size (NMAS) mixtures are used in order for the lift thickness to NMAS ratio to be maintained in the range of 3:1 to 5:1 for

ensuring adequate compaction (Brown et al. 2004). A few agencies' gradations, aggregate quality, and mix design requirements in thin HMA overlay constructions are summarized in the National Asphalt Pavement Association (NAPA) report by Newcomb (2009). Sometimes the underlying existing pavement needs to be milled when surface distresses (e.g., segregation, raveling, or block cracking) are evident.

Thin HMA overlays are often applied to address function problems, such as roughness, cracking (longitudinal, transverse, and block), raveling/weathering, friction loss, and bleeding. Generally, a thin overlay is too thin to add additional structural (or load-carrying) capacity to the existing pavement; however, when the overlay gets thicker or repetitive applications are applied, greater structural benefits in terms of load-carrying capability is possible (Peshkin et al. 2011). Thin HMA overlays can also contribute to the improvement of pavement strength, including impermeability properties, thus minimizing moisture damage and oxidative aging from water and air infiltration, respectively (Lubinda and Scullion 2008). Comparing to slurry seals and chip seals, thin HMA overlays are normally used on higher volume routes or as an alternative to these treatments. When properly placed on pavements without structural problems, thin HMA overlays can provide excellent extended service life and performance.

Recent studies suggest that thin HMA overlay is one of the most frequently used preservation techniques for HMA pavements (Morian et al. 2011; Cuelho et al. 2006; and Smith et al. 2011). The performance of thin HMA overlay varies among highway agencies, as stated in many reports. Previous studies show that the service life of thin HMA overlays may vary from 2 to 12 years (Geoffroy 1996; Hicks et al. 1999; Johnson

2000; Wade et al. 2001; Peshkin et al. 2004; Liu et al. 2010; Liu and Gharaibeh 2012). Some highway agencies, such as the Illinois Department of Transportation, reported superior performance on their thin overlay projects when targeted to pavement meeting specified criteria (Reed 1994). The wide use of thin HMA overlay in pavement preservation makes it an ideal candidate for developing PRS.

Specifications for Thin HMA Overlays

The construction specifications from 14 state highway agencies were reviewed. It was found that a very small proportion of these agencies have separate specifications specific for thin HMA overlays. Most state DOTs include this treatment in their specifications for HMA pavements, stone mastic asphalt, open graded friction course, etc. with or without minor modifications. Table 2 summarizes the current specifications for thin HMA overlays used in Michigan, Texas, Kansas, and Florida. Materials and construction quality measures and payment methods are presented in this table.

Based on the literature review, a few initial material and construction quality characteristics are used as AQCs by some states and may have an impact on the performance of thin HMA overlays. They are thus candidate AQCs in the PRS under development, as listed below:

- HMA overlay thickness
- Asphalt binder content
- Percent air voids in laboratory HMA mixture
- Aggregate gradation (percent passing #8 and #200 sieves)
- Initial IRI, immediately measured after an overlay treatment

Table 2 Construction Specifications for Thin HMA Overlays

State	Materials Quality Measures (Pre-construction)		During and Post-construction Quality Measures	Payment Methods
	Material Type	Quality Measure		
Michigan	Bond Coat (SS1h)	N/A	Tackcoat application rate HMA application rate Asphalt content Air voids Aggregate gradation (#8, #80, and #200 sieve)	Payment = contracted unit price × sq yd of application
	HMA Mixture	Marshall air voids		
		Voids of Mineral Aggregate		
		Marshall Stability		
		Marshall Flow Value		
		Percent Fines (passing #200 sieve)		or Payment = contracted unit price for special mix × tons of mix used
	Aggregate	Percent Crushed Face		
		LA Abrasion Loss		
		Aggregate Wear Index		
		Aggregate Angularity Index		
		Gradation		
	Asphalt	Performance Grading*		
Texas	Asphalt	Performance Grading*	Asphalt binder content (P_b) No. 8 sieve (P_8) No. 200 sieve (P_{200}) In-place air voids (V_a) Lab-modeled density (G_{mb}) International Roughness Index Joint Density (In-place)	Payment = contracted unit price × tons of HMA used
	Aggregate	SA CA QMP		
		Deterious material		
		Decantation, %, max		
		Micro-Deval abrasion loss		
		Los Angeles abrasion loss		
		Magnesium sulfate soundness		
		Coarse aggregate angularity		
		Flat and elongated particles		
		Linear shrinkage		
		Sand equivalent		
		Gradation		
Kansas	Asphalt	Performance Grading*	Air voids (V_a) at Ndesign Density (G_{mb}) Thickness Profile index	Payment = contracted unit price × tons of HMA used
	Aggregate	Gradation		
		Plasticity index		
		Clay content		
		Coarse aggregate angularity		
		Fine aggregate angularity		
		Soundness		
		Abrasion loss		
		Flat and elongated particles		
		Linear shrinkage		
Florida	Asphalt	Performance Grading*	Asphalt binder content (P_b) No. 8 sieve (P_8) No. 200 sieve (P_{200}) Air voids (V_a) at Ndesign Density (G_{mb}) Smoothness using straightedge	Payment = contracted unit price × tons of HMA used
	Aggregate	Gradation		
		Sand equivalent		
		Clay content		
		Coarse aggregate angularity		
		Fine aggregate angularity		
		Soundness		
		Abrasion loss		
		Flat and elongated particles		
		Linear shrinkage		
		Shale content		

* Performance grading of asphalt refers to all the superpave binder testing performed on original, RTFO aged, and PAV aged binder to determine its high and low temperature properties and thereby classify them into PG grade.

PRESERVATION TREATMENT PERFORMANCE PREDICTION MODELS

Performance prediction models are the most critical component in PRS. Through these models, the AQCs of thin HMA overlays are related to pavement long-term performance and life-cycle cost of the treatment. As discussed earlier, the ability to related AQCs to in-service performance allows for developing rational pay adjustment schemes.

Existing Models for Predicting the Performance of Thin HMA Overlays

The review of past studies revealed a lack of promising performance prediction models in the literature. Most existing models predict pavement performance (represented by either individual distress or a composite index) as a function of age, traffic, climatic parameters, without considering the initial material and construction quality of the treatment. Below are a few thin HMA overlay performance models developed in studies by other researchers.

Morian et al. (1998) developed linear regression models using the LTPP data for predicting pavement composite rating score (CRS) as a function of traffic, environment, and site-specific variables. CRS is a composite 0-100 scale performance indicator, computed based upon distress conditions including fatigue cracking, longitudinal cracking, transverse cracking, and patching. The CRS model for thin HMA overlays has the following form:

$$CRS = 43.3486 + 1.88071(EZ) + 6.137(Age) + 4.37(IC) + 6.122(SG)$$

where EZ is environmental zone (dry-no freeze, dry-freeze, wet-no freeze, wet-freeze), Age is year of pavement preservation treatment, IC is original pavement condition level (good, fair, and poor), and SG is subgrade type (fine verses coarse).

Eltahan et al. (1999) employed the Kaplan-Meier method to develop a model that predicts the probability of failure of thin HMA overlay treatments at any given time as expressed in the following form.

$$F(t_r) = 1 - \left\{ \frac{n-1}{n} \times \cdots \times \frac{n-(r-1)}{n-(r-1)+1} \times \frac{n-r}{n-r+1} \right\}$$

where $F(t_r)$ is the probability of treatment failure at a given time, n is the total number of sections, and r is the rank of the section at a given time.

Labi et al. (2007) fitted exponential models for predicting IRI on thin HMA overlays using pavement management data from Indiana, which has the following form:

$$y = e^{\beta_1 + (\beta_2 \times AATT + \beta_3 \times AFDX) \times t}$$

where y is the IRI value for a treated pavement section at a given year, AATT is annual average daily truck traffic, AFDX is average annual freeze index, t is the pavement age at which IRI is being estimated, and β_1, β_2, and β_3 are regression coefficients.

Chen and Zhang (2011) used New Mexico pavement data to investigate the applicability of IRI-based pavement deterioration prediction models of four forms – the NCHRP, Al-Omari-Darter, Dubai, and New Mexico Department of Transportation (NMDOT) models. In the four models, the NCHRP and NMDOT models predict other performance indicators (e.g., PSI) based on IRI, while the Al-Omari-Darter and Dubai

models predict IRI based on other factors (e.g., age). The Al-Omari-Darter and Dubai models have the following forms:

$$\text{Al-Omari-Darter Model}: \quad IRI = 0.796e^{0.0539(Age)}$$
$$\text{Dubai Model}: \quad IRI = 57.56RD - 334.28$$
$$IRI = 136.19SD - 116.36$$

where Age is the age of the pavement section since the original construction or last overlay, *RD* is the rut depth, and *SD* is the standard deviation of rut depth.

It is obvious that these models are not adequate for being used in PRS as none of them has included any initial material and construction characteristics that were listed in the previous section. In addition, these models are too simple for predicting pavement post-treatment performance, as they usually consider a very limited number of variables, which restricts their capability of capturing actual in-service treatment performance. A preliminary analysis of the LTPP Specific Pavement Studies Experiment 3 (SPS-3) data indicated that field post-treatment performance data commonly shows large variations and does not follow obvious patterns or trends, making it essential to devise a promising approach for developing pavement post-treatment performance models.

Performance Indicators of Thin HMA Overlays

Performance prediction models used in PRS include acceptance quality characteristics, along with other influential factors, as predicator variables; on the other side of the model will be pavement performance, which is usually represented by different forms of distress (e.g., fatigue cracking, longitudinal cracking, transverse cracking, and rutting) and pavement smoothness [e.g., International Roughness Index

(IRI)], especially in the Mechanistic Empirical Pavement Design Guide (MEPDG). Selection of appropriate performance indicator for thin HMA overlays is important in the PRS because it helps define the failure of the pavement that receives a thin HMA overlay treatment.

IRI was originally produced in a research effort led by the World Bank that aimed to establish a universal and transportable index for quantifying pavement roughness. IRI is defined as the cumulative relative displacement of the axle with respect to the frame of a reference quarter-car per unit distance traveled over the pavement profile at a speed of 80 km/h (Sayers et al. 1986).

In this dissertation, IRI was used as the performance criterion to characterize thin HMA overlays and underlying pavement structure. Using IRI as the performance criterion was determined for several reasons. First, it is one of the most commonly used performance criteria for new HMA pavements (ARA 2004; Choi et al. 2004; Fugro and ASU 2011; Haider and Dwaikat 2011). Secondly, in the construction specifications of many highway agencies (such as TxDOT and FDOT), the initial IRI measurement immediately after a thin HMA overlay treatment is used as a post-construction quality measure for making pay adjustment purposes. Thirdly, a pilot application of the pavement prediction under development finds that IRI models tend to give the most promising predictions that are closer the field observations in the LTPP database, comparing to other considered distress types, such as alligator cracking and rutting. These features make IRI an ideal performance indicator for justifying the quality of thin HMA overlay treatments.

A REVIEW OF EXISTING IRI MODELS FOR HMA PAVEMENT

With an aim of developing IRI models for thin HMA overlays, a review of existing IRI models for HMA pavement in the literature was conducted.

The existing pavement structure is a complex system and usually consists of multiple pavement layers, such as the HMA surface layer, granular/stabilized base, and subgrade. Some pavement sections also include an HMA binder course between the surface layer and base, or a granular/stabilized subbase between the base and subgrade. Considering abundant information contained in each layer, a great number of variables need to be taken into consideration for predicting overall pavement performance. Ideally, these variables include pavement material properties, traffic loading, and environmental factors such as temperature, rainfall, and freezing index (Owusu-Abaio 1998).

Over the past decades, numerous efforts have been made to develop pavement performance models that aim to address one of the commonly used performance indicators in HMA pavement design, including distresses (e.g., rutting, alligator cracking, longitudinal cracking, and transverse cracking), serviceability (e.g., present serviceability index and roughness) ,and surface friction (Huang 2004). For example, in the SHRP Early Analysis, Simpson et al. (1994) developed regression equations for predicting the variation of IRI for HMA pavements on granular base in different climatic regions. Their model for the Wet-Freeze climatic region has the following form:

$$\Delta IRI = N^{B}10^{C}$$

where ΔIRI is the difference in IRI compared to the construction year (in/mile), N is the number of cumulative KESALs (1 KESALs = 1000 ESALs), and B and C are determined using the following equations:

$$B = b_0 + b_1 x_1 + b_2 x_2 + \cdots + b_n x_n$$

$$C = c_0 + c_1 x_1 + c_2 x_2 + \cdots + c_n x_n$$

where x_1 is the asphalt viscosity at 140 ^{o}F, x_2 is the air voids, x_3 is the logarithm of HMA layer thickness, x_4 is the base thickness, x_5 is the annual number days > 90^{o}F, and x_6 is the product of freeze index and air voids in HMA mix.

Many of these predictive models were mostly developed based on regression analysis on localized data base, resulting in very limited usefulness in practice (Huang 2004). Some researcher developed pavement roughness models using the neural network approach (La Torre et al. 1998; Roberts and Attoh-Okine 1998). These models either considered only a small number of independent variables or were based on local pavement performance data, preventing them from being used in a generalized PRS system.

The NCHRP Study 01-37A, namely "*Development of the 2002 Guide for the Design of New and Rehabilitated Pavement Structures:* Phase II," adopted a mechanistic-empirical approach to damage analysis of HMA pavements. This approach involves computing the pavement structural responses to load (i.e., stresses/strains), translating them into damage, and accumulating the damage into distresses, which reduce pavement performance over time. It implemented damage functions for fatigue

cracking (bottom-up and top-down), rutting by computing the plastic deformation in all layers, and pavement roughness (Papagiannakis and Masad 2008). The mechanistic-empirical performance prediction models were calibrated using field performance observations from three large-scale pavement experiments: the Minnesota Road Research (MnRoad) Project, the WesTrack Project, and the LTPP Program. These models were implemented in the MEPDG software, which was developed under the NCHRP 01-37A.

The IRI model proposed in the NCHRP 01-37A guide is regression-based, using the other computed distresses as the main independent variables. It was developed in three forms to accommodate three types of pavement design.

1. For HMA pavements on unbound granular bases, the IRI model has the following form:

$$IRI = IRI_0 + 0.463\left[SF\left(e^{\frac{age}{20}} - 1\right)\right] + 0.00119\left(TC_L\right)_T + 0.1834\left(COV_{RD}\right) + 0.00384\left(FC\right)_T + 0.00736\left(BC\right)_T + 0.00115\left(LC_{SNWP}\right)_{MH}$$

where IRI_0 is the initial (as constructed) pavement roughness, $(TC_L)_T$ is the total length of transverse cracks (low, medium, and high severity levels), COV_{RD} is the coefficient of variation in rut depth, $(FC)_T$ is the fatigue cracking in the wheel-paths, $(BC)_T$ is the area of block cracking (percent of total lane area), $(LC_{SNWP})_{MH}$ is the length of moderate and high severity sealed longitudinal cracks outside the wheel-paths, *age* is the age the section in years, and *SF* is a site factor, expressed as

$$SF = \left(\frac{R_{SD} * \left(P_{.075} + 1 \right) * PI}{2 * 10^4} \right) + \left(\frac{\ln\left(FI + 1 \right) * \left(P_{.02} + 1 \right) * \ln\left(R_m + 1 \right)}{10} \right)$$

where R_m and R_{SD} are the mean and standard deviation in annual rainfall, $P_{.075}$ and $P_{.02}$ are the subgrade percent finer fractions for grain sizes 0.075 mm and 0.02 mm, *FI* is the average annual freezing index, and *PI* is the plasticity index of the subgrade.

2. For HMA pavements on asphalt treated bases, the IRI model has the following form:

$$IRI = IRI_0 + 0.0099947\left(Age \right) + 0.0005183\left(FI \right) + 0.000235\left(FC \right)_T + 18.36\left[\frac{1}{\left(TC_s \right)_H} \right] + 0.9694\left(P \right)_H$$

where $(TC_s)_H$ is the average spacing of high severity transverse cracks, and $(P)_H$ is the area of high severity patches.

3. For HMA pavements on chemically treated bases, the IRI model has the following form:

$$IRI = IRI_0 + 0.00732\left(FC \right)_T + 0.07647\left(SD_{RD} \right) + 0.0001449\left(TC_L \right)_T + 0.00842\left(BC \right)_T + 0.0002115\left(LC_{NWP} \right)_{MH}$$

In another NCHRP Project 9-22 “Beta Testing and Validation of HMA PRS” conducted by Fugro Inc. and Arizona State University (ASU), the researchers developed closed form solutions for three major distresses (rutting, fatigue cracking, and thermal cracking) that predict the simulation of the MEPDG distress predictions (Fugro and ASU

2011). Their research and the resulted Quality-Related Specification Software (QRSS) used the Initial IRI (actual degree of smoothness obtained by the contractor, not predicted through models) in its analyses for adjusting the pay factor. The QRSS rutting and fatigue cracking models are based on relating the dynamic modulus calculated with the respective effective temperature to the pavement distress. The QRSS thermal cracking model is based on relating the calculated creep compliance to the pavement distress.

The literature review of existing pavement performance prediction models indicates that the mechanistic-empirical performance models incorporated in the MEPDG software are the most promising at current stage and widely accepted by the pavement community (Graves and Mahboub 2006; Tarefder and Sumee 2011; Aguiar-Moya et al. 2009; Ahn et al 2009; Guclu et al. 2009). Another advantage of the MEPDG models is that these models are developed based on nation-wide database (i.e., not limited to particular locality) and well-tested. Therefore, this dissertation made an effort to develop performance models that predict the simulation results of IRI prediction using MEPDG.

The literature and practically trial runs of the MEPDG show that the MEPDG is a computation-intensive program, requiring many input factors including material properties, climate, and traffic. Because the MEPDG consists of a finite element (FE) or a multilayer linear elastic analysis (Aguiar-Moya and Prozzi 2011), running a single instance using the MEPDG requires considerable amount of time, generally 20 to 40 minutes per run depending on the complexity of the pavement design. Additionally, the

source code for the MEPDG distress prediction models is not accessible, making it impossible to directly integrate the MEPDG analysis into the PRS simulations. These barriers make it necessary to develop reliable and rapid-form pavement roughness models that can predict the MEPDG distress analysis results.

A REVIEW OF THE ARTIFICIAL NEURAL NETWORKS MODELING APPROACH

In this research, efforts were made to develop IRI models for HMA pavement that simulate the MEPDG IRI models introduced in Section 2.6. Due to the complexity of pavement structure and the number of predictors used for predicting IRI, the artificial neural networks (ANNs) approach was used in this study for modeling purposes. An introduction about ANNs is provided in the following part of this section.

What is ANNs

An ANNs is a machine that is designed to model the way in which the human brain performs a particular task or function of interest by employing a massive interconnection of simple computing cells referred to as *neurons* or *processing units*. Haykin (2008) defined ANNs as

"*A neural network is a massively parallel distributed processor made up of simple processing units that has a natural propensity for storing experimental knowledge and making it available for use. It resembles the brain in two respects: 1) knowledge is acquired by the network from its environment through a learning process;*

2) interneuron connection strengths, known as synaptic weights, are used to store the acquired knowledge."

ANNs has many useful features, making it a powerful tool in modeling. The first feature is that it has the ability to represent any arbitrary nonlinear relationships. Although in regression analysis linear relationships (or at best pre-specified nonlinearity) are often needed, ANNs can find its own function without the constraint of linearity. Additionally, ANNs has the ability of generalizing a relationship from a small subset of data, to remain relatively robust in the presence of noisy inputs or missing input parameters, and to adapt and continue to learn in the face of changing environments linearity (Roberts and Attoh-Okine 1998). Another feature of ANNs is that it can find good approximate solutions to complex (large-scale) problems that are intractable (Haykin 2008). These advantages made ANNs an ideal approach for developing existing pavement IRI models in this study.

An ANNs consists of a large number of neurons, which are interconnected by means of directed links, and each directed link has an associated weight. The weights acquired through the training process represent abstracted information from the data set, which is used by the ANNs to solve particular problems. To construct an ANNs, three key components need to be first determined: 1) the network architecture; 2) the neuron activation function; and 3) the learning method.

Architecture

Selection of the network architecture is an important step in the ANNs modeling process as it is intimately linked with the learning algorithm used to train the network

(Haykin 2008). The efforts generally include determination of input and output variables, number of hidden layers, and number of hidden neurons in each hidden layer. Usually an ANNs with too few hidden neurons is unable to learn sufficiently from the training data set, whereas an ANNs with too many hidden neurons will allow the network to memorize the training set instead of generalizing the acquired knowledge for unseen patterns (Lawrence and Fredrickson 1994). In general, there are three fundamental ANNs architectures (Haykin 2008):

- Single-layer feedforward networks, in which the input layer of source codes are projected directly onto the output layer of neurons, but not vice versa (in the sense of "*feedforward*").
- Multilayer feedforward networks, in which one or more hidden layers are used to intervene between the input and output layers. By doing this, the network is enabled to extract higher-order statistics from its input.
- Recurrent networks, in which at least one feedback loop is included.

Among these architectures, multilayer feedforward ANNs are the one most commonly used in many scientific studies. The backpropagation learning algorithm, introduced later in this section, requires an input and an output layer and at least one hidden layer (Alsugair and Al-Qudrah 1998). The number of hidden layers and the number of neurons in a hidden layer(s) are selected based on the problem complexity. Studies have proved that any continuous function can be approximated by using a three-layered network (Funahashi 1989; Hornik et al. 1989). In practice, most ANNs applications found in the literature used one hidden layer in the final models. This

research also used one hidden layer ANNs for developing existing pavement performance models. A typical fully connected feedforward ANNs is shown in Figure 4. Note that in this study, the ANNs output layer has only one neuron, which represents IRI.

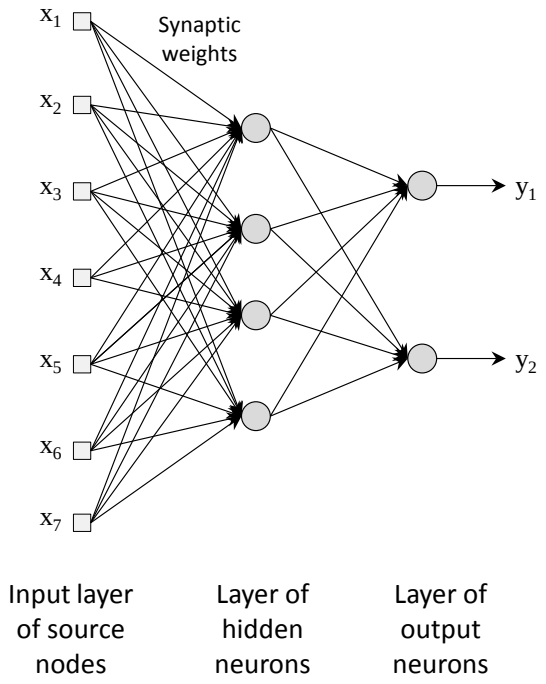

Figure 4 A typical 7-4-2 fully connected feedforward ANNs architecture.

Activation Function

Each neuron in an ANNs works as a processing units, taking in inputs and giving output to the next layer. It functions in a way of distributed parallel computation. The processing of each neuron is simply a weighted summation that is transferred via activation function, which is shown as the following equation:

$$O_j = f\left(\sum_{i=1}^{n} x_i w_i\right)$$

where O_j is the output of the jth neuron, f is the activation function, x_i is the ith input, w_i is the connection weight associated with the ith input, and n is the total number of input in that layer. Five typical transfer functions are generally used as neuron activation functions, including: 1) linear; 2) linear threshold; 3) step; 4) sigmoid (or hyperbolic tangent sigmoid); and 5) Gaussain. Among these, the sigmoid function is mostly commonly used owing to its concise form and differentiability. In this study, the sigmoid function and linear threshold function were used for hidden layer and output layer, respectively. The two functions have the following mathematical expressions (Rooij et al. 1996):

1. Sigmoid function

$$f(y) = \frac{1}{1+e^{-a(y)}}$$

$$y = \sum_{i=1}^{n} w_i x_i$$

2. Linear threshold function

$$f(y) = \begin{cases} -1, & if\ y \le -1 \\ y, & if\ -1 < y < 1 \\ 1, & if\ y \ge 1 \end{cases}$$

where y is the input to the transfer function, and a is the gain of the sigmoid function.

Learning

The learning process in an ANNs is one of developing a mapping between the output data and the input data, so that the weight values in the network are adjusted to reflect the characteristics of the input data. This process is generally achieved by adjusting the signs and magnitudes of the weight values according to learning rules that seek to minimize a cost or an error function. All learning methods can be classified into two categories: supervised learning and unsupervised learning. In supervised learning, a target value is included as part of each pattern within the training data. In unsupervised learning, there is not target value; instead, the set of data which contains the facts is repeatedly applied to the network until a stable network output is obtained. It relies on local information during the learning process by organizing presented data and discovering its emergent collective properties (Yang et al. 2003).

The backpropagation method in supervised learning is widely used in many studies for network learning (Najjar et al. 1996; Alsugair and Al-Qudrah 1998). The backpropagation learning algorithm uses gradient descent search in the weight space to minimize the error between the target output and the actual output. A typical network error is the mean square error (MSE), which is defined as follows:

$$E_{total} = \frac{1}{2}\sum_{j=1}^{n}\sum_{k=1}^{m}\left(T_k^{(j)} - Y_k^{(j)}\right)^2$$

where E_{total} is the square of the output error for all the patterns in the data sample, $T_k^{(j)}$ is the target value of the kth output for the jth pattern, $Y_k^{(j)}$ is the actual kth output for the jth

pattern, *n* is the number of patterns in the data sample, and *m* is the number of neurons in the output layer.

Then the error is minimized by backpropagation through the neural network. During this process, the error contribution caused by each layer is computed and distributed backward, and the corresponding weight adjustments (through learning rules) are made to minimize the error. Using the gradient descent method, the backpropagation weight adjustment is associated with the derivative of the error with respect to each weight, according to the delta rule, and can be expressed as follows (Rooij et al. 1996):

$$\Delta w_{jk}(t+1) = -\eta \frac{\partial E_{total}}{\partial w_{jk}}(t+1) + \mu \Delta w_{jk}(t)$$

where $\Delta w_{jk}(t+1)$ is the weight adjustment for training iteration $t + 1$ between the jth neuron and the kth neuron in the next layer, η is the learning rate, and μ is a momentum term used to achieve rapid convergence and avoid numerical vibration during training.

The ANN training approach used in this research is batch training, in which the weights are adjusted after all samples are processed. This training approach guarantees the network error E_{total} to decrease gradually and convergence can be speeded up. The ANN training process is considered complete based on some criteria. In this research, the magnitude of the gradient of performance, MSE, and the number of validation checks are used to terminate the training process. When the magnitude of the gradient is below 10^{-5} or the number of successive iterations that the validation performance fails to decrease reaches 6, the training process will stop. These values are default values in the Matlab Neural Network Toolbox.

CHAPTER III

MODELING APPROACH FOR PREDICTING POST-TREATMENT PAVEMENT PERFORMANCE

OVERVIEW

PRS depend on quantified relationships between various initial quality characteristics and performance. A modeling approach for predicting post-treatment pavement performance was developed and is discussed in this chapter. This approach, named "Two-Component Modeling Approach" (TCMA), consists of two model components. The first component consists of a set of artificial neural networks (ANNs) for predicting the performance of original pavement structure (i.e., before a preservation treatment is applied). The second component consists of Bayesian linear models that predict the beneficial effects due to a preservation treatment, exhibited as reduced deterioration in pavement. In this research, TCMA was applied to thin HMA overlays for developing pavement roughness models that will be used in the PRS.

THE TWO-COMPONENT MODELING APPROACH

As discussed in Section 2.3, pavement preservation treatments are not aimed to add substantial structural capacity to the existing pavement; instead, they are used to correct surface defects and retard the initiation and propagation of distresses in the original pavement layers. Eventually, however, the distresses in the original layers will develop and reflect on the treatment surface after a certain period of time. This mechanism is depicted graphically in Figure 5.

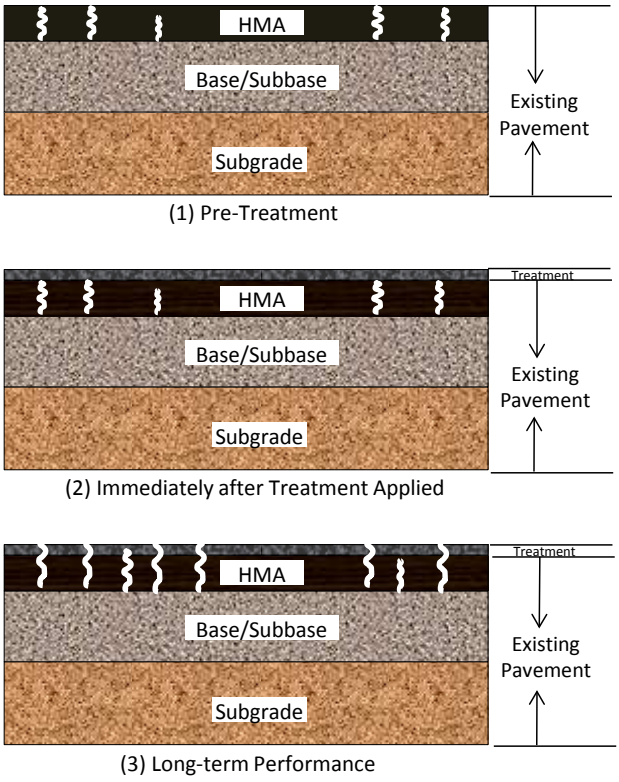

Figure 5 Distress development mechanism for pavement preservation treatments.

The existing pavement distresses (e.g., cracking and roughness) are immediately covered (i.e., reduced to zero) or alleviated (i.e., reduced to a lower amount) after the treatment layer is placed, as shown in the top two parts of Figure 5. With time and increasing traffic loading on the treatment layer, the distress grow in extent and severity, propagate upward, and eventually reflected on the surface, as shown in the bottom part of Figure 5. Therefore, the performance of pavement preservation treatments is affected by three major categories of factors: 1) the initial quality characteristics of the treatment; 2) the condition of the original pavement; and 3) other important site factors such as traffic and climatic conditions.

The TCMA modeling approach, developed as part of this research, simulates the above distress development mechanism of pavement preservation treatments illustrated in Figure 5. TCMA is illustrated graphically in Figure 6.

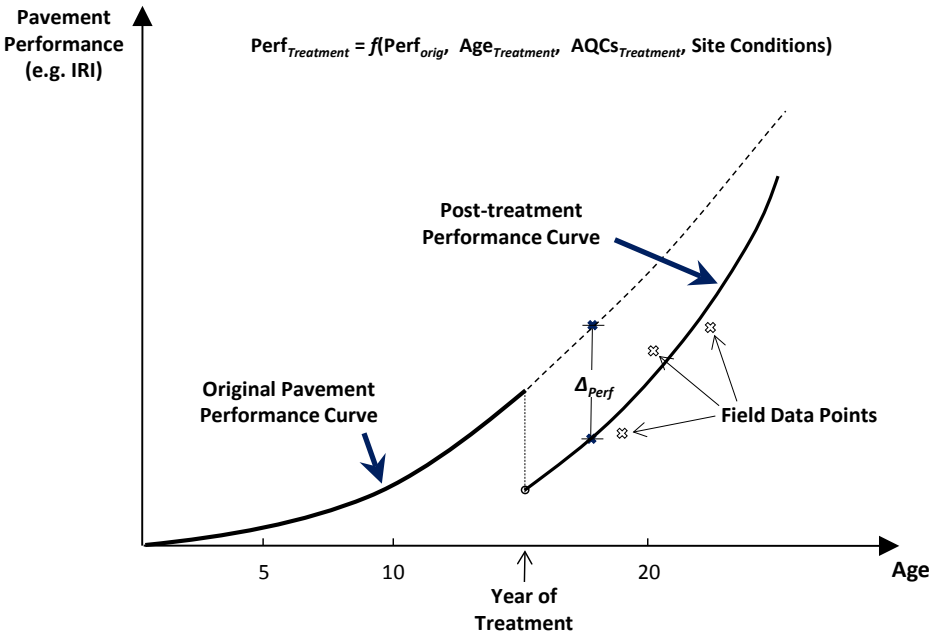

Figure 6 A modeling approach for predicting preservation treatment performance.

In this approach, the performance of a pavement preservation treatment is modeled as a function of the AQCs of the treatment, the treatment age, the condition of the original pavement structure, and site conditions (traffic loading, climate, etc.). The final model includes two tightly-coupled components:

- The first component is used to predict the performance of the existing (i.e. original) pavement. The inputs to this component include material properties and structural characteristics of the pavement layers (e.g., HMA layer(s),

base/subbase, and subgrade), age of the pavement, climate conditions, and traffic factors. The performance prediction using this component is represented by the "*Original Pavement Performance Curve*" in Figure 6. The solid part of this curve refers to the performance of existing pavement before a preservation treatment is applied. The dotted part of this curve refers to the conceptual performance of existing pavement if no preservation treatment is applied. Eq. 1 is a generalized model form of the first component.

$$Perf_{orig} = f\left(materials_{orig}, structure_{orig}, age_{orig}, traffic, climate\right) \quad \text{(Eq. 1)}$$

In practice, there are many different pavement designs (i.e., layer compositions of HMA surface, binder course, base, and subbase). This model component may vary for different original pavement designs.

- The second component, represented by "Δ_{perf}" in Figure 6, is used to predict the reduction in distress or roughness, which is induced by application of the preservation treatment. Immediately after the treatment, the existing pavement distress or roughness is brought down to a lower level. For some distresses (e.g. alligator cracking), the amount of cracks after treatment would be reduced to close to zero; whereas an initial post-treatment IRI would be typically 60-70 in/mile. In the MEPDG software, the default initial IRI is 63 in/mile (≈ 1 m/km), which is set based on the LTPP pavement profile data (ARA 2004). Inputs to this component include the AQCs of the treatment,

age of the treatment, traffic factors, and climate conditions. The general form of the second component can be expressed as in Eq. 2.

$$\Delta_{perf} = f\left(AQCs_{trmt}, age_{trmt}, traffic, climate\right) \quad \text{(Eq. 2)}$$

When the two components are developed, the treatment's future performance can be predicted by combining the predictions from the two components, as shown in Eq. 3. The pavement post-treatment performance is illustrated by the "*Post-Treatment Performance Curve*" in Figure 6.

$$Perf_{trmt} = Perf_{orig} - \Delta_{perf} \quad \text{(Eq. 3)}$$

An example is given here for predicting pavement IRI after a thin HMA overlay treatment was applied. The first step is to predict the IRI of the existing pavement over a given analysis period. In this step, information about the existing pavement layers needs to be obtained from appropriate data sources, such as state DOT's pavement management systems. Using the first model component (i.e., Eq. 1), the IRI of the existing pavement is predicted as a set of time series values (typically successive data points in time spaced at uniform intervals). In the second step, the treatment AQCs measured during the quality assurance and quality control process of the overlay treatment, along with other necessary information, are input into the second component (i.e., Eq. 2) to predict the reduction in IRI in different years after the thin HMA overlay treatment was applied. The last step is to obtain the post-treatment IRI in different years

by subtracting the reduction in IRI estimated in the second step from the predicted IRI in the first step.

PREDICTION OF IRI FOR HMA PAVEMENT TREATED WITH A THIN HMA OVERLAY – MODEL COMPONENT 1

The above modeling approach was applied to develop a model for predicting IRI for HMA pavement treated with a thin HMA overlay. The IRI model incorporated in the MEPDG for HMA pavement was used as the bases for developing the first component (i.e., prediction of IRI of existing pavement) of this model. A rapid form of the MEPDG IRI model was developed using artificial neural networks. The following steps were followed to develop the first component of this model:

- **Step 1: Prepare a pavement dataset of adequate sample size for simulation**. Important pavement layers properties that are influential on future performance are identified based on past pavement studies in the literature and available data in the LTPP database. In this step, the statistics (e.g., range and distribution) of each key pavement property and site factor were obtained from the LTPP data. Then this research used the Latin Hypercube Sampling (LHS) procedure for generating the input data set to be used in MEPDG simulations. LHS was used to generate all possible combination of the model inputs within their ranges. The LHS procedure will be introduced in a later section of this chapter.
- **Step 2**: **Input the sample data into MEPDG and ran the simulations.**

This step was one of the most time-consuming tasks during the simulation because about three thousands cases were input into the MEPDG. A script was written using AutoIt to facilitate the input process on a case-by-case basis. A very useful feature of MEPDG was that it allows for running multiple simulation cases under the "Batching" mode.

- **Step 3: Extract the MEPDG simulation results into a dataset.** After each run, the MEPDG generates an output file in Excel format that contains detailed information about the pavement design, site conditions, and predicted performance data over the pavement design life. Another script was writing using Matlab to read necessary pavement and performance data into one dataset, which was used as the basis for developing performance models for existing pavement (i.e., the first component of the overall prediction model).
- **Step 4: Develop reliable and rapid-form of pavement roughness prediction models.** In this step, the artificial neural networks modeling approach was applied to develop the first component of the IRI model using the dataset generated from the MEPDG simulation results. The details and advantages of this modeling technique are discussed in the next chapter of this dissertation.

PREDICTION OF IRI FOR HMA PAVEMENT TREATED WITH A THIN HMA OVERLAY – MODEL COMPONENT 2

It was observed that the IRI data in the LTPP database have a high propensity of being incomplete (i.e., missing IRI values for some years within the study period) and highly variable (i.e., without clear patterns). For example, Figure 7 displays the actual IRI values observed at two Wyoming LTPP test sections that received thin HMA overlays in 1991. Section 56-A310 had consecutive IRI measurements while 56-B310 did not have values for some years. In contrast, 56-B310 had a clear increasing pattern in its IRI measurements, whereas the pattern for 56-A310 was not clear. This type of incomplete and variable performance data made the development of deterministic performance models unviable.

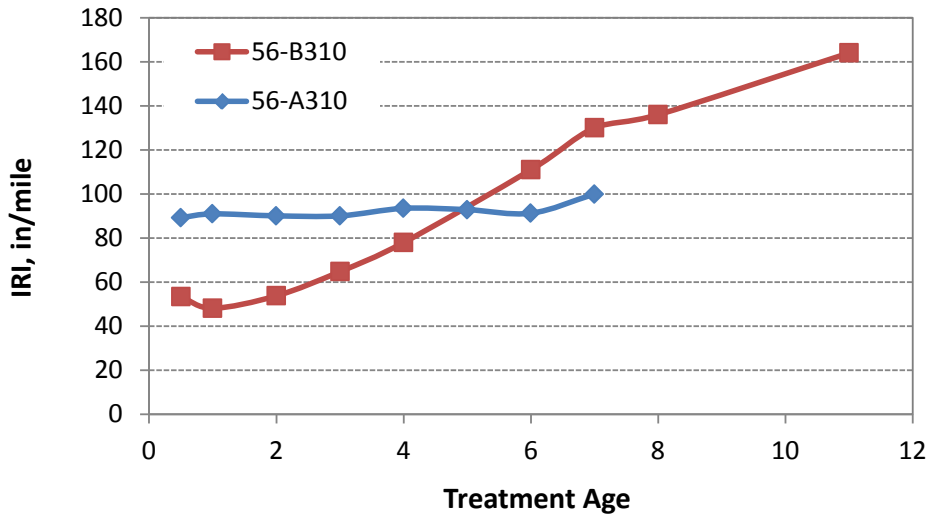

Figure 7 IRI measurements for example LTPP sections treated with thin HMA overlay.

In this research, Bayesian regression was used due to its power to incorporate uncertainty, which is specially reality in pavement preservation performance data. The other advantage is its ability to incorporate expert opinions (used as priors) to supplement historical data where quality data is not available (Amador and Mrawira 2011). Instead of predicting in the form of a single value for the response variable, Bayesian regression models generate probability distributions for the response variable (i.e., IRI reduction in this study), which is more in line with commonsense interpretations (Congdon 2001). Another desired property of the Bayesian approach is that it avoids the maximization of any function, which is required and numerically difficult in classical linear or non-linear modeling approaches (Train 2001).

DATA USED FOR DEVELOPING PERFORMANCE PREDICTION MODEL

The Long-Term Pavement Performance (LTPP) Data is used for developing the IRI prediction model. The LTPP program is a large-scale pavement experiment that was initiated in 1986 as part of the Strategic Highway Research Program (SHRP) to evaluate the long-term performance of pavement consisting of various material and layer compositions. It was first funded by the SHRP during 1987 to 1992; then the Federal Highway Administration (FHWA) assumed the management and funding of the LTPP program (Ali and Tayabji 1998).

The LTPP includes two classes of studies: the General Pavement Studies (GPS), and the Specific Pavement Studies (SPS). The GPS experiments were designed to study the performance of existing pavements; whereas the SPS experiments were designed to study the performance of specially constructed, maintained, or rehabilitated pavement

sections, incorporating a controlled set of experimental design and construction features. For HMA pavements, the SPS experiments included four specific preventive maintenance treatments (designated as "SPS-3"): 1) chip seals; 2) crack sealing; 3) slurry seals; and 4) thin HMA overlays. A control section (untreated pavement) was also included for each SPS test section for comparison purposes. The total number of test sections is nearly 800 for the GPS experiments and 1,262 for the SPS experiments. These sections were exposed to in-service traffic monitored by weight-in-motion (WIM) systems (Elkins et al. 2003). Pavement performance data has been collected at these sections for over 20 years through four regional contracting agencies under the oversight of the FHWA. The data is assembled into a massive database, which is publicly accessible at the LTPP DataPave web-based database or by inquiry. The whole database is composed of a total of 14 modules that contains similar sets of tables.

This research used the data from the Inventory, Maintenance, Rehabilitation, Monitoring, Specific Pavement Studies, Test, Traffic, Climate, and Administration modules. The IRI data computed from raw pavement longitudinal profile data is stored in the MON_PROFILE_MASTER table of the Monitoring module. Normally, the profile data were collected for at least five repeat measurement passes on the same day using inertial profilers.

In this research, a HMA overlay treatment that has a thickness of below 2.0 inches was regard as thin HMA overlay. The 2.0 inches cutoff value was selected based on an analysis of the SPS-3 thin HMA overlay data, in which the thin HMA overlay treatments ranged between 0.5 and 2.0 inches. The initial data set included 148 test

sections that had received a thin HMA overlay treatment. These pavement sections have 25 different pavement layouts (or pavement designs). A histogram of these pavement layouts is shown in Figure 8. The most commonly observed pavement layout at these sections was “GB_BC_OSL”, followed by “GS_GB_BC_OSL”, “GS_GB_OSL”, and “GB_OSL” (shaded area in Figure 8). These four pavement layouts accounted for about 60% of all observed layouts of the LTPP test sections that had received a thin HMA overlay treatment. As a result, this research used four dominating pavement layouts only. Figure 9 graphically depicts the layout compositions in each of the four pavement layouts used in this research. Furthermore, those sections with incomplete pavement data or suspicious values were excluded from further study. The final dataset consists of 88 LTPP test sections. Thin HMA overlay treatments were applied at these sections during the period of 1989 to 2003. A map showing the locations of these overlay treatments is presented in Figure 10. It can be seen that these locations had a reasonable coverage of the climatic and geographical conditions in the U.S.

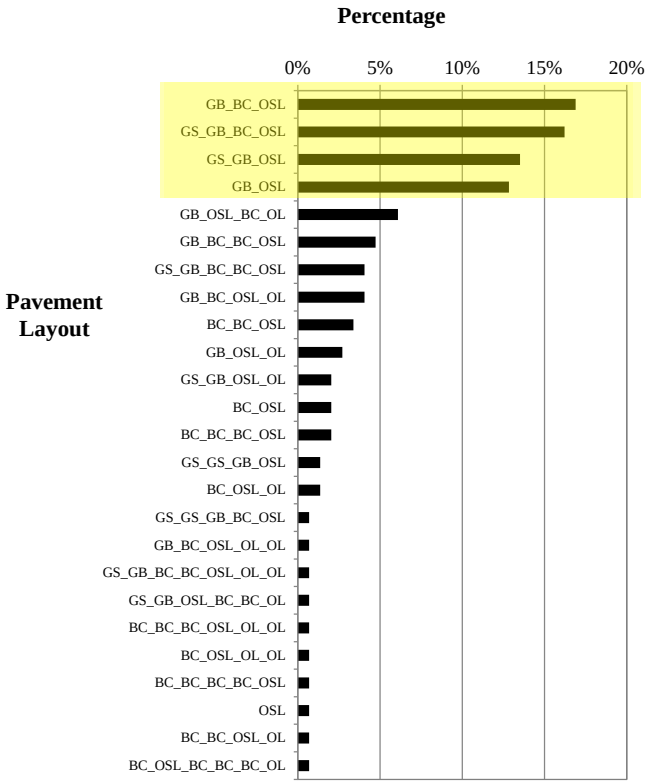

Figure 8 Pavement layouts of all LTPP thin HMA overlay sections. (*GS* = Granular Subbase; *GB* = Granular Base; *BC* = Binder Course; *OSL* = Original Surface Layer; *OL* = Overlay. A subgrade is present for all sections, thus not shown. Example: *GB_BC_OSL* indicates the pavement consists of from top to down, an original HMA surface, a binder course, a granular base, and subgrade.)

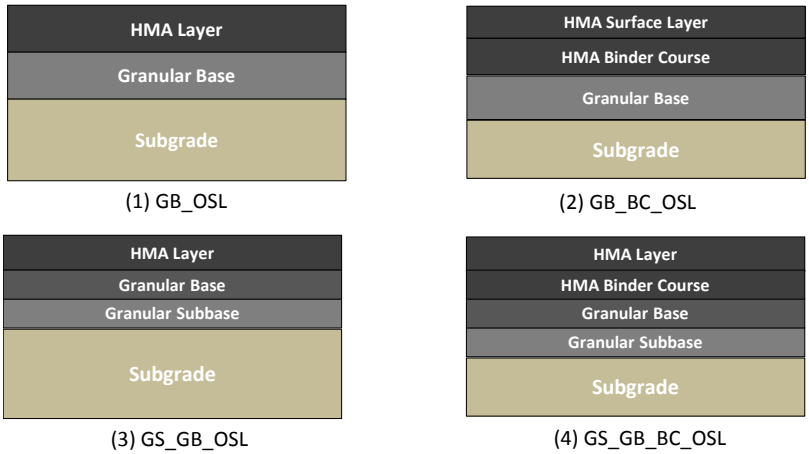

Figure 9 Layout compositions of four dominating pavement layouts in the research dataset.

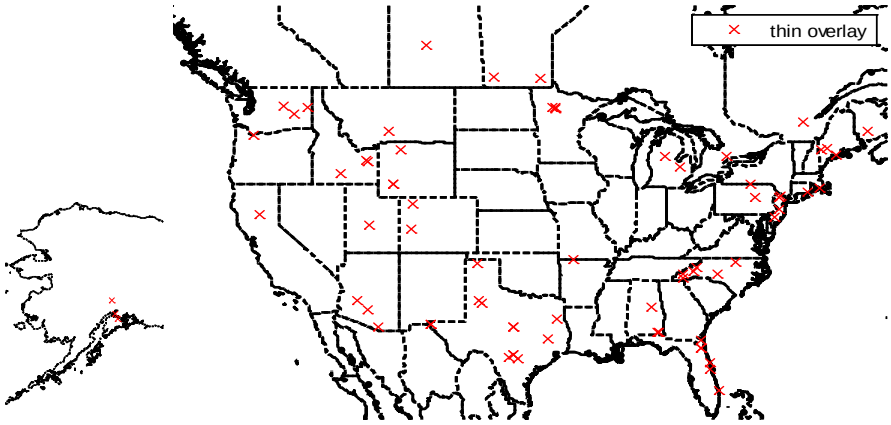

Figure 10 Locations of the thin HMA overlay treatments included in the research dataset.

Tables 3 through 5 provide summary statistics (i.e., minimum, maximum, mean, and standard deviation) of the site conditions, important properties of HMA layers, and underlying courses of the LTPP sections used in this study, respectively.

Table 3 Site Conditions

Variables	LTPP Data			
	Min	Max	Mean	Stdev
Average air temperature, °F	34.5	74.5	52.9	43.8
Annual rainfall, in	7.6	84.8	33.1	17.2
Freeze index, °F-days	0	1820	476.1	580.5
Initial two-way AADTT, *veh*/day	40	1,900	320	319
AADTT compound growth rate, %	0.4	14.5	4.5	3.1

Table 4 Characteristics of Existing (Pre-treatment) HMA Layers

Layer	Variables	LTPP Data			
		Min	Max	Mean	Stdev
HMA Surface Layer	Thickness, in	0.7	12.6	2.9	2.1
	Effective asphalt content, %	3.7	7.7	5.5	0.8
	Air voids, %	1.9	10.0	4.8	1.9
	Unit weight, pcf	131.6	166.6	145.3	5.2
	Cum. % retained 3/4” sieve	0.0	8.0	0.6	1.5
	Cum. % retained 3/8” sieve	0.0	39.0	14.8	10.1
	Cum. % retained #4 sieve	13.0	59.0	39.7	8.3
	% passing #200 sieve	1.0	10.5	5.7	1.6
Binder Course	Thickness, in	1.0	8.3	3.9	2.0
	Effective asphalt content, %	3.5	7.1	4.9	0.8
	Air voids, %	1.8	9.6	4.8	1.8
	Unit weight, pcf	131.0	162.2	147.4	6.3
	Cum. % retained 3/4” sieve	0.0	26.0	6.4	7.3
	Cum. % retained 3/8” sieve	1.0	50.5	28.1	15.5
	Cum. % retained #4 sieve	19.0	65.0	48.2	11.1
	% passing #200 sieve	3.2	9.6	5.9	1.7

Table 5 Characteristics of Existing (Pre-treatment) Base, Subbase, and Subgrade

Layer	Variables	LTPP Data			
		Min	Max	Mean	Stdev
Granular Base	Thickness, in	1.0	25.6	9.2	4.4
	Plasticity index	0	12	2.3	3.0
	Liquid limit	0	32	11.4	11.4
	% passing #200 sieve	0.5	38.5	14.1	8.5
	% passing #40 sieve	5	67	29.8	13.2
	% passing #10 sieve	13	80	47.1	14.2
	% passing #4 sieve	16	89	59.3	13.2
	% passing 1" sieve	39	100	96.0	7.8
	Max dry unit weight, pcf	109.5	147.5	134.7	7.5
	Opt. moisture content, %	4.5	16.0	7.4	2.0
Granular Subbase	Thickness, in	3.0	38.2	11.8	6.8
	Plasticity index	0	11	1.9	3.3
	Liquid limit	0	32	9.9	11.0
	% passing #200 sieve	3.2	31.1	12.9	6.3
	% passing #40 sieve	8	99	41.7	26.7
	% passing #10 sieve	19	100	59.8	25.2
	% passing #4 sieve	30	100	69.3	22.3
	% passing 1" sieve	62	100	93.0	9.0
	Max dry unit weight, pcf	107	149.5	128.5	13.0
	Opt. moisture content, %	5.0	18.0	9.1	3.2
Subgrade	Plasticity index	0	33	7.2	8.2
	Liquid limit	0	65	20.0	16.4
	% passing #200 sieve	0.3	91.8	29.7	23.6
	% passing #40 sieve	12	99	63.0	25.0
	% passing #10 sieve	20	100	75.7	23.2
	% passing #4 sieve	23	100	81.6	20.1
	% passing 1" sieve	63	100	95.1	8.3
	Max dry unit weight, pcf	96.0	140.5	116.2	10.3
	Opt. moisture content, %	6.0	22.0	12.8	3.8

The asphalt binder used in the HMA layers of these LTPP sections included the following types (which are based on conventional viscosity or penetration grading systems): AC-2.5, AC-5, AC-10, AC-20, AC-30, AC-40, PEN40-50, PEN60-70, PEN85-100, PEN120-150, and PEN200-300. The viscosity of the asphalt binder at a reference temperature (70°F used as default in this study) was determined using the ASTM viscosity temperature relationship defined as follows (Fugro and ASU 2004):

$$\log\log\eta = A + VTS\log\left(459.7 + T_R\right) \qquad \text{(Eq. 4)}$$

where η is the viscosity in *cP*, *A* is the regression intercept, *VTS* is the regression slope of viscosity temperature susceptibility, and T_R is the reference temperature in °F. The *A* and *VTS* values recommended by MEPDG and computed viscosity values for different asphalt binders are provided in Table 6.

Table 6 Viscosity of Typical Asphalt Binders

Asphalt Binder	A	VTS	Viscosity@70°F (10^6 Poise)
AC-2.5	11.5167	-3.8900	2.10
AC-5	11.2614	-3.7914	3.81
AC-10	11.0134	-3.6954	7.10
AC-20	10.7709	-3.6017	13.03
AC-30	10.6316	-3.5418	42.67
AC-40	10.5338	-3.5104	23.01
PEN40-50	10.5254	-3.5047	32.87
PEN60-70	10.6508	-3.5537	21.95
PEN85-100	10.8232	-3.6210	12.86
PEN120-150	11.0897	-3.7252	5.66
PEN200-300	11.8107	-4.0068	0.74

Source: *Fugro and ASU 2004.*

Figures 11 through 16 show histograms of the variables in the LTPP data that were categorized into traffic factors, HMA surface, binder course, granular base, granular subbase, and subgrade. It can be seen that some variables, such as effective binder content and unit weight, exhibit a pattern of normal distribution; however the distributions of a lot of input variables can hardly be identified.

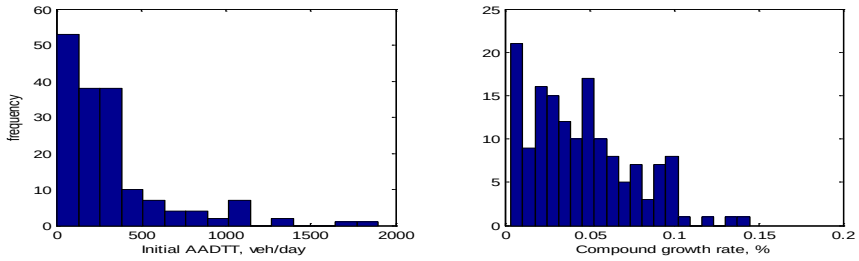

Figure 11 Histograms of traffic factors.

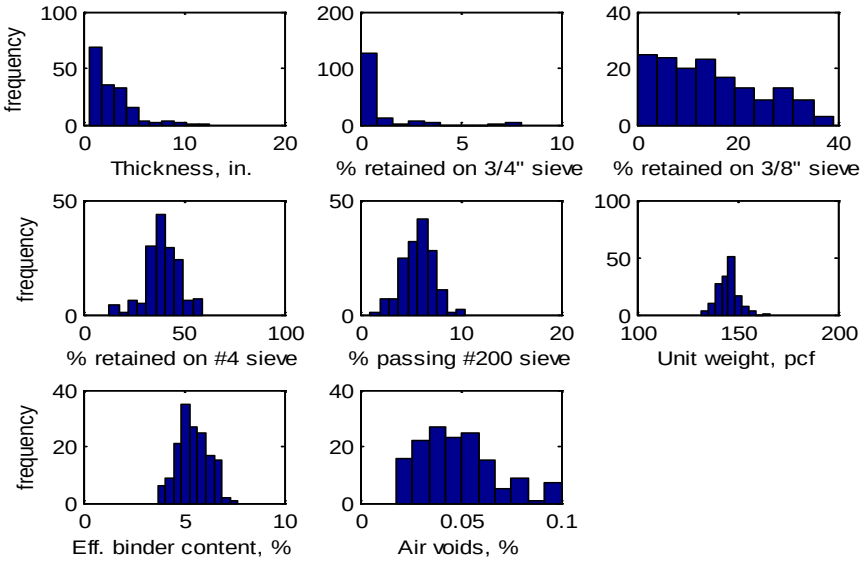

Figure 12 Histograms of HMA surface properties.

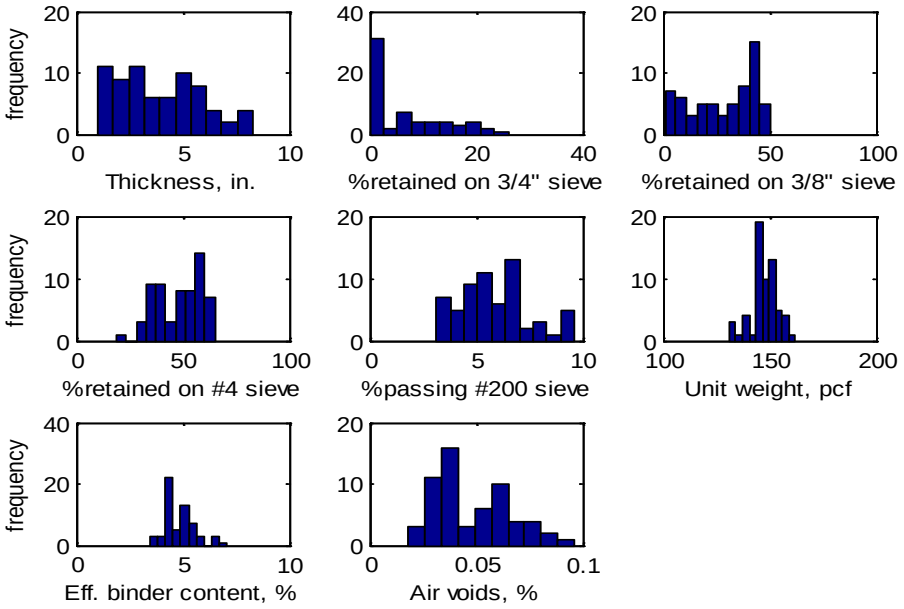

Figure 13 Histograms of binder course properties.

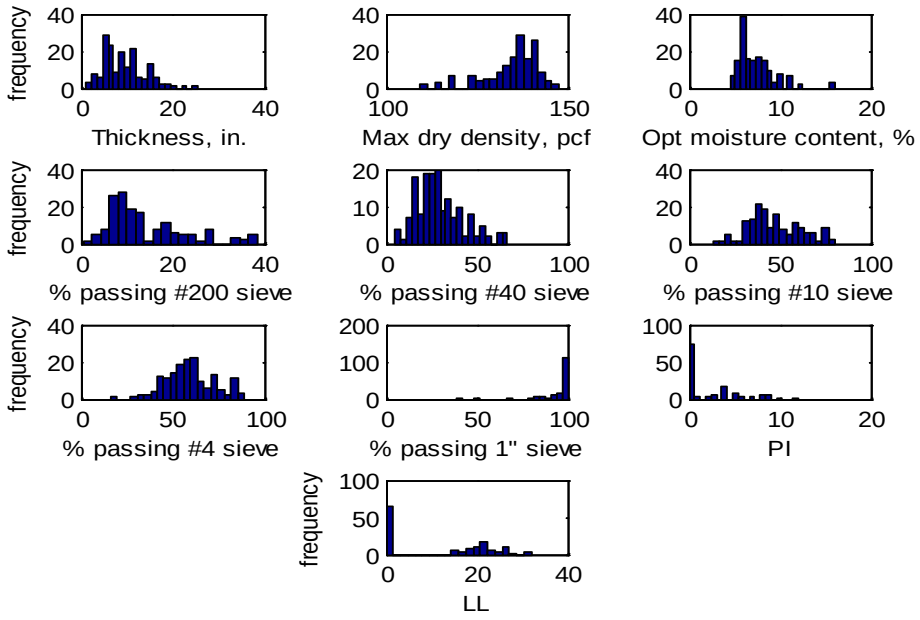

Figure 14 Histograms of base properties.

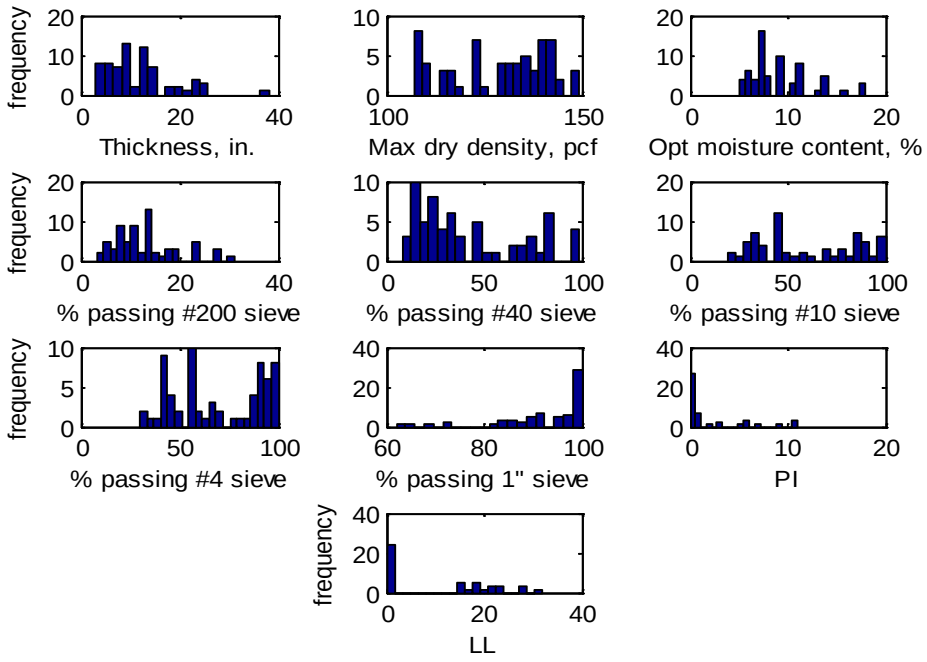

Figure 15 Histograms of subbase properties.

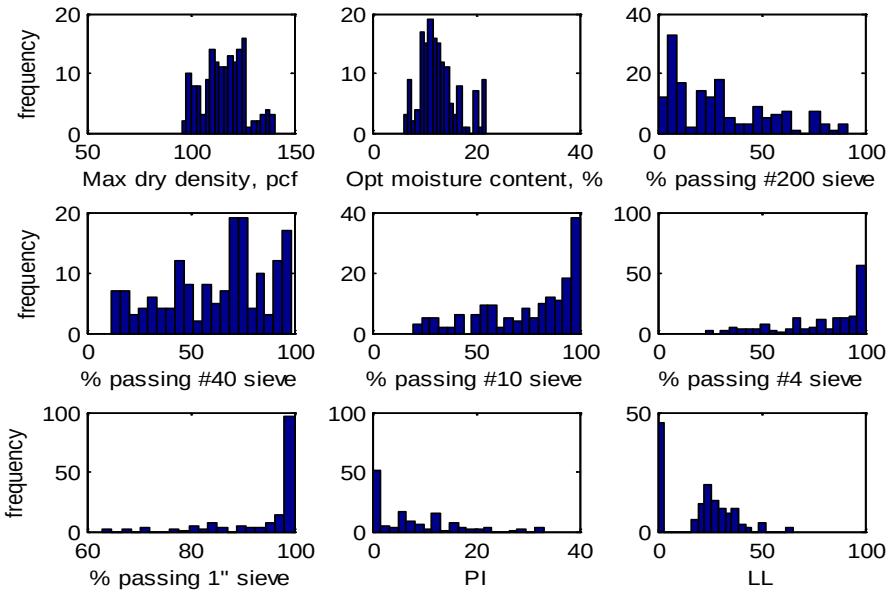

Figure 16 Histograms of subgrade properties.

CHAPTER IV

DEVELOPMENT OF IRI PREDICTION MODEL FOR HMA PAVEMENT TREATED WITH THIN HMA OVERLAYS

OVERVIEW

This chapter describes the development of IRI prediction model for HMA pavement treated with thin HMA overlays. As discussed earlier, this model consists of two tightly-coupled components. The first component is used to predict the IRI of the existing (i.e., original) pavement. The second component is used to predict the reduction in IRI induced by application of the thin HMA overlay. The development of these two components of the model is discussed in this chapter.

DEVELOPMENT OF IRI PREDICTION MODEL FOR EXISTING HMA PAVEMENT

This component of the model consists of ANNs that mimic the IRI prediction model used in the MEPDG. To develop these ANNs, thousands of HMA pavement design cases were generated based on the LTPP dataset using the Latin hypercube sampling (LHS) technique. MEPDG was then used to predict IRI for these design cases. Finally, ANNs were developed to relate IRI to the input parameters of these design cases.

Generation of Input and Output Dataset for MEPDG IRI Prediction Model

The MEPDG input variables for thousands of simulated designs were drawn from probability density functions that represent the LTPP histograms (i.e., Figures 11 through 16 discussed earlier) using the LHS technique. The MEPDG default values were

used for other inputs (such as the vehicle classification distribution and monthly adjustment factors) that are not available in the LTPP data set. The asphalt binder for HMA layers in each case were randomly generated from the 11 types listed in Table 6.

LHS is widely used in engineering studies, especially sensitivity analysis of complex models (Kleijnen 1997; Mrawira et al. 1999; Orobio and Zaniewski 2011). LHS is a stratified random procedure which provides an efficient way of sampling variables from their distributions (Iman and Canover 1980). In LHS, probability distributions of the input variables are prescribed first. Then the cumulative distribution for each variable is divided into equiprobable intervals. A value is selected randomly from each interval and placed in a Latin square, (see Figure 17).

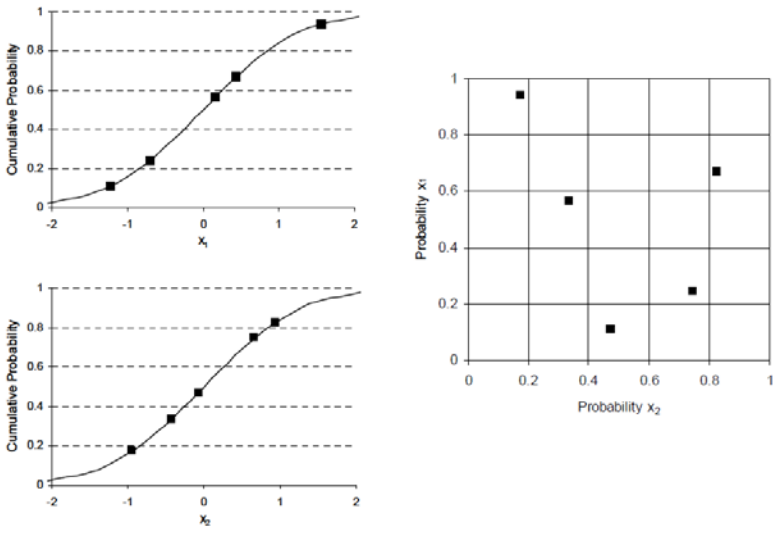

Figure 17 Example of LHS: a) Random stratified sampling of variables x1 and x2 at five intervals (left); and b) Random pairing of sampled x1 and x2 forming a Latin hypercube (right).

The LHS sample sizes included 600 design cases for Layout-1, 700 for Layout-2, 700 for Layout-3, and 1000 for Layout-4. The summary statistics of the input variables used in the LHS data generation process are provided in Table A-1 of the Appendix.

The input values for the simulated design cases were input into MEPDG in a batch mode. and simulations were ran for every pavement layout. As each case consisted of a large number of input variables, manual input was very time-consuming, and may result in input errors. To facilitate this process, a script was written using AutoIt, which read the inputs row by row from the spreadsheet that contained the simulation data, called the MEPDG application into the design environment, and wrote each input variable in the corresponding place in MEPDG. Each run of the MEPDG simulation took about 20 to 40 minutes, depending on the complexity of pavement structure. Another script was written using Matlab to automatically extract the input values and IRI predictions into a summary spreadsheet for developing the ANNs that mimic the MEPDG IRI model.

ANNs Models for Predicting IRI of Existing Pavement

One ANN was developed for each one of the four pavement layouts using the final dataset of inputs and outputs of the MEPDG IRI prediction model. Recap that 600 simulations were performed for Layout-1, 700 for Layout-2, 700 for Layout-3, and 1000 for Layout-4. In all the simulations, a 30-year analysis period was used. This resulted in a total of 30*n patterns in the ANN dataset for each pavement layout. For example, in the Layout-1 data, each simulation resulted in 30 patterns, with each pattern consisting

of the same pavement layer properties and climate conditions but a different age value. As a result, the total number of patterns for Layout-1 equaled 18,000 (i.e., 30*600).

Development of these ANNs for existing pavements was conducted using the Neural Network Toolbox incorporated in the Matlab R2012b. This toolbox offers a user-friendly interface and allows the user to easily adjust the parameters and functions that define the ANNs when necessary.

Before training the ANNs, the data was randomly divided into three subsets. The first subset was the training set, used for computing the gradient and updating the network weights and biases. The second subset was the validation set. The error on the validation set was monitored during the training process. The network weights and biases were maintained at the minimum of the validation set error. The test subset error was not used during training, but used for comparing different models. In this study, 70% of the data was used for training purpose and 15% of the data was used for validation and testing purposes, respectively.

At the very beginning of the training process, the input and target values in the raw data were scaled through data transformation to fall within a specified range, usually [-1, 1]. The primary purpose of data transformation was to modify the distribution of the input variables so that they could better match the distribution of the predicted distribution (Shi 2000). When the dataset was transferred between [-1, 1], a small change in a normalized input within the range would have a greater influence on the output, making the training of the ANN become faster (Nourani and Sayyah Fard 2012).

In the Matlab environment, the data transformation process was carried out using the "*mapminmax*" function, as follows:

$$x' = \frac{(y_{\max} - y_{\min})(x - x_{\min})}{(x_{\max} - x_{\min})} + y_{\min} \qquad \text{(Eq. 5)}$$

where *x'* is the input value after transformation, y_{max} is the upper bound of the normalized interval (i.e., 1), y_{min} is the lower bound of the normalized interval (i.e., -1), *x* is the original input value, x_{max} is the maximum value in the data set corresponding to the input neuron, and x_{min} is the minimum value in the data set corresponding to the input neuron.

Similar to the regular regression process, the objective of ANNs modeling is to attain a set of weight matrices, which represent the underlying knowledge from the sample data after many iterations of training. Before the modeling process, the architecture of the IRI ANNs was not available to or known by the researcher, thus they were selected based on a decision-making process. This process involved determining the number of layers in the network, the number of neurons in the hidden layer, and the variables that were included in the input layer. Selection of the variables used in the input layer was based on the literature and data availability in the LTPP database. When this process was finished, the patterns contained in the data set were trained, validated, and tested.

Figure 18 displays the architecture of a typical *30-15-1* network used for Layout-1. This ANNs had 30 input neurons, 15 neurons in the hidden layer, and one output neuron. The activation function was "*tansig*" for the hidden neurons and "*satlins*' for

the output neuron. Similar configurations were used for developing ANNs for the other three pavement layouts, with a different number of neurons in the input and hidden layers.

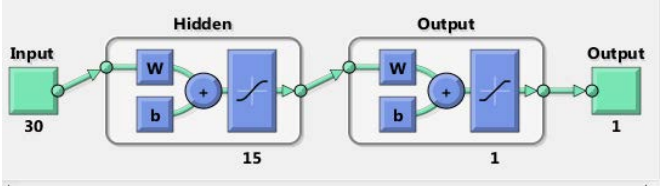

Figure 18 A typical 30-15-1 ANN for Layout-1.

The algorithms for the "*tansig*" and "*satlins*" transfer functions were as follows (Beale et al. 2012):

$$\text{tan sig}: \quad f(y) = \frac{2}{1+e^{-2y}} - 1$$

$$\text{satlins}: \quad f(y) = \begin{cases} -1, & \text{if } y \le -1 \\ y, & \text{if } -1 < y < 1 \\ 1, & \text{if } y \ge 1 \end{cases} \qquad \text{(Eq. 6)}$$

where y is the input to the neuron, and $f(y)$ is the output of the neuron.

Two forms of performance prediction accuracy measures were used for evaluating the ANNs for IRI prediction. The first measure was the coefficient of determination (R^2) and the second was the root of mean square error (RMSE). The R^2 is calculated using the following equation:

$$R^2 = 1 - \frac{\sum \left(IRI_{act} - IRI_{pred} \right)^2}{\sum \left(IRI_{act} - IRI_{avg} \right)^2} \qquad \text{(Eq. 7)}$$

where IRI_{act} is the actual IRI values, IRI_{pred} is the predicted IRI values using ANNs, and IRI_{avg} is the average IRI value. The RMSE is mathematically expressed as follows:

$$RMSE = \sqrt{\frac{\sum_{i=1}^{n}\left(IRI_{act,i} - IRI_{pred,i}\right)^2}{n}} \quad \text{(Eq. 8)}$$

where n is the total number of patterns in the sample data. The closer the *RMSE* to 0 and the closer the R^2 to 1, the more accurate the ANN would be.

ANNs Modeling Results for IRI

The ANNs and fitting statistics for the four pavement layouts are summarized in Table 9. The modeling results indicated that when more neurons were used in the hidden layer, the training process usually took a longer time to reach acceptable accuracy (i.e., MSE gradient magnitude < 10^{-5} or the no. of validation iterations > 6). The R^2 tended to be higher when more neurons were used in the hidden layer. Generally, the R^2 for the training subset was slightly higher than that for the validation and testing subsets in all the ANNs architectures. When the developed ANNs were used for making IRI predictions on the test subsets, which were not used in the network development, the R^2 values were very high (greater than 0.95), indicating adequate generalization of the ANNs. There was also a tendency that the RMSE values of these ANNs became lower when more hidden neurons were used, but it was also observed that when the number of hidden neurons reached 15, the reduction in RMSE became very insignificant. Therefore, it was concluded that 15 hidden neurons were adequately enough for the IRI ANNs for all four pavement layouts.

Based on Table 7, ANNs architectures 30-15-1, 39-15-1, 32-15-1, and 47-15-1 were selected for pavement layouts 1 through 4, respectively. The input variables included in the ANNs of layouts 1 through 4 are presented in Table 8. Plasticity index and liquid limit values were not included for the Layout-3, because of insufficient data points in the LTPP database. Detailed information about these ANNs and their computer programming code are provided in the appendix of this dissertation.

Table 7 Summary Statistics of the ANNs of Layouts 1 to 4

Layout	ANN Architecture	# of Iterations	Training Time (min)	Training		Validation		Testing	
				R^2	RMSE (in/mile)	R^2	RMSE (in/mile)	R^2	RMSE (in/mile)
1	30-9-1	109	3.1	0.954	7.91	0.951	8.43	0.95	8.41
	30-11-1	333	18.3	0.961	6.84	0.958	7.43	0.956	7.62
	30-13-1	136	16.3	0.965	6.12	0.963	6.57	0.961	6.55
	30-15-1*	248	29.3	0.967	5.48	0.965	6.02	0.963	6.16
	30-17-1	265	35.7	0.964	5.54	0.97	7.05	0.961	6.76
	30-19-1	176	34	0.972	5.21	0.971	5.39	0.961	5.44
2	39-9-1	312	20.3	0.99	3.54	0.99	3.64	0.989	3.6
	39-11-1	675	22.4	0.989	3.71	0.988	3.78	0.989	3.77
	39-13-1	210	27.2	0.996	2.38	0.995	2.46	0.995	2.53
	39-15-1*	758	29.3	0.996	2.18	0.995	2.56	0.995	2.43
	39-17-1	447	37.8	0.997	2.17	0.996	2.36	0.996	2.38
	39-19-1	127	39.4	0.998	2.11	0.997	1.87	0.997	1.87
3	32-9-1	327	15.9	0.957	10.34	0.954	10.59	0.956	10.97
	32-11-1	223	22.7	0.98	7.13	0.977	7.28	0.978	7.58
	32-13-1	304	27.5	0.98	7.33	0.979	7.06	0.98	7.2
	32-15-1*	124	14.7	0.987	5.70	0.981	6.01	0.982	6.21
	32-17-1	137	20.2	0.988	5.67	0.983	5.97	0.981	6.25
	32-19-1	287	52.8	0.989	5.65	0.985	5.96	0.985	6.11
4	47-9-1	1000	181.4	0.988	3.87	0.987	4.02	0.987	3.96
	47-11-1	1000	180.8	0.976	5.28	0.977	5.49	0.976	5.43
	47-13-1	478	90.9	0.994	2.77	0.993	2.96	0.993	2.9
	47-15-1*	770	216.1	0.994	2.7	0.993	2.89	0.994	2.79
	47-17-1	219	83.7	0.99	3.6	0.989	3.79	0.988	3.81
	47-19-1	358	211	0.993	2.8	0.994	2.93	0.993	2.97

***** *indicates the corresponding ANN was selected as the final model for that layout.*

Table 8 Input Variables Used in the ANNs of Layouts 1 to 4

Categories	Input Variables	Pavement Layout			
		1	2	3	4
Site Factors	Average air temperature, °F	√	√	√	√
	Annual rainfall, in	√	√	√	√
	Freeze index, °F-days	√	√	√	√
	Initial two-way AADTT, *veh*/day	√	√	√	√
	Compound growth rate, %	√	√	√	√
HMA Surface Layer	Thickness, in	√	√	√	√
	Effective asphalt content, %	√	√	√	√
	Air voids, %	√	√	√	√
	Unit weight, pcf	√	√	√	√
	Cumulative % retained 3/4" sieve	√	√	√	√
	Cumulative % retained 3/8" sieve	√	√	√	√
	Cumulative % retained #4 sieve	√	√	√	√
	% passing #200 sieve	√	√	√	√
	Asphalt Viscosity (10^6 Poise)	√	√	√	√
Binder Course	Thickness, in	×	√	×	√
	Effective asphalt content, %	×	√	×	√
	Air voids, %	×	√	×	√
	Unit weight, pcf	×	√	×	√
	Cumulative % retained 3/4" sieve	×	√	×	√
	Cumulative % retained 3/8" sieve	×	√	×	√
	Cumulative % retained #4 sieve	×	√	×	√
	% passing #200 sieve	×	√	×	√
	Asphalt Viscosity (10^6 Poise)	×	√	×	√
Granular Base	Thickness, in	√	√	√	√
	Plasticity index	√	√	×	√
	Liquid limit	√	√	×	√
	% passing #200 sieve	√	√	√	√
	% passing #40 sieve	√	√	√	√
	% passing #4 sieve	√	√	√	√
	Max dry unit weight, pcf	√	√	√	√
	Optimum moisture content, %	√	√	√	√
Granular Subbase	Thickness, in	×	×	√	√
	Plasticity index	×	×	×	√
	Liquid limit	×	×	×	√
	% passing #200 sieve	×	×	√	√
	% passing #40 sieve	×	×	√	√
	% passing #4 sieve	×	×	√	√
	Max dry unit weight, pcf	×	×	√	√
	Optimum moisture content, %	×	×	√	√
Subgrade	Plasticity index	√	√	×	√
	Liquid limit	√	√	×	√
	% passing #200 sieve	√	√	√	√
	% passing #40 sieve	√	√	√	√
	% passing #4 sieve	√	√	√	√
	Max dry unit weight, pcf	√	√	√	√
	Optimum moisture content, %	√	√	√	√

Figure 19 shows the IRI predicted using ANNs against the IRI predicted using the MEPDG for the training, validation, and testing subsets in layouts 1 through 4. The strong correlation between the MEPDG predictions and the ANN predictions is evident in these charts, suggesting that these ANNs can substitute the MEPDG IRI model for the four pavement design layouts considered in this research.

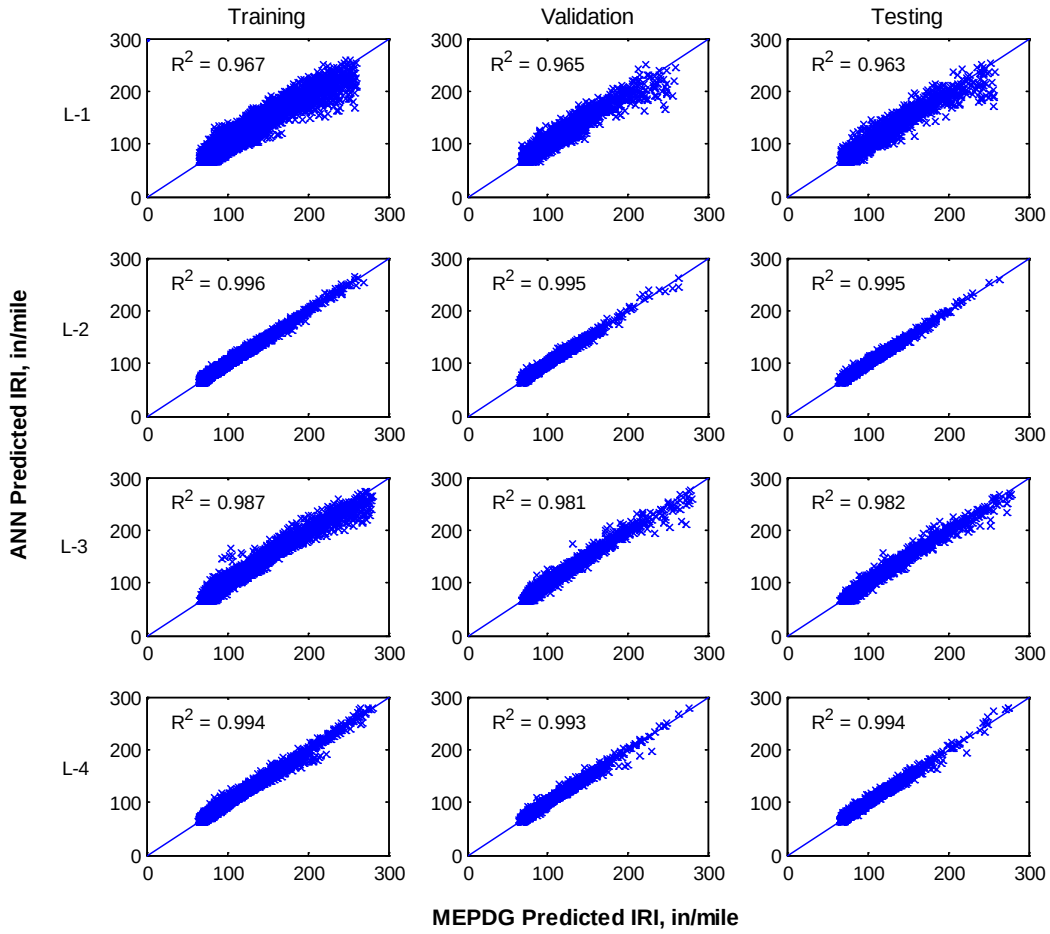

Figure 19 ANN predictions vs. MEPDG simulation data for three subsets: training, validation, and testing.

ANNs Checking with LTPP Data

In this section, the IRI predictions using the ANNs were compared to the measured IRI values recorded in the LTPP dataset for the year prior to or the year in which the thin overlay was placed. The results are shown in Figure 20. The R-square values for these comparisons range from 0.6 to 0.72, indicating reasonable predicative capability of the ANNs when they are used for predicting IRI on actual LTPP test sections.

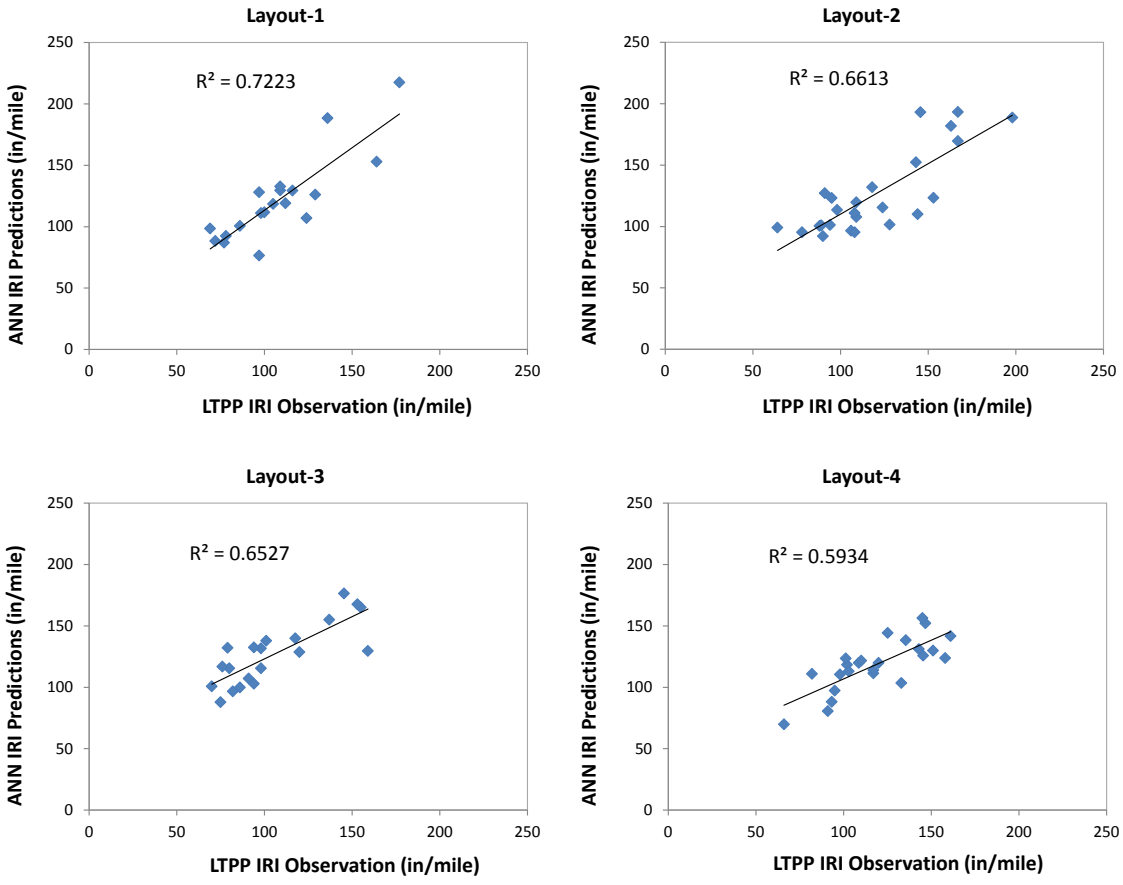

Figure 20 ANN Predictions versus actual IRI observations in the LTPP database.

Calibration of ANNs

The use of ANNs for predicting the IRI of some LTPP test sections showed adequate accuracy as shown in Figure 20; however in order to be used in practical cases (i.e., predicting IRI development of existing HMA pavements), calibration of the developed ANNs using local pavement and performance measurement data is needed. A good sample of such data is the LTPP database that consists of both pavement design information and field performance measurement. Other resources include pavement management system (PMS) database administered by state highway agencies.

The calibration process can be done by following a few steps. First, a dataset that consists of actual pavement data and field IRI measurement should be prepared. Then it can be used solely as the calibration sub-dataset or aggregated with the calibration sub-dataset from the MEPDG simulation data for calibration purposes. Eventually, the final ANN is developed by adapting its weight matrix so that the IRI predictions using the ANN are closer to actual field observations.

This calibration mechanism is displayed in Figure 21. For example, some field IRI measurement value at certain pavement age is available (this is the case for many of LTPP test sections, especially SPS sections). Without calibration using localized dataset, the predictions using the ANNs tend to underestimate the IRI development of this section. After a localized calibration is applied, the weight matrix of the ANNs is adapted, and the predicted IRI curve using the calibrated ANNs shifts to the side of field observations, making the predictions more realistic and much closer to field measurements.

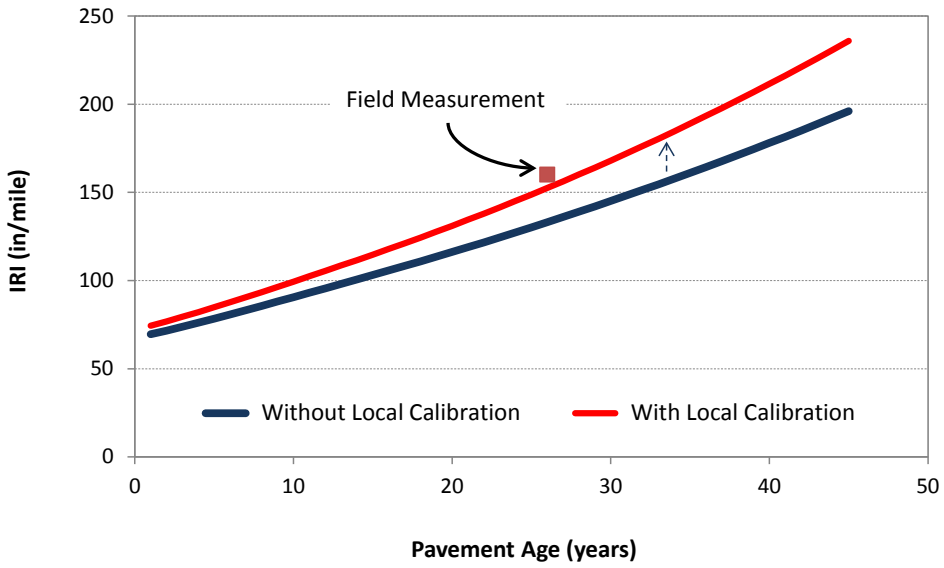

Figure 21 A demonstration of the effect of calibrating IRI ANNs using local data.

In this dissertation, this section just provides a mechanism for calibrating the IRI ANNs. Actual calibration using a certain localized pavement dataset is not the focus of this study.

Sensitivity Analysis of the ANNs

Similar to traditional regression analysis, the relative significance or contribution of each input variable to the IRI prediction can be studied through sensitivity analysis. Sensitivity analysis of the ANNs can be performed by two ways: 1) study the information stored in the weights, and 2) take the first order partial derivative between the output variable and the input variables (Nourani and Sayyah Fard 2012; Shekharan 1999). The first method (i.e., the weight method) was adopted in this study as it

involves less computation while gives similar results to the second method (i.e., the partial derivative method).

In the weight method, the output layer connection weights are partitioned into input node shares (Garson 1991). The weights along the paths from the input to the output indicate the relative predictive importance of input variables. The weights are used to partition the sum of effects on the output neuron with the following equation, using absolute values of all weights (Shekharan 1999):

$$RC = \frac{\sum_{j}^{h}\left(\frac{w_{ij}O_j}{\sum_{i}^{v} w_{ij}}\right)}{\sum_{i}^{v}\left[\sum_{j}^{h}\left(\frac{w_{ij}O_j}{\sum_{i}^{v} w_{ij}}\right)\right]} \quad \text{(Eq. 9)}$$

where *RC* is the relative contribution of each input variable, *v* is the number of input variables, *h* is the number of hidden neurons, w_{ij} is the connection weight between the *j*th hidden neuron and the *i*th input variable, and O_j is the connection weight between the output neuron and the *j*th hidden neuron. The calculated RC values range between 0 and 1. A larger RC value indicates a greater effect of the corresponding input variable on the predicted IRI.

Using Equation 6, the relative contribution of input variables to IRI prediction for all four pavement layouts was computed into percentage values, as summarized in Table 9. For each layout, the sum of RCs of all input variables equals 100%.

Table 9 Relative Contribution of Input Variables in the ANNs

Category	Variables	RC (%)			
		Layout-1	Layout-2	Layout-3	Layout-4
Site factors	Air Temperature (F)	5.9	2.1	4.2	1.9
	Rainfall (in)	2.3	3.0	1.9	2.4
	Freeze Index (F-Days)	5.2	1.2	2.1	3.0
	AADTT (veh/day)	3.6	4.9	7.4	2.2
	Traffic Growth Rate (%)	4.0	8.3	2.8	4.2
	Age (year)	4.3	5.7	5.2	5.1
HMA Surface Layer	Thickness (in)	9.0	8.8	11.2	16.3
	Effective Binder Content (%)	6.9	3.2	5.0	3.9
	Air Voids (%)	6.4	0.5	6.6	1.0
	Unit Weight (pcf)	1.5	3.1	1.8	1.6
	% Retained on ¾" Sieve	0.9	2.1	1.5	0.2
	% Retained on 3/8" Sieve	1.2	0.7	2.4	2.5
	% Retained on #4 Sieve	5.2	3.0	2.0	0.8
	% Passing #200 Sieve	2.3	2.4	2.8	0.8
	Viscosity (10^6 Poise)	2.9	1.1	1.4	0.6
Binder Course	Thickness (in)	-	5.3	-	8.3
	Effective Binder Content (%)	-	1.2	-	0.3
	Air Voids (%)	-	3.2	-	6.2
	Unit Weight (pcf)	-	3.8	-	0.6
	% Retained on ¾" Sieve	-	1.2	-	0.3
	% Retained on 3/8" Sieve	-	2.3	-	1.9
	% Retained on #4 Sieve	-	0.6	-	1.6
	% Passing #200 Sieve	-	0.7	-	0.6
	Viscosity (10^6 Poise)	-	0.4	-	1.6
Granular Base	Thickness (in)	2.1	1.4	2.5	1.3
	Plasticity Index	1.3	1.2	-	0.8
	Liquid Limit	1.8	0.5	-	0.7
	% Passing #200 Sieve	2.3	1.5	2.8	2.2
	% Passing #40 Sieve	1.7	2.6	2.9	1.9
	% Passing #4 Sieve	4.7	2.8	2.8	1.7
	Max Dry Unit Weight (pcf)	3.2	2.6	2.0	2.6
	Optimum Moisture Content (%)	4.9	4.4	4.4	0.9
Granular Subbase	Thickness (in)	-	-	2.0	0.7
	Plasticity Index	-	-	-	1.7
	Liquid Limit	-	-	-	1.8
	% Passing #200 Sieve	-	-	2.8	0.2
	% Passing #40 Sieve	-	-	2.4	0.9
	% Passing #4 Sieve	-	-	2.4	0.6
	Max Dry Unit Weight (pcf)	-	-	2.7	1.1
	Optimum Moisture Content (%)	-	-	1.3	1.6
Subgrade	Plasticity Index	1.8	2.0	-	1.7
	Liquid Limit	2.3	1.8	-	1.3
	% Passing #200 Sieve	3.2	2.1	2.4	1.2
	% Passing #40 Sieve	1.5	1.0	2.2	2.6
	% Passing #4 Sieve	3.0	5.0	2.1	1.8
	Max Dry Unit Weight (pcf)	1.7	0.4	1.9	0.5
	Optimum Moisture Content (%)	2.6	1.9	2.1	2.1

For all layouts, the thickness of HMA surface layer had the largest RC value, and site factors, such as temperature and traffic factors, played an important role in IRI predictions. When a binder course was present in the pavement structure, its thickness also became a significant factor, as evidenced by 5.3% and 8.3% RC values for layouts 2 and 3, respectively. However, the relative contribution of some factors, such as air voids of the HMA surface layer, exhibited significant variation among different layouts by dropping from more than 6% (i.e., in layouts 1 and 3) to less than 1% (i.e., in layouts 2 and 4). The cause of this phenomenon might be due to the inclusion of a binder course in the pavement design. It can be seen that in layouts 2 and 4, air voids in the binder course layer had relatively larger RCs than those of the HMA surface layer.

It can also be seen that the RCs of the input variables from granular layers and subgrade hardly exceeded 4%, in contrast to site factors and HMA layer properties. This is an indication that, in terms of predicting IRI by simulating the MEPDG, the HMA layer properties (such as thickness, asphalt binder content, and air voids) and site conditions played a more important role than the material properties of the underlying granular layers and subgrade. Table 9 also shows that no variable had very low RC values in all the ANNs, thus no input variable was removed from the model.

DEVELOPMENT OF A BAYESIAN MODEL FOR PREDICTING REDUCTION IN IRI DUE TO TREATMENT

Introduction

This section discusses the development of the second component of post-treatment performance prediction models. Instead of predicting in the form of a single value for the response variable, Bayesian regression models generate probability distributions for the response variable (i.e., IRI reduction in this study), which is more in line with commonsense interpretations (Congdon 2001).

In Bayesian regression, uncertainty in the model parameters is expressed as probabilities, through Bayesian theorem. Bayesian theorem combines prior knowledge of certain event probabilities with observed data (likelihood) in order to produce an adjusted expression of the event probabilistic distribution, called the posterior, which can be expressed as follows:

$$P(\theta \mid x) = \frac{P(x \mid \theta) P(\theta)}{\int P(x \mid \theta) P(\theta) d\theta} \quad \text{(Eq. 10)}$$

where $P(\theta \mid x)$ denotes the posterior probability beliefs about the parameter θ given the data *x*, $P(x \mid \theta)$ is the likelihood of the data given the parameter θ, and $P(\theta)$ is the prior beliefs about the parameter. Therefore, the learning process in Bayesian inference is one of modifying one's initial probability statements about the predicted parameter prior to observing the data to updated or posterior knowledge incorporating both prior knowledge and the data in hand (Congdon 2001).

Bayesian regression is similar to traditional regression in the sense that a functional form (equation) relates a response to explanatory factors. However, Bayesian regression embeds the equation as the mean of a probabilistic distribution of the predictions and incorporates the precision (inverse of the variance) to capture uncertainty (Amador and Mrawira 2012). The Bayesian analysis begins by defining each of the model terms and their functional relation in a multivariate regression model.

Recap from Equation #2 that the IRI reduction due to thin HMA overlay was modeled as a function of acceptance quality characteristics (AQCs), site conditions, and treatment age. Therefore, the Bayesian linear models developed in this research have the following form:

$$\log(\Delta IRI) = \beta_0 + \sum_{i=1}^{l} \beta_i * AQC_i + \sum_{j=1}^{m} \beta_j * SF_j + \beta_{l+m+1} Age + \varepsilon \qquad \text{(Eq. 11)}$$

where ΔIRI is reduction in IRI due to treatment (thin HMA overlay in this case), β is parameter coefficients, *SF* is site factors (e.g., annual average daily truck traffic and rainfall), *Age* is treatment age, ε is error item [subject to a normal distribution $N(0, \sigma^2 I)$], *l* is the number of AQCs, and *m* is the number of site factors considered in the regression. The natural logarithm of ΔIRI is used as the response variable to avoid predicted reduction in IRI from being negative values.

The major interest in Bayesian regression focuses on updating prior knowledge about parameters with the data in hand, and then drawing samples from the posterior density of the regression parameters to assess whether the effects of all or particular

predictors on the response variable is significant. Suppose the *ΔIRI* Bayesian model has the following simplified form:

$$Y = X\beta + \varepsilon \qquad \text{(Eq. 12)}$$

where Y is performance vector ($n \times 1$), X is the input data matrix ($n \times p$), β is the regression coefficients, ε is error item ~ $N(0, \sigma^2 I)$, n is the number of observations, and p is the number of predictors.

As no information currently exists about the values, ranges, or densities of the predictors of *ΔIRI*, noninformative priors were used in this research, as suggested by Hoff (2009) and Congdon (2011). The main idea in using noninformative priors was that if the prior distribution cannot represent real prior information about the parameters, then it should be as minimally informative as possible. The resulting posterior distribution would then represent the posterior information of someone who begins with little knowledge of the population being studied.

Let the precision term, $\tau = 1/\sigma^2$, and suppose that τ is unknown and so to be considered a variable parameter along with β. One of the commonly used noninformative priors is as follows:

$$p(\beta, \tau) \propto \tau^{-1} \qquad \text{(Eq. 13)}$$

It is used so that the log of σ^2 is essentially uniform on $(-\infty, \infty)$ (Congdon 2001). The corresponding joint posterior distribution is then expressed as

$$\pi(\beta,\tau \mid y) \propto \tau^{(n+1)/2} \exp\left[-(n-p)s^2\tau/2\right] \exp\left[-\frac{\tau}{2}(\beta-\hat{\beta})X'X(\beta-\hat{\beta})\right] \quad \text{(Eq. 14)}$$

From the second term in the above equation, the posterior distribution of β can be seen to be a multivariate normal distribution conditional on $\hat{\beta}$ and τ as

$$\beta \mid \hat{\beta},\tau \sim N\left(\hat{\beta},\tau^{-1}\left(X^T X\right)^{-1}\right) \quad \text{(Eq. 15)}$$

where $\hat{\beta}$ is the ordinary least squares estimate of β and can be calculated as $\hat{\beta} = \left(X^T X\right)^{-1} X^T y$.

The posterior distribution of τ follows a scaled chi-square distribution as

$$\tau \mid y \sim \chi^2\left(v, s^2\right) \quad \text{(Eq. 16)}$$

where v is the degrees of freedom ($n - p$), and s^2 is the standard estimate of the residual variance and calculated as $s^2 = \left(Y - X\hat{\beta}\right)\left(Y - X\hat{\beta}\right)/(n-p)$.

This research used the GENMOD procedure in SAS (Statistical Analysis System) for developing Bayesian linear models for the four pavement layouts. This procedure can conduct a Bayesian analysis of the regression model by using Gibbs sampling (SAS OnlineDoc). Gibbs sampling is a Markov Chain Monte Carlo (MCMC) algorithm for sampling from a specified multivariate probability distribution when direct sampling is difficult due to the complexity of model, which is the case in this research as each *ΔIRI* model may include 10 or more predictors. This method is widely used in statistical studies (Hoff 2009).

The Gibbs sampling method draws samples from each parameter in the posterior density, while regarding all other parameters as fixed. Thus, it requires the joint posterior distribution decomposed into full conditional distributions for each parameter in the model and then it samples from them. Given full conditional distributions $p(\beta|\tau,Y)$ and $p(\tau|\beta,Y)$ and assuming the current state of the parameters at iteration t, the sampling procedures in this method can be briefly described as follows (Hoff 2009):

1. Sample $\beta^{(t+1)} \sim p(\beta|\tau^{(t)},Y)$;
2. Sample $\tau^{(t+1)} \sim p(\tau|\beta^{(t+1)},Y)$;
3. Sampled parameters at iteration $t + 1 = \{\beta^{(t+1)}, \tau^{(t+1)}\}$.

The GENMOD procedure used noninformative uniform priors by default. The number of burn-in iterations before the Gibbs sampling chains were saved was 2,000. Additional 10,000 iterations were generated after the burn-in, which produced the posterior distributions of the parameters and the predictive model for *ΔIRI*. Trace, autocorrelation, and density plots for each model parameters, were generated for diagnosing where the chain of posterior samples has converged. Figure 22 shows some sample diagnostic plots for a variable, which indicate an excellent evidence of convergence and also shows that the posterior distribution of the parameter approximately follows normal distribution. The Bayesian analysis outputs include the posterior estimates (mean and standard deviation) and 95% highest posterior density (HPD) regions. The 95% HPD region represents a subset C of coefficient values such that $P(\beta \in C \mid Y) \geq 5\%$, given that the volume of C is as small as possible.

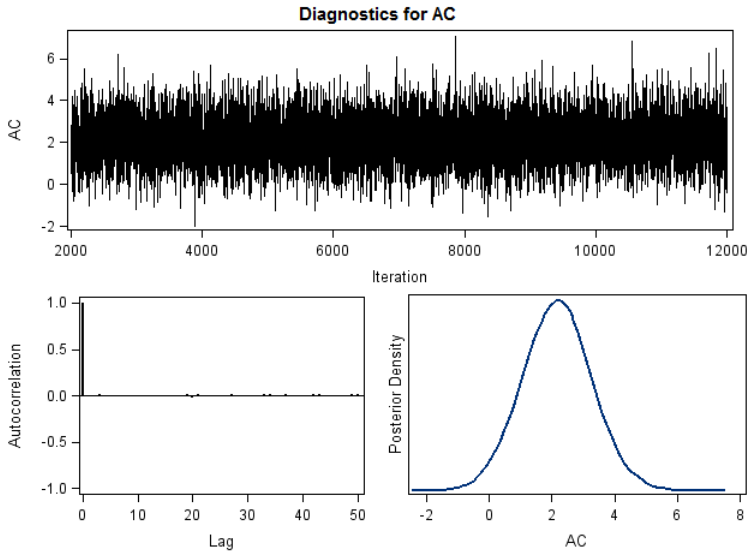

Figure 22 Sample diagnostic plots for the asphalt content (AC) variable.

Fitness Assessment of Bayesian Models

After the Bayesian models were developed, next important step was to assess their goodness of fit through some performance measures. Some measures for this purpose included the deviance information criterion (DIC), predictive concordance (PC), and Bayesian p-values.

Deviance Information Criterion

DIC is used as a model assessment measure. A smaller DIC indicates a better fit to the data set. Since DIC increases with model complexity, a simpler model is preferred. DIC can be compared across different models as long as the predictors do not change between models. As a rule of thumb, if two models differ in DIC by more than three, the one with the smaller DIC is considered better fitting (Spiegelhalter et al. 2002).

Letting β be the parameters of the model, the deviance information formula is

$$DIC = \overline{D(\beta)} + p_D \qquad \text{(Eq. 17)}$$

where $D(\beta)$ is the deviance, defined as $D(\beta) = 2\left(\log\left(f(y)\right) - \log\left(p(y \mid \beta)\right)\right)$, $f(y)$ is a standardizing term that is a function of the data alone, $p(y|\beta)$ is the likelihood function with the normalizing constants, $\overline{D(\beta)}$ is the posterior mean of the deviance, approximated by $\frac{1}{L}\sum_{l=1}^{L} D\left(\beta^{(l)}\right)$, in which L is the number of iterations in the sampling and $\beta^{(l)}$ is the lth iteration parameters, and p_D is the effective number of parameters, which is the difference between the posterior mean of the deviance and the deviance evaluated at the posterior mean of the parameters, expressed as $\overline{D(\beta)} - D\left(\overline{\beta}\right)$ (Neelon et al. 2010).

Predictive Concordance

The posterior predictive distribution is either the replication of y given the model (usually represented as y^{rep}), or the prediction of a new and unobserved y (usually represented as y^{new}). Gelfand (1996) suggested that any y_i that is in either 2.5% tail area of y_i^{rep} should be considered an outlier. The percentage of y_is that are not outliers is called the "predictive concordance" (PC). Gelfand (1996) suggests that the goal is to attempt to achieve 95% PC. In the case of a lower PC, say 80%, the discrepancy between the model and data is undesirable because the model does not fit the data well and many outliers have resulted. On the other hand, if the PC is too high, say 100%, the

model may have been overfitted, and it may be worth considering a more parsimonious model (Statisticat LLC 2013).

Bayesian P-Values

A Bayesian form of p-value can be estimated with a variety of test statistics (Gelman et al. 1996). For instance, the minimum or maximum observed y is compared to the minimum or maximum y^{rep} from posterior predictive prediction. The Bayesian p-value is to report the discrepancy between y and y^{rep}.

In this research, the Bayesian p-value is estimated based on a discrepancy statistic suggested by Link and Barker (2010). The following steps describe how to estimate the Bayesian p-values. Let y_i (i = 1, 2, …, n) denote the ith observation in data, and $y_i^{(h)}$ denote the expected value computed for each set of parameters based on the hth draw (h=1, 2, …, M) for a chain of length M. Note that n is the sample size, and M is the number of MCMC draws. The values T_1^{obs}, …, T_M^{obs}, are obtained using

$$T_h^{obs} = \sum_{i=1}^{N} \frac{\left(y_i - y_i^{(h)}\right)^2}{y_i^{(h)}} \qquad \text{(Eq. 18)}$$

Another set of values T_1^{rep}, …, T_M^{rep}, are obtained using

$$T_h^{rep} = \sum_{i=1}^{N} \frac{\left(y_i^{rep} - y_i^{(h)}\right)^2}{y_i^{(h)}} \qquad \text{(Eq. 19)}$$

where y_i^{rep} is the ith draw from the posterior predictive distribution for y_i.

The Bayesian p-value is estimated by the proportion of $T^{rep} > T^{obs}$ for all M cases. A plot of T^{rep} versus T^{obs} can be draw to graphically illustrate the calculation of Bayesian p-values. A Bayesian p-value close to 0.5 represents good model fit, and p-values near 0

or 1 indicate lack of fit. Generally, p-values between 0.2 and 0.8 represent adequate fit (Neelon et al. 2013). Figure 23 shows a sample scatterplot. The Bayesian p-value is estimated by the proportion of points above the equality line. In this sample, the p-value is 0.284.

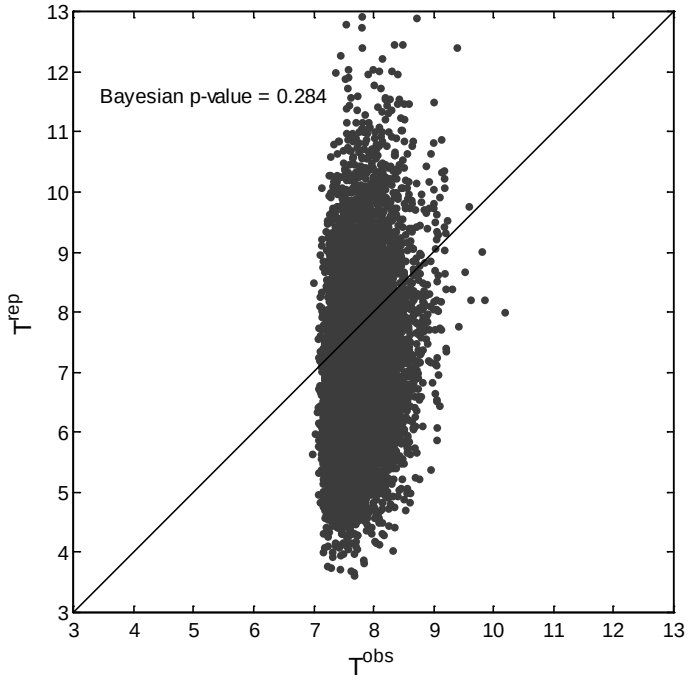

Figure 23 A sample scatterplot of predictive T^{rep} versus observed T^{obs}.

Data Used for Development of Bayesian Linear Models

The data used for developing the Bayesian linear models was prepared from 88 LTPP test sections that had received thin HMA overlay treatments and had complete data about the existing pavement layers. For these sections, IRI progression in the original pavement over a certain analysis period was predicted using the ANNs

previously developed in this research. The observed post-treatment IRI values over several years were deducted from the predicted IRI values in the original pavement in the same post-treatment years (refer to Figure 6) to obtain the reduction in IRI (*ΔIRI*) values at different ages of the thin HMA overly treatment.

Information about the quality characteristics in thin HMA overlay treatments and site factors were collected from the LTPP data. This information along with treatment age and *ΔIRI* values was formed into a data set for the Bayesian regression process. In the final regression data set, 19 test sections were included for Layout-1, 25 for Layout-2, 20 for Layout-3, and 24 for Layout-4. The thin HMA overlay acceptance quality characteristics (AQCs) considered in Bayesian regression included the following:

- Overlay thickness
- Asphalt content
- Percent air voids in laboratory-molded HMA mix
- % aggregate passing #8 sieve
- % aggregate passing #200 sieve
- Initial IRI (immediately measured after overlay placement)

These items were selected because they are used as quality measures in current specifications for thin HMA overlays by some states (i.e., Florida, Kansas, Michigan, and Texas) (NCHRP 2011). The site factors included annual average air temperature, average annual rainfall, freezing index, and average annual daily truck traffic. Unit weight of HMA mix, which is the weight of a specific volume of HMA mix, was also used as an independent variable in the regression model to characterize the HMA mix.

In additional to these input variables, second-order terms, such as the interactive effects between some of these variables (e.g., asphalt content, air voids, thickness, and unit weight) and the quadratic terms of asphalt content and air voids, were also considered in the modeling process to account for nonlinear relationships. As previously mentioned, the logarithm of *ΔIRI* was used as response variable to avoid producing negative values for the response variable. Table 10 summarizes the acronyms of all the variables and some of their applicable ranges based on the data used for modeling. Application of the Bayesian regression models outside these ranges should be performed with caution.

Table 10 Applicable Ranges of Independent Variables in the Bayesian Models

Variables	Acronym	Layout1		Layout2		Layout3		Layout4	
		Min	Max	Min	Max	Min	Max	Min	Max
Logarithm of ΔIRI	log(ΔIRI)	-	-	-	-	-	-	-	-
Temperature, (°F)	Temp	38	72	35	70	34	75	35	70
Rainfall (in.)	Rain	7	54	10	65	9	85	10	57
Freeze Index (°F-Days)	FI	0	1,150	0	1,500	40	1,500	0	1,850
AADTT (veh/day)	AADTT	100	2,900	80	2,600	80	2,200	120	1,850
Overlay Thickness (in.)	Thick	0.5	2.0	0.8	2.0	0.8	2.0	1.0	2.0
% Passing #8 Sieve	PP8	18	61	29	61	7	46	15	51
% Passing #200 Sieve	PP200	2.0	8.0	2.0	10	1.0	7.0	2.0	7.5
Asphalt Content (%)	AC	3.0	7.5	3.5	7.0	3.5	7.0	4.0	8.5
Air Voids (%)	AV	3.0	6.5	2.0	8.5	2.0	7.5	1.5	6.5
Initial IRI (in./mile)	IRI_0	55	135	60	135	60	140	55	135
Unit Weight (lb/ft^3)	UW	134	150	133	153	133	149	132	164
Treatment Age (years)	Age	1	18	1	21	1	18	1	22
Quadratic Term of AC	AC2	-	-	-	-	-	-	-	-
Quadratic Term of AV	AV2	-	-	-	-	-	-	-	-
Interaction of AC and AV	AC_AV	-	-	-	-	-	-	-	-
Interaction of Thick and UW	Thick_UW	-	-	-	-	-	-	-	-
Interaction of Rain and AC	Rain_AC	-	-	-	-	-	-	-	-
Interaction of FI and AC	FI_AC	-	-	-	-	-	-	-	-
Interaction of FI and AV	FI_AV	-	-	-	-	-	-	-	-

Before the data presented in Table 10 was used for modeling, it was first standardized (i.e., $z = (X - \mu)/\sigma$), except for treatment age, to avoid significant differentiation in the magnitudes of regression coefficients between different independent variables. As a result, the posterior distributions of regression coefficients were based on the standardized data.

Results of Bayesian Linear Regression

A variety of forms of linear models, based on inclusion of different independent variables, were fitted using the Bayesian regression method. The aforementioned performance measures were derived for these models for comparisons. An appropriate model should meet the following criteria:

- Include important AQCs;
- Outperform rival models in observance of performance measures;
- Be simpler when possible.

The model fitting statistics are summarized in Tables 11 through 14 for pavement layouts 1 through 4, respectively. The independent variables in each model are presented in the second column. The model performance measures (i.e., DIC, PC, and p-value) were used to select the most appropriate model for each layout. The last column contains RMSE (i.e., root mean squared error) values, estimated using ordinary least squares regression. Smaller RMSEs indicate better fit of the model to actual data. For each layout, the most appropriate model is marked with the ***** sign (e.g., Model #4 for layout-1), indicating best matching of the model with aforementioned criteria.

Table 11 Fitting Statistics of ΔIRI Bayesian Prediction Model for Layout-1

Model	Included Independent Variables	# of Obs	Model Performance				
			DIC	pD	PC (%)	p-value	RMSE
1	Rain FI AADTT Thick PP8 PP200 UW AC AV IRI0 Age	130	188.6	13.5	97.7	0.323	0.472
2	Rain FI AADTT Thick PP8 PP200 UW AC AC2 AV AV2 IRI0 Age		177.4	15.6	97.7	0.313	0.448
3	Rain FI AADTT PP200 UW AC AC2 AV AV2 Thick_UW Rain_AC FI_AC IRI0 Age		155.9	16.7	96.9	0.283	0.411
4*	Rain AADTT PP8 PP200 UW AC AC2 AV AV2 Thick_UW Rain_AC FI_AC FI_AV IRI0 Age		148.8	17.8	96.9	0.318	0.409
5	Rain FI AADTT Thick PP8 PP200 AC AC2 AV AV2 Thick_UW Rain_AC FI_AC FI_AV IRI0 Age		155.6	18.8	96.9	0.280	0.407
6	Rain FI AADTT Thick PP8 PP200 UW AC AC2 AV AV2 Thick_UW Rain_AC FI_AC FI_AV IRI0 Age		156.6	19.9	96.9	0.287	0.407
7	Temp Rain FI AADTT Thick PP8 PP200 UW AC AC2 AV AV2 Thick_UW Rain_AC FI_AC FI_AV IRI0 Age		157.9	20.9	96.9	0.293	0.407
8	Temp Rain FI AADTT Thick PP8 PP200 UW AC AC2 AV AV2 AC_AV Thick_UW Rain_AC FI_AC FI_AV IRI0 Age		156.4	22.0	96.9	0.298	0.403

Table 12 Fitting Statistics of ΔIRI Bayesian Prediction Model for Layout-2

Model	Included Independent Variables	# of Obs	Model Performance				
			DIC	pD	PC (%)	p-value	RMSE
1	Temp AADTT Thick PP8 UW AC AC2 AV AV2 Thick_UW IRI0 Age	146	49.4	14.6	93.2	0.313	0.266
2	Temp AADTT Thick PP8 PP200 UW AC AC2 AV AV2 Thick_UW IRI0 Age		49.0	15.6	95.2	0.33	0.266
3	Temp Rain AADTT Thick PP8 PP200 UW AC AC2 AV AV2 Thick_UW IRI0 Age		48.7	16.6	95.2	0.333	0.267
4*	Temp Rain AADTT Thick PP8 PP200 UW AC AC2 AV AV2 Thick_UW Rain_AC FI_AC IRI0 Age		47.8	18.8	95.2	0.35	0.268
5	Temp Rain AADTT Thick PP8 PP200 UW AC AC2 AV AV2 AC_AV Thick_UW Rain_AC FI_AC IRI0 Age		51.6	19.7	95.2	0.340	0.269
6	Temp Rain AADTT Thick PP8 PP200 UW AC AC2 AV AV2 AC_AV Thick_UW Rain_AC FI_AC FI_AV IRI0 Age		53.7	20.8	95.2	0.341	0.269

Table 13 Fitting Statistics of ΔIRI Bayesian Prediction Model for Layout-3

Model	Included Independent Variables	# of Obs	Model Performance				
			DIC	pD	PC (%)	p-value	RMSE
1	AADTT PP200 AC AV AV2 AC_AV Rain_AC FI_AC IRI0 Age	117	86.9	12.6	96.6	0.534	0.306
2	AADTT Thick PP8 PP200 AC AV AV2 AC_AV Rain_AC FI_AC IRI0 Age		67.8	14.7	95.7	0.495	0.307
3*	FI Thick PP8 PP200 UW AC AC2 FI_AC FI_AV IRI0 Age		59.7	13.6	97.4	0.498	0.291
4	Rain FI AADTT Thick PP200 AC AC2 AV AV2 AC_AV Thick_UW Rain_AC FI_AV IRI0 Age		71.9	17.8	97.4	0.513	0.309
5	Rain FI AADTT Thick PP8 PP200 AC AC2 AV AV2 AC_AV Thick_UW Rain_AC FI_AV IRI0 Age		69.3	18.9	96.6	0.493	0.31
6	Temp Rain FI AADTT Thick PP8 PP200 AC AC2 AV AV2 AC_AV Thick_UW Rain_AC FI_AV IRI0 Age		69.7	20	96.6	0.494	0.311
7	Temp Rain FI AADTT Thick PP8 PP200 UW AC AC2 AV AV2 AC_AV Thick_UW Rain_AC FI_AC FI_AV IRI0 Age		68.1	22.2	97.4	0.501	0.314

Table 14 Fitting Statistics of ΔIRI Bayesian Prediction Model for Layout-4

Model	Included Independent Variables	# of Obs	Model Performance				
			DIC	pD	PC (%)	p-value	RMSE
1	Temp Rain FI AADTT Thick PP8 PP200 UW AC AV IRI0 Age	245	148.7	14.4	96.7	0.358	0.317
2	Rain AADTT Thick PP8 PP200 UW AC AV Thick_UW FI_AC FI_AV IRI0 Age		152.3	15.3	97.1	0.362	0.319
3*	Rain FI AADTT Thick PP8 PP200 AC AV AV2 AC_AV Thick_UW FI_AV IRI0 Age		132.8	16.4	97.1	0.364	0.306
4	Temp Rain AADTT Thick PP8 PP200 UW AC AV Thick_UW FI_AC FI_AV IRI0 Age		152.5	16.4	96.7	0.368	0.319
5	Temp FI AADTT Thick PP8 PP200 UW AC AV Thick_UW Rain_AC FI_AC FI_AV IRI0 Age		154.6	17.4	97.1	0.359	0.319
6	Temp FI AADTT Thick PP8 PP200 UW AC AV AC_AV Thick_UW Rain_AC FI_AC FI_AV IRI0 Age		156.9	18.5	97.1	0.37	0.320
7	Temp Rain FI AADTT Thick PP8 PP200 UW AC AV AC_AV Thick_UW Rain_AC FI_AC FI_AV IRI0 Age		156.2	19.4	97.1	0.359	0.319
8	Temp Rain FI AADTT Thick PP8 PP200 UW AC AC2 AV AC_AV Thick_UW Rain_AC FI_AC FI_AV IRI0 Age		157.4	20.5	97.1	0.359	0.319
9	Temp Rain FI AADTT Thick PP8 PP200 UW AC AC2 AV AV2 AC_AV Thick_UW Rain_AC FI_AC FI_AV IRI0 Age		141.2	21.5	97.6	0.374	0.308

Tables 15 through 18 present the posterior estimates and 95% highest posterior density (HPD) regions for the predictors included in the selected models. Analogous to traditional regression, the relationship between the predictors and *ΔIRI* can be noticed by observing the 95% HPD regions. For instance, unit weight of the asphalt mix has a 95% HPD region between 0.0107 and 0.5304, indicating that when the unit weight get higher, the reduction in IRI tends to be higher, with the other variables fixed. Notice that the 95% HPD regions of variable *Age* were negative for all four pavement layouts, meaning the effect on reducing IRI decreases as the overlay course ages.

Some variables, such as AC, AV and IRI_0 in Layout-1 model, contain the null value in their 95% HPD regions. These variables can be regarded as less predictive, compared to those variables with a 95% HPD of either positive or negative only (such as UW and AC2 in the Layout-1 model). Nevertheless, these variables are widely used in many pavement models and specifications. They were regarded as important quality characteristics of thin HMA overlays, and remained in the final models.

Table 15 Posterior Estimates of the ΔIRI Bayesian Prediction Model for Layout-1

Variables	Posterior Mean	Posterior Std. dev.	95% HPD Region	
			Lower End	Upper End
Intercept	3.7628	0.0654	3.6355	3.8905
Rain	-2.5552	0.8823	-4.2307	-0.7549
AADTT	-0.1265	0.0825	-0.2883	0.0337
PP8	0.3463	0.0845	0.1705	0.5011
PP200	-0.2595	0.1014	-0.4558	-0.0619
UW	0.2815	0.1322	0.0107	0.5304
AC	2.1683	1.0987	-0.0834	4.2324
AC2	-2.9080	1.2051	-5.2617	-0.5415
AV	1.2566	1.2699	-1.2417	3.6953
AV2	-0.9575	1.2038	-3.2269	1.4529
Thick_UW	0.1204	0.0599	0.00573	0.2385
Rain_AC	2.8635	0.9558	0.9464	4.7170
FI_AC	0.9880	0.3692	0.2615	1.7045
FI_AV	-1.1557	0.3533	-1.8364	-0.4531
IRI_0	0.0314	0.1252	-0.2131	0.2760
Age	-0.0807	0.0106	-0.1011	-0.0597

Table 16 Posterior Estimates of the ΔIRI Bayesian Prediction Model for Layout-2

Variables	Posterior Mean	Posterior Std. dev.	95% HPD Region	
			Lower End	Upper End
Intercept	3.7813	0.0478	3.6849	3.8723
Temp	-0.0263	0.0794	-0.1825	0.1278
Rain	0.3759	0.2878	-0.1799	0.9469
AADTT	0.0166	0.0371	-0.0566	0.0888
Thick	1.5754	1.5247	-1.2993	4.7455
PP8	0.0327	0.0448	-0.0541	0.1206
PP200	0.0539	0.0327	-0.0126	0.1157
UW	0.3511	0.2501	-0.1578	0.8308
AC	1.3122	0.7479	-0.1231	2.8255
AC2	-0.9303	0.7305	-2.3418	0.5128
AV	0.8731	0.2258	0.4217	1.3030
AV2	-0.9778	0.2126	-1.3815	-0.5573
Thick_UW	-1.7493	1.6664	-5.2017	1.3820
Rain_AC	-0.4126	0.3776	-1.1465	0.3313
FI_AC	0.0580	0.0901	-0.1186	0.2368
IRI_0	-0.1951	0.0587	-0.3104	-0.0797
Age	-0.0644	0.00691	-0.0785	-0.0511

Table 17 Posterior Estimates of the ΔIRI Bayesian Prediction Model for Layout-3

Variables	Posterior Mean	Posterior Std. dev.	95% HPD Region	
			Lower End	Upper End
Intercept	3.7666	0.0505	3.6686	3.8659
FI	-1.7556	0.3495	-2.4564	-1.0783
Thick	0.2452	0.0728	0.3922	0.1046
PP8	0.0611	0.0373	-0.0159	0.1304
PP200	-0.1670	0.0575	-0.2835	-0.0583
UW	-0.0183	0.1123	-0.2424	0.2014
AC	-1.4250	0.6275	-2.6804	-0.2144
AC2	1.3449	0.5453	0.2394	2.3937
FI_AC	0.9364	0.2805	0.3992	1.4964
FI_AV	0.5412	0.1255	0.3009	0.7954
IRI_0	-0.3248	0.0721	-0.4653	-0.1821
Age	-0.0529	0.0070	-0.0659	-0.0385

Table 18 Posterior Estimates of the ΔIRI Bayesian Prediction Model for Layout-4

Variables	Posterior Mean	Posterior Std. dev.	95% HPD Region	
			Lower End	Upper End
Intercept	3.9230	0.0380	3.8493	3.9961
Rain	-0.2164	0.0297	-0.2762	-0.1604
FI	-0.5968	0.1433	-0.8909	-0.3245
AADTT	0.00209	0.0453	-0.0849	0.0902
Thick	0.7984	0.1550	0.4920	1.0977
PP8	0.0737	0.0275	0.0191	0.1263
PP200	-0.2670	0.0252	-0.3178	-0.2187
AC	0.5121	0.2194	0.0642	0.9269
AV	-0.5815	0.3465	-1.2532	0.1189
AV2	0.8302	0.1861	0.4535	1.1801
AC_AV	-0.7552	0.4654	-1.6656	0.1573
Thick_UW	-0.7097	0.1615	-1.0284	-0.3960
FI_AV	0.3370	0.1499	0.0465	0.6384
IRI_0	-0.1391	0.0554	-0.2475	-0.0326
Age	-0.0629	0.00404	-0.0708	-0.0550

To justify the predictive capability of the developed Bayesian models, they were applied to some randomly selected thin HMA overlay treatments in LTPP for predicting

the treatment effect in reducing IRI. The predictions are displayed in Figure 24. The dots represent actual *ΔIRI* values, while the lines represent the mean values and 95% confidence interval of *ΔIRI* predicted using the Bayesian models. The graphs show that although the variability in actual *ΔIRI* values is significant, the predicted distribution using the Bayesian models (represented by mean and standard deviation) can generally envelope this variability. So the predictive capability of the developed Bayesian regression models was justified.

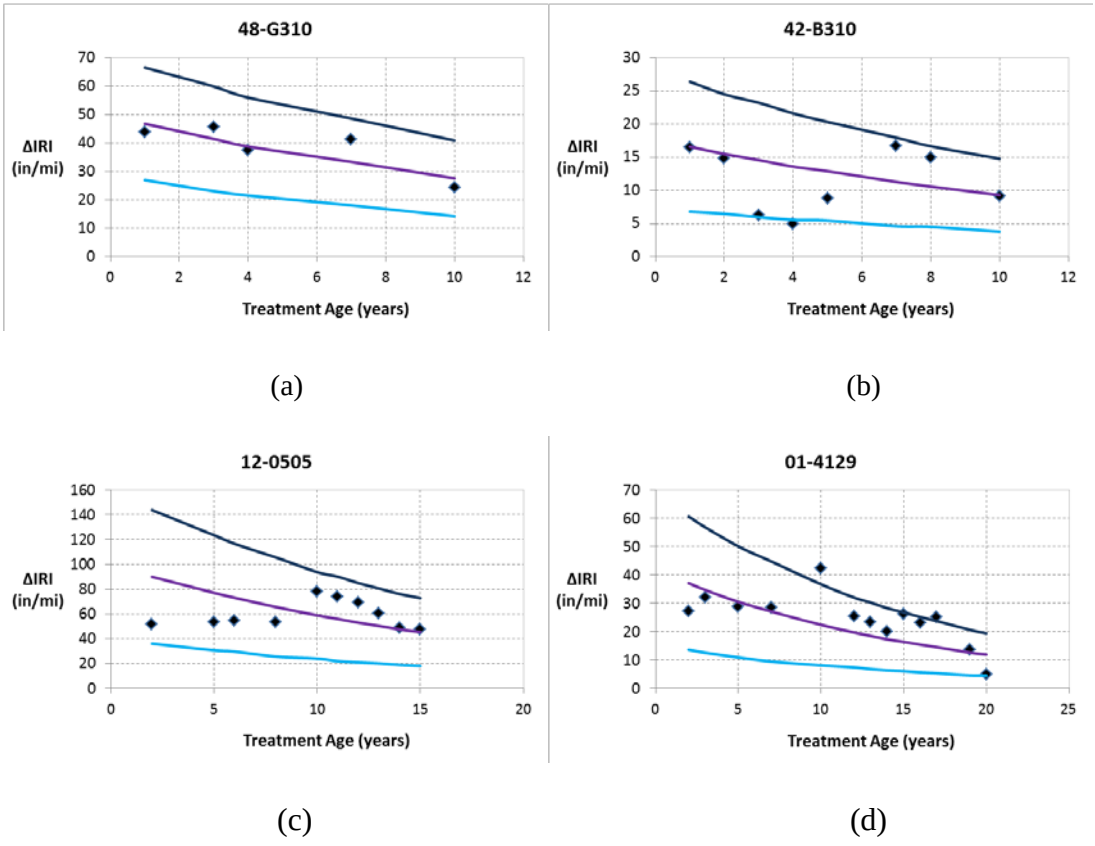

Figure 24 Bayesian model predictions for randomly selected LTPP test sections: (a) Layout-1; (b) Layout-2; (c) Layout-3; and (d) Layout-4.

CONCLUDING REMARKS

In this chapter, the most critical element in PRS (i.e., pavement post-treatment performance prediction models) was developed. A novel modeling approach, "Two-Component Modeling Approach," was devised to predict pavement post-treatment performance. As the name implies, the model consists of two major components, which predict the existing pavement performance and distress or roughness reduction due to treatment, respectively. In this approach, the effect of the underlying pavement structure on post-treatment performance is considered, which was never accounted for in previous endeavors of developing performance prediction models for preservation treatments.

New models were developed using this approach for predicting IRI of asphalt pavement treated with thin HMA overlay. ANNs were developed for predicting the IRI of the existing asphalt pavement and Bayesian regression models were developed for predicting the reduction in IRI due to thin HMA treatment. The goodness of fit statistics of these models indicated that these models are sufficiently reliable to be adopted in PRS for making long-term pavement performance predictions.

CHAPTER V

PRS METHODOLOGY FOR PAVEMENT PRESERVATION TREATMENTS

OVERVIEW

This chapter describes the development of a simulation-based performance-related specifications (PRS) methodology for pavement preservation treatments. In this methodology, the acceptance unit of a preservation treatment, namely *lot*, is divided into smaller units, namely *sublot*. As-designed and as-constructed measurements of AQCs, along with other necessary inputs, are used to predict the performance of the as-designed and as-constructed lots using the performance prediction models discussed earlier. The performance predictions are integrated into the PRS methodology, and eventually pay adjustment for a treatment lot is determined based on the economic value of performance lost or gained due to the differences between the treatment's as-designed (i.e., target) and as-constructed level of quality.

INTRODUCTION

PRS is defined as specifications that describe the desired levels of key materials and construction AQCs (e.g., layer thickness, asphalt content, and air voids) that have been found to correlate strongly with fundamental engineering properties (e.g., dynamic modulus) that predict pavement performance (TRB 2009). These AQCs should be amendable to acceptance testing at the time of construction. True PRS not only describe the desired levels of these AQCs but also use the measured AQCs to predict subsequent pavement performance (e.g., post-treatment performance in this research), thus

providing the basis for rational acceptance and price adjustment decisions. Thus, a promising PRS methodology should possess the capacity to relate the materials and construction quality of preservation treatments to the estimated performance and life-cycle cost (LCC) of a given treatment lot. The pay adjustment for a lot is computed based on the difference between the LCCs associated with the as-designed (target) treatment and the LCCs associated with the as-constructed (actual) treatment. A general framework for the developed PRS methodology in this research is presented in Figure 25. In this research, performance is measured in terms of IRI. A treatment lot is considered failed (i.e., require a new treatment application or reconstruction) when it reaches a certain IRI threshold value.

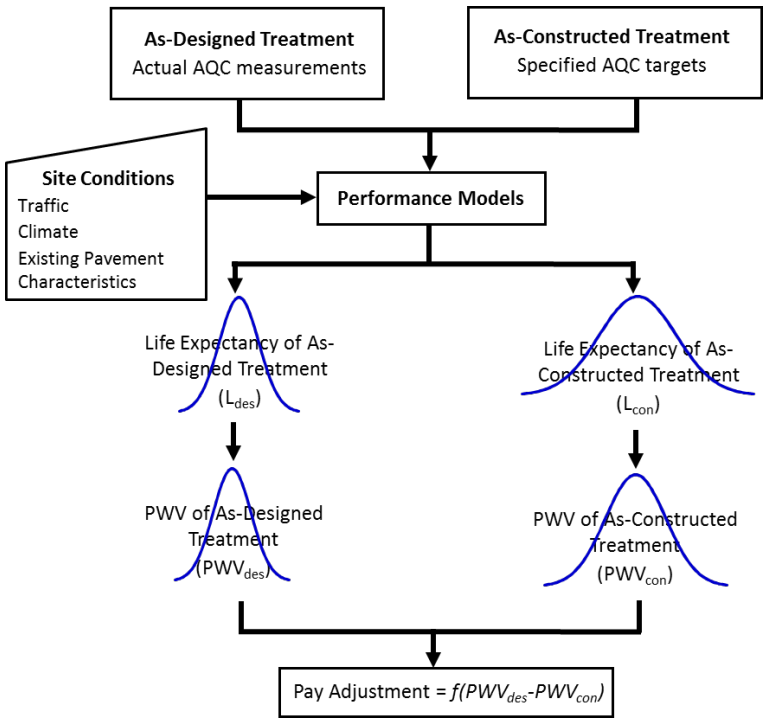

Figure 25 A general PRS framework for pavement preservation treatments.

In this framework, target AQC values are defined in the specifications and actual AQC values are measured in the lab or field. Same site condition (e.g., traffic, climate, and existing pavement characteristics) values are used for both as-designed and as-constructed treatments. Pavement performance prediction models (e.g., the two-component ΔIRI prediction model discussed earlier) are used to predict the future performance based on the AQC values and other factors. Service life of preservation treatment is defined here based on predicted performance as "number of years until user-defined IRI threshold values are reached." As in this research the treatment performance is predicted as probability distributions, the resulting estimated service life is also expressed as probability distributions, as shown in Figure 24. Then the present worth values (PWVs) of as-designed lot and as-constructed lot are estimated through LCC analysis (LCCA). In LCCA, the treatment's initial cost and the costs of future maintenance and rehabilitation (M&R) options expected to be incurred over the analysis period are included. The final step is to establish rational pay adjustment decisions based on the difference between the PWVs of the as-designed and as-constructed treatments.

DEFINITIONS OF KEY PRS ELEMENTS

Key elements in the PRS methodology are defined according to TRB (2009) and summarized as follows:

- **Lot:** This is the amount of treatment that may be accepted or rejected based on the deviation of the as-constructed quality level from the as-designed quality level. Each AQC of a lot is assumed to be normally distributed. A treatment lot can be measured in different units, depending on the treatment

type. For example, a thin HMA overlay lot may be measured in tonnage, whereas a chip seal lot may be measured in number of gallons for asphalt material and cubic yards for aggregate.

- **Sublot:** Each lot may be divided into 3 to 5 sublots of approximately equal size for sampling stratification purposes.
- **Sample Size:** This refers to the number of measurements taken randomly from a lot. Typically, at least one unit of the sample is taken from each sublot. It is important that each sample unit should be taken from a randomly-selected location within each sublot. Randomness of sampling is a vital assumption upon which statistical acceptance procedures are based.
- **AQC:** Inherent measurable treatment characteristics that affect pavement performance, are under the control of the contractor, and are measurable at or near the time of construction. The performance prediction model developed in this research allows for considering up to six AQCs for thin HMA overlays: overlay thickness, percent aggregate passing #8 and #200 sieves, unit weight of HMA mix, asphalt content, air voids, and initial IRI right after treatment.
- **Analysis Period:** Period of time over which future preservation and maintenance associated costs are to be considered in the LCC analysis.
- **As-Constructed Lot Present Worth Value (PWV_C):** The estimated post-treatment PWV that represents the as-constructed treatment lot quality. It heavily depends on the measured AQC values of the as-constructed lot. In this research, PWV_C is represented by a probability distribution.

- **As-Designed Lot Present Worth Value (PWV_D):** The estimated post-treatment PWV that represents the as-designed treatment lot quality. It is based on the as-designed target values for the AQCs. In this research, PWV_D is represented by a probability distribution.
- **Performance Indicator:** A key distress or a composite index that describes the condition of the pavement. In a PRS methodology, a performance indicator is predicted as a function of AQCs and site conditions.
- **Performance Indicator Threshold:** A predetermined value for a performance indicator (e.g., IRI in this research). Beyond this threshold, a treated pavement is marked as "Failed" and further M&R options need to be considered.
- **Pay Factor (PF):** The percent of the bid price that the contractor is paid for the treatment lot. A PF greater than 100 percent is provided for a lot that exceeds the as-designed quality and a PF less than 100 percent is provided for a lot that falls short of the as-designed quality.

SIMULATION-BASED PRS METHODOLOGY

The general PRS framework discussed earlier was further developed into a detailed simulation-based PRS methodology that can take inputs including AQC values and site conditions, and through simulations give pay adjustment recommendations. Figure 26 depicts this detailed PRS methodology.

In this methodology, a treatment lot is divided into multiple sublots. Samples are taken from each sublot for each AQC. The AQC values, site conditions, and treatment

age are then input into the ΔIRI prediction model (discussed earlier). The performance of each sublot is predicted and checked against predefined performance threshold value to determine the service life range of each sublot. The life distributions of all sublots within the same lot are aggregated through data sampling to obtain the life distribution of the whole lot. Subsequently, the life distribution of the whole lot is used in the LCCA process to derive the PWV distribution of the lot. The service life and the LCCA computation processes are discussed next.

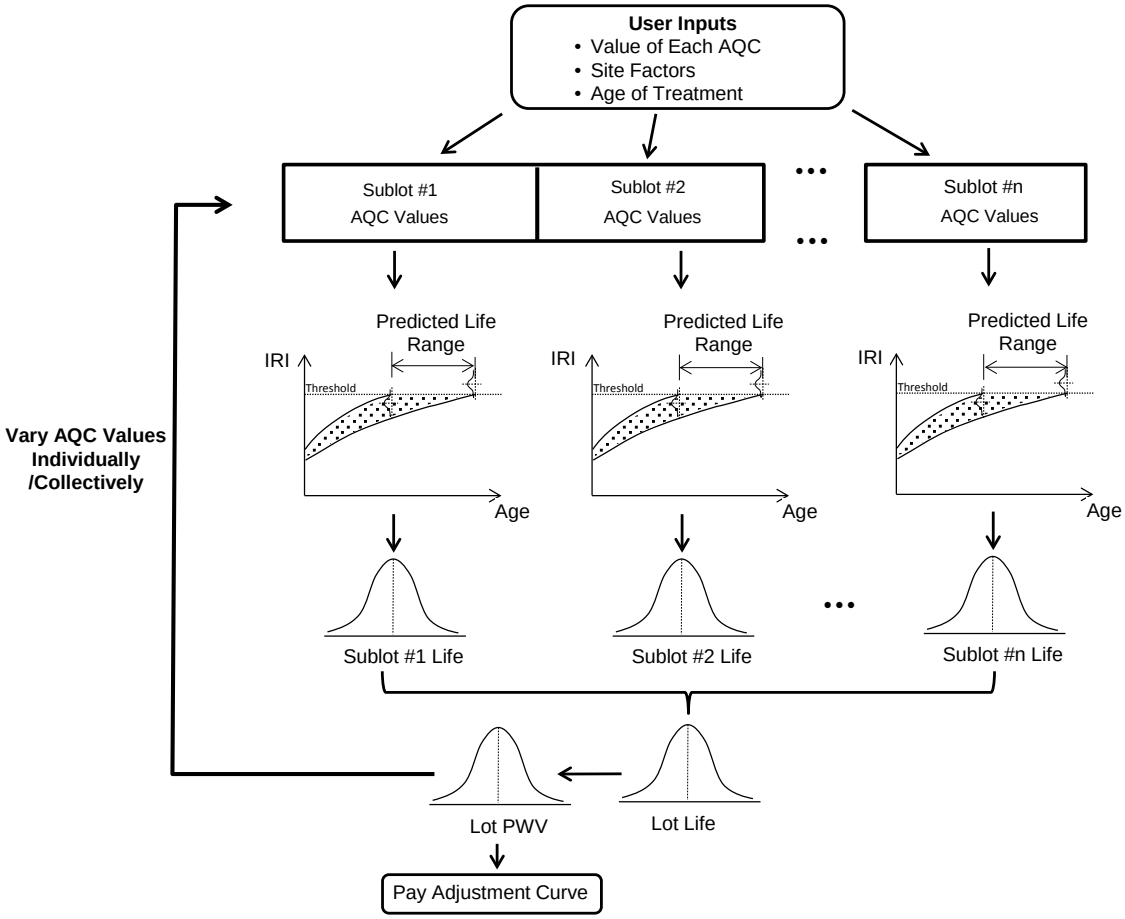

Figure 26 A simulation-based PRS methodology for pavement preservation treatments.

Determination of Treatment Service Life

The end of service life of a preservation treatment (e.g., thin HMA overlay) has defined by the occurrence of either of the following two events (Liu and Gharaibeh 2013):

- Application of a subsequent preservation or rehabilitation treatment.
- Reaching pre-determined threshold values of performance indicator.

In this research, the determination of treatment service life was based on the second event (i.e., the IRI progression reaches or exceeds a pre-determined threshold value). The IRI progression was predicted as a function of AQCs, site characteristics, and age. A graph depicting how to derive the treatment service life based on predicted IRI probability distribution is shown in Figure 27. A confidence level, α (e.g., 95%) needs to be specified first. At any given treatment age, the predicted IRI follows a normal distribution, expressed as $N(\mu, \sigma^2)$. The predicted treatment service life is a range of time period that is determined as follows:

- The lower end of service life range (denoted as SL_L^{α}) is defined as the age at which the cumulative probability density of predicted IRI above the threshold limit exceeds $(1 - \alpha)$. For example, let's take the 95% confidence level. When the treatment age reaches five years, the upper endpoint of the 95% confidence interval of predicted IRI exceeds the threshold value [i.e., the shaded area of normal distribution below the threshold line becomes less than 95% (see Figure 27)]. As a result, the $SL_L^{.95}$ is determined to equal to five years.

- The upper end of service life range (denoted as SL_U^{α}) is defined as the age at which the cumulative probability density of predicted IRI above the threshold limit exceeds α. For example, let's take the 95% confidence level again. When the treatment age reaches eight years, the lower endpoint of the 95% confidence interval of predicted IRI exceeds the threshold value [i.e., the shaded area of normal distribution below the threshold line becomes less than 5% (see Figure 27)]. As a result, the $SL_U^{.95}$ is determined to equal to eight years.
- The predicted treatment service life is assumed to follow a normal distribution. The statistics of the normal distribution (i.e., mean and standard deviation) can be estimated based on SL_L^{α}, SL_U^{α}, and confidence level α.

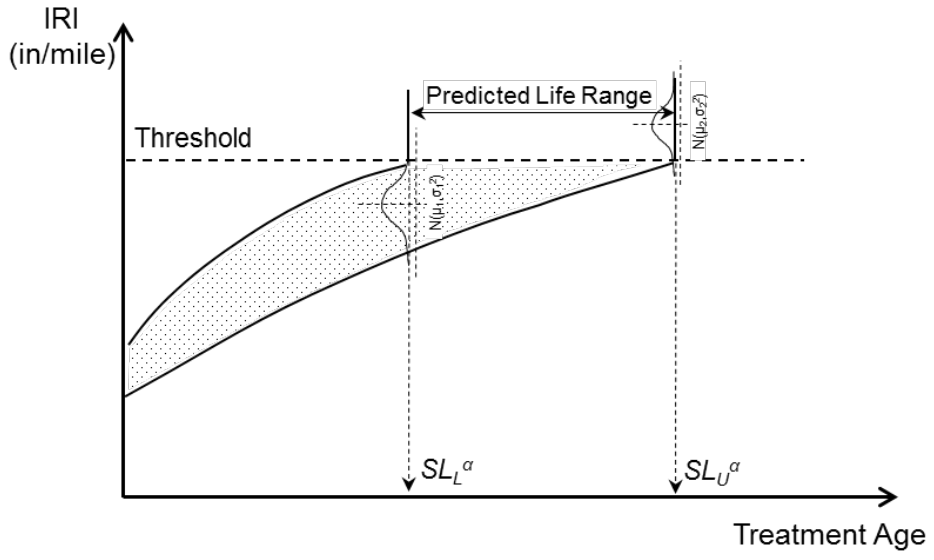

.

Figure 27 A graphical illustration of determining treatment service life.

Selection of the IRI threshold is important in the definition of treatment service life. Federal Highway Administration (FHWA) recommends that for new asphalt and asphalt overlaid asphalt pavements, terminal IRI threshold value that define end of service life should not be over 170 in/mile (Shafizadeh and Mannering 2003). In the MEPDG, the default terminal IRI for asphalt pavements is set at 172 in/mile, very close to the FHWA recommendation. Some state highway agencies have their threshold values for IRI. For example, Indiana Department of Transportation (InDOT) specifies that when the IRI is above 150 in/mile, a thin HMA overlay shall be considered to improve the surface roughness (INDOT 2013). Baus and Stires (2010) mentioned that the IRI thresholds values recommended by AASHTO for use in judging pavement trial design are 160 in/mile for interstate highways, and 200 in/mile for lower class pavements. Based on the literature, an IRI threshold value between 150 and 170 in/mile is appropriate for defining the failure of a preservation treatment.

Lifecycle Cost Analysis

Figure 28 shows an LCCA diagram for estimating the PWV of preservation treatment constructions. In LCCA, the costs of initial treatment and future treatment(s) and the service life of each treatment are needed. The salvage value (SV) can be calculated using the prorated life method (Walls III and Smith 1998):

$$SV = \frac{RL}{SL} \times Cost_{Future} \qquad \text{(Eq. 20)}$$

where *RL* is the remaining life after the analysis period, *SL* is the treatment service life, and $Cost_{Future}$ is the construction cost of future treatment. The PWV is calculated by discounting future treatment costs at various points in time back to the base year as follows:

$$PWV = Cost_{Init} + \sum_{k=1}^{N}\left[Cost_{Future}\left(\frac{1}{(1+i)^{n_k}}\right)\right] \qquad \text{(Eq. 21)}$$

where $Cost_{Init}$ is the construction cost of initial treatment, i is the discount rate, k is the number of cost items in the analysis (k = 1 to N), n_k is the year at which the kth cost item is applied.

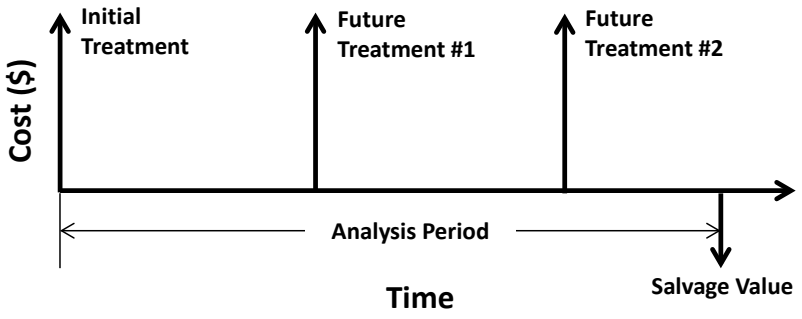

Figure 28 A typical LCCA diagram for a pavement preservation treatment.

In the PRS simulations, the same type of treatment as the initial one were applied at needed time points in the future. Thus, the same treatment costs and service life are used for initial and future treatments in the LCCA. As can be induced from the LCCA diagram, the PWV has a negative relationship with treatment service life. The longer the

treatment service life, the less number of future treatments are needed, and therefore the lower the PWV is.

A PF is determined based on the PWV distributions of as-designed and as-constructed treatment lot and bid price of the lot. The formula for PF calculation is as follows:

$$PF = \frac{BID + \left(PWV_D^{\alpha} - PWV_C^{\alpha}\right) \times P}{BID} \times 100\% \qquad \text{(Eq. 22)}$$

where *BID* is the bid price ($), $PWV_D{}^{\alpha}$ is the present-worth value of as-designed lot at α confidence level, $PWV_C{}^{\alpha}$ is the present-worth value of as-designed lot at α confidence level, and *P* is the probability of PWV between $PWV_D{}^{\alpha}$ and $PWV_C{}^{\alpha}$ (see Figures 30 and 31).

In the PF computation, the probability term *P* is included to account for the variability incorporated in the PWV distributions of as-designed and as-constructed treatments. It can represent a probability of economic saving when the as-constructed treatment has superior quality to the as-designed treatment, or a probability of economic loss when the as-constructed treatment has inferior quality to the as-designed treatment. These scenarios are reflected in Figures 29 through 31 and summarized as follows:

1. **On-Target quality**: In this case, the as-constructed and as-designed PWV distribution curves are identical (i.e., $PWV_C{}^{\alpha} = PWV_D{}^{\alpha}$, as shown in Figure 29), and the pay factor is expected to be 100%. This happens when the mean and standard deviation values of the AQCs of the as-constructed lot are equal or very close to the target values.

2. **High quality**: In this case, the as-constructed PWV distribution curve shifts to the left of the as-designed PWV distribution curve (i.e., $PWV_C^{\alpha} < PWV_D^{\alpha}$, as shown in Figure 30), and the pay factor is expected to be greater than 100%. This happens when the mean and standard deviation values of the AQCs of as-constructed lot are superior to the target values.
3. **Poor quality**: In this case, the as-constructed PWV distribution curve shifts to the right of the as-designed PWV distribution curve (i.e., $PWV_C^{\alpha} > PWV_D^{\alpha}$, as shown in Figure 31), and the pay factor is expected to be less than 100%. This happens when the mean and standard deviation values of the AQCs of as-constructed lot are inferior to the target values.

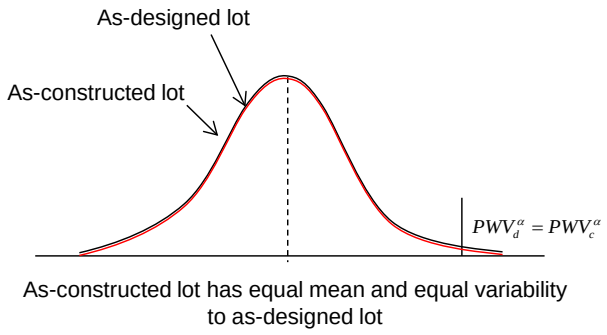

Figure 29 Scenario of on-target quality treatment: receiving PF = 100%.

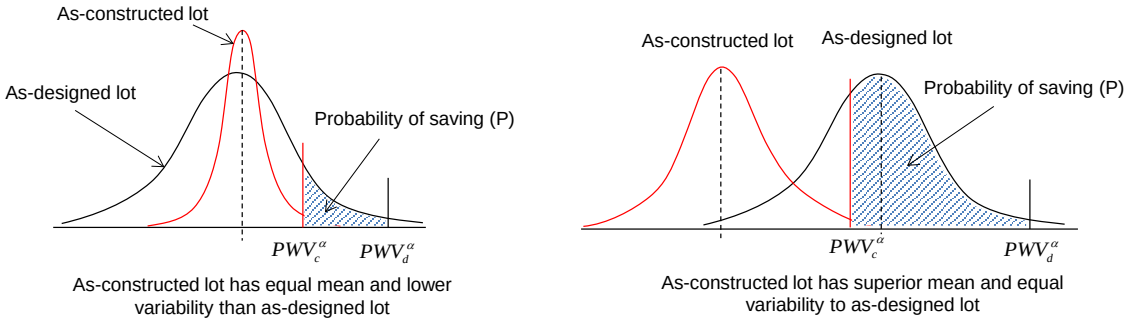

Figure 30 Scenario of high-quality treatment: receiving PF > 100%.

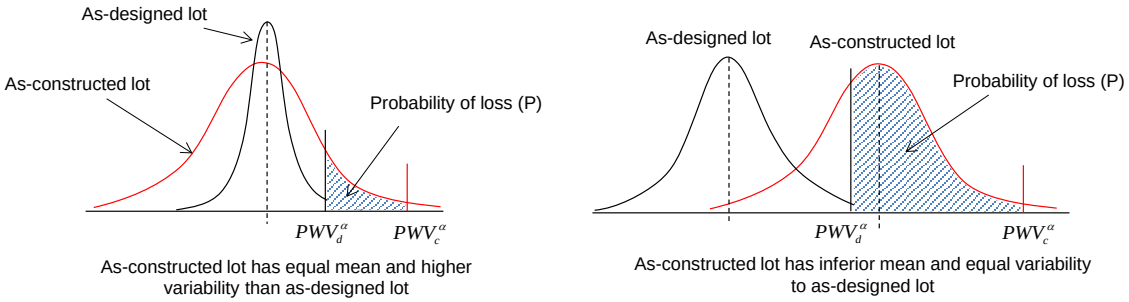

Figure 31 Scenario of poor-quality treatment: receiving PF < 100%.

At the end of this PRS methodology, pay factor curves can be developed by plotting pay factors against different quality levels of the AQCs. Conceptual PF curves for various quality scenarios are shown in Figure 32. It is important to emphasize that only one AQC is allowed to vary at a time when developing such pay factor curves, with the other AQCs set to their target values.

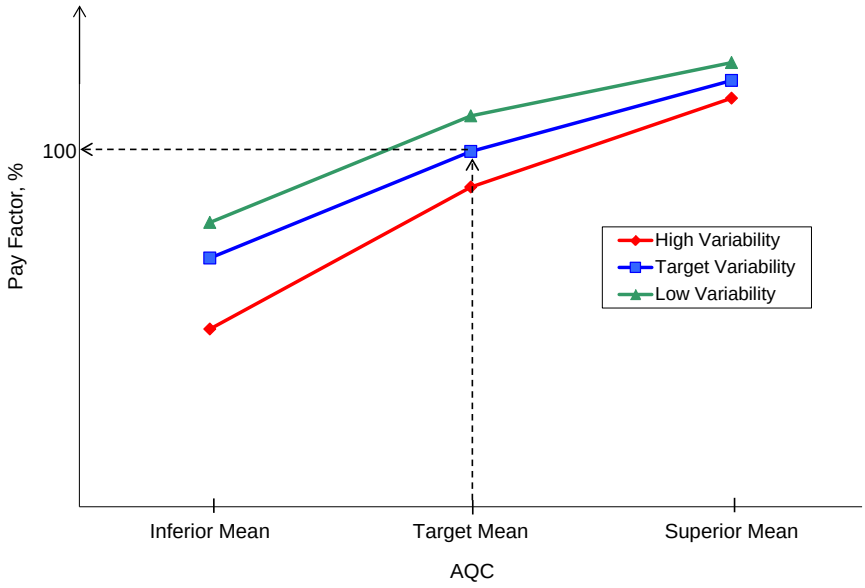

Figure 32 Pay factor curves for various quality scenarios.

CONCLUDING REMARKS

Current materials and construction specifications for pavement preservation treatments have little or no methodical linkage between initial quality of the treatment and its future performance. Consequently, current pay adjustment methods greatly depend on subjective judgments of the relationships between the treatment initial quality and its future performance. This chapter describes a novel PRS methodology that was devised for pavement preservation treatments. This methodology consists of quantitative probabilistic models for predicting pavement performance (e.g., IRI) as a function of key AQCs and other site factors. The predicted performance indicator is then used to derive probability frequency distributions for the service life and the lifecycle cost (measured in terms of PWV) of the treatment. Finally, the devised methodology computes rational pay adjustment factors based on the difference between the PWVs of the as-constructed and as-designed treatments on a lot-by-lot basis.

CHAPTER VI

APPLICATION OF THE DEVELOPED PRS METHODOLOGY TO CASE STUDIES

INTRODUCTION

In previous chapters, the PRS methodology and its core elements (i.e., post-treatment performance prediction models and AQCs) were discussed. In this chapter, the developed methodology is applied to real-world cases of thin HMA overlay treatments of LTPP sections.

One case study was performed for each pavement layout (totaling four case studies). In all these case studies, the reliability level was set at 95%. Various values were assigned to the AQCs to test their impact on the final pay factor. It is important to mention that the input data was reasonably selected and checked with the applicable range of predicators in the performance models (refer back to Table 10 in Chapter 4).

In all the case studies, the final PF of a treatment lot were within the range from 80% to 110%, which is very common in current specifications of many highway agencies. A PF below 80% indicates the quality of the thin HMA overlay is not acceptable and replacement of the treatment layer should be considered. On the other hand, the contractor will receive a maximum payment of 110% of the bid price, which represents a maximum 10% reward owing to exceptional treatment quality.

The following sections describe the case studies in the order of pavement layouts.

IMPLEMENTATION OF THE PRS METHODOLOGY

Implementation of the developed PRS methodology was carried out by incorporating its elements into a computational tool programmed in Excel VBA. The process described in Figure 33 was followed to simulate various quality scenarios for each case study and to derive pay factor curves for a treatment lot.

Data on site conditions, existing pavement properties, and the AQCs (i.e., mean and standard deviation values) is read into the simulation spreadsheet. Simulated AQC samples are drawn based on given distribution statistics for each sublot. Then, on a sublot-by-sublot basis, the service life distributions are estimated and the life distribution of the lot is derived.

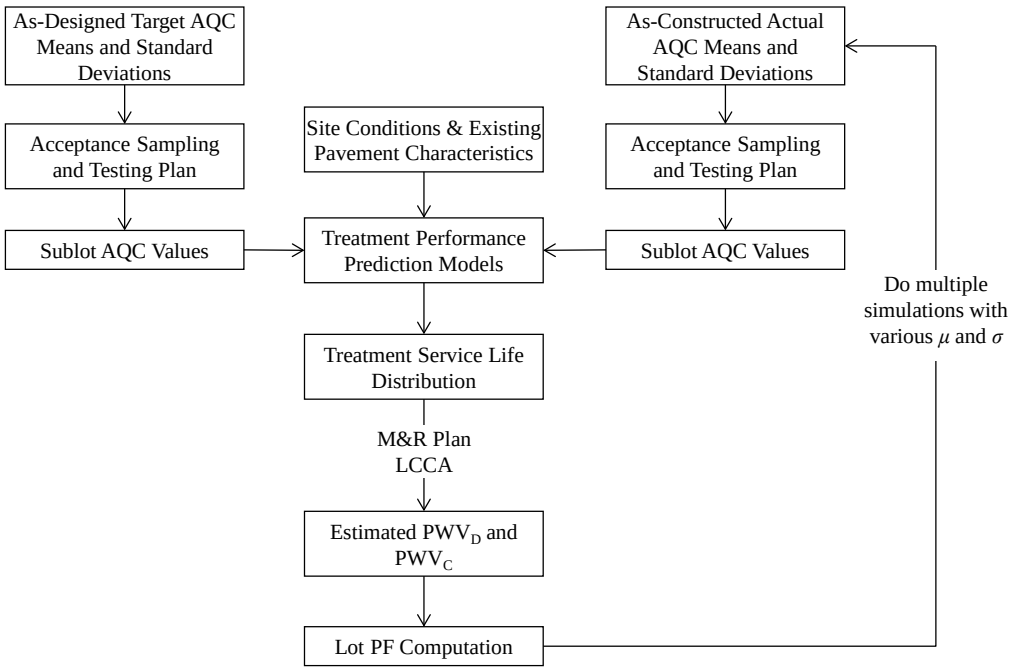

Figure 33 Process used to derive PF curves for a treatment lot.

CASE STUDY FOR PAVEMENT LAYOUT-1

Section Information

The LTPP SPS-3 test section 48-G310 was selected for cross-sectional Layout-1 case study. This section is located on Texas Highway 322 in Rusk County, Texas, with two lanes in each direction. The original pavement at this section was constructed in August, 1972; and the thin HMA overlay treatment was applied on October 15, 1990. Crushed stone was used for constructing the granular base, and sand was used for the subgrade.

This section has an annual air temperature of 64.5 ^{o}F, an annual rainfall of 48.7 in, and a freeze index of 18.8 ^{o}F-days, on average. The initial average annual daily truck traffic (AADTT) was 96 trucks per day in each direction, with a 5.8% compound growth rate. A current view of this roadway section is displayed in Figure 35.

Figure 34 Current view of section 48-G310 in Rusk County, TX.

The pavement consists of three layers: HMA surface layer, granular base, and subgrade. Table 19 summarizes the material and construction properties of the pre-treatment pavement layers and the AQC values of the thin HMA overlay treatment at this section.

Table 19 Pavement Characteristics of Section 48-G310

Layer	Attributes/AQC	Values
Thin HMA Overlay	Overlay Thickness (in)	1.5
	% Passing #8 Sieve	37.0
	% Passing #200 Sieve	3.0
	Asphalt Content (%)	5.5
	Air Voids (%)	6.0
	Initial IRI (in/mile)	88
Original HMA Surface Layer	Thickness (in)	3.4
	Effective Binder Content (%)	5.0
	Air Voids (%)	3.7
	Unit Weight (pcf)	139.2
	Cum. % Retained on ¾″ Sieve	0
	Cum. % Retained on 3/8″ Sieve	0
	Cum. % Retained on #4 Sieve	38
	% Passing #200 Sieve	4
	Asphalt Viscosity (10^6 poise)	18.31
Granular Base	Thickness (in)	11.3
	Plasticity Index	4
	Liquid Limit	21
	% Passing #200 Sieve	27.8
	% Passing #40 Sieve	67.0
	% Passing #4 Sieve	83.0
	Max Dry Unit Weight (pcf)	135.5
	Opt. Gravimetric Water Content (%)	7.5
Subgrade	Plasticity Index	16
	Liquid Limit	34
	% Passing #200 Sieve	2.6
	% Passing #40 Sieve	79.0
	% Passing #4 Sieve	100
	Max Dry Unit Weight (pcf)	110.5
	Opt. Gravimetric Water Content (%)	12.5

IRI and Service Life Predictions

Figure 36 shows the predicted IRI values in different years at this section. It is noticed that the predicted IRI in the 18th year is about 117 in/mile, very close to the field observed 112 in/mile recorded in the LTPP database. The blue curve represents the IRI predictions on the original pavement, while the green curve represents the predicted mean IRI after the thin HMA overlay was placed. The prediction indicates that the IRI on the original pavement reaches the failure threshold value (i.e., 170 in/mile) at an age of 33 years. Placement of the thin HMA overlay is expected to bring IRI down to a mean value of 84 in/mile in the first year.

Based on the predicted IRI mean and standard deviation values, the service life of this thin HMA overlay has a mean of 7.5 years and a standard deviation of 1.3 years. With 95% confidence, the predicted service life is between 5 to 10 years.

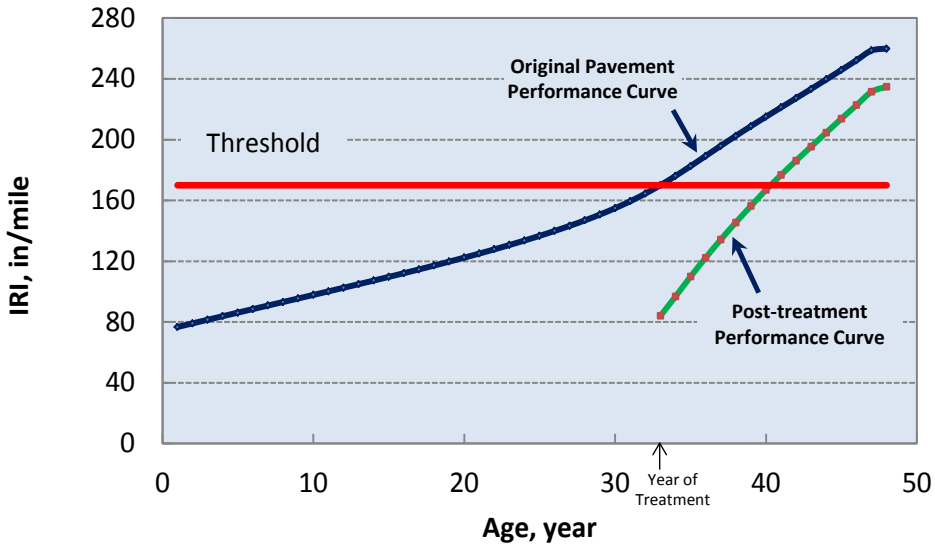

Figure 35 IRI predictions for Section 48-G310.

Pay Factor Curves

In the thin overlay pay adjustment simulations, a lot size of 3,000 tons of HMA mix was used, and each lot consisted of six sublots. Each sublot was sampled once and tested for each AQC. Thus, the sample size for each lot is six. The unit cost of HMA mix was assumed to be $55 per ton. An analysis period of 20 years was used in all the PRS simulations.

The s target mean and standard deviation values for each AQC of the thin HMA overlay are presented in Table 20. Note that the measured AQC values of the thin HMA overlay listed in Table 19 were used as target mean values. Target standard deviation values were selected based on NCHRP research (i.e., Hughes 1996), highway agency construction specifications (e.g., TxDOT 2004 Standard Specifications) and engineering judgments, as shown in Table 20.

Table 20 Case Study #1: AQC Target Mean and Standard Deviation Values

AQC Targets	Thick (in)	PP8 (%)	PP200 (%)	AC (%)	AV (%)	IRI_0 (in/mile)
Mean	1.5	37.0	3.0	5.5	6.0	88.0
Std. Dev.	0.20	2.50	0.80	0.20	0.90	5.0

For the as-constructed lot, the simulations were performed on seven levels of each AQC's mean value and three levels of each AQC's standard deviation. Therefore, each AQC was simulated for 21 combinations of mean and standard deviation levels. The simulation results, represented by PF curves, are shown in Figure 37.

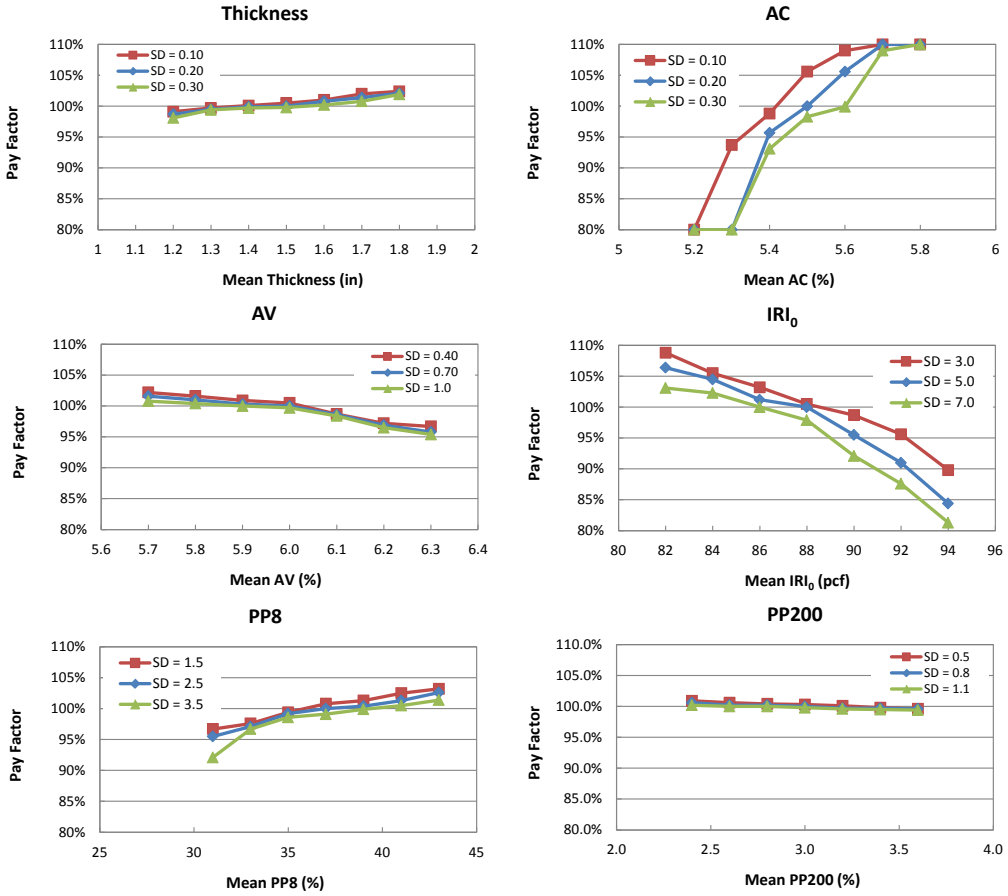

Figure 36 Pay factor curves for case study #1.

The PF curves in Figure 37 exhibit clear patterns of PF at different levels of the mean and standard deviation of AQCs. For overlay thickness, asphalt content, and % aggregate passing #8 sieve, the lot PF increases as any of these three AQCs increases (the other AQCs remain fixed) within the given ranges. For the other three AQCs (i.e., air voids content, % aggregate passing #200 sieve, and initial IRI), the lot PF decreases when any of these three AQCs increases within the given ranges. As the lot PF has a direct relationship with its service life, the PF curves indicate that in this particular case,

larger mean values of thickness, AC, and PP8 are favorable, whereas smaller mean values of PP200, AV, and IRI_0 are favorable.

The standard deviation of AQC values has also an impact on the lot PF. For all AQCs, a lot with a smaller standard deviation tends to have a higher PF than that with a larger standard deviation, as can be seen from the PF curves in Figure 37.

The effect of the AQCs on the magnitude of the PF varies. By observing the graphs in Figure 37, it can be seen that AC and IRI_0 means are most influential on the lot PF (i.e., the PF varies from 80% to 110% for the simulated AQC levels). The PF curves for PP200 has the smallest variation among different AQC levels, indicating much less influence of PP200 on contractor payment than the other AQCs. From this case study, it can be concluded that establishment of PF curves for all considered AQCs can help not only determine the effect of individual AQC on PF, but also compare between a set of AQCs and identify those important AQCs affecting the PF (through affecting treatment service life and PWV).

CASE STUDY FOR PAVEMENT LAYOUT-2

Section Information

The LTPP SPS-3 test section 16-C310 was selected for cross-sectional Layout-2 case study. This section is located on Highway US-15 in Bonneville County, Idaho, with two lanes in each direction. The original pavement at this section was constructed in October, 1969; and the thin HMA overlay treatment was applied on September 24,

1990. Crushed stone was used for constructing the granular base, and silty sand was used for the subgrade.

This section has an annual air temperature of 44.2 °F, an annual rainfall of 12.0 in, and a freezing index of 637.6 °F-days, on average. The initial AADTT was 356 trucks per day in each direction, with a 7.7% compound growth rate. A current view of this roadway section is displayed in Figure 38.

Figure 37 Current view of section 16-C310 in Bonneville County, Idaho.

The pavement at this section consists of four layers: HMA surface layer, binder course, granular base, and subgrade. Table 21 summarizes the material and construction properties of pre-treatment pavement layers and the AQC values of the thin HMA overlay treatment at this section.

Table 21 Pavement Characteristics of Section 16-C310

Layer	Attributes/AQC	Values
Thin HMA Overlay	Overlay Thickness (in)	1.7
	% Passing #8 Sieve	49.1
	% Passing #200 Sieve	5.5
	Asphalt Content (%)	5.3
	Air Voids (%)	4.2
	Initial IRI (in/mile)	76
Original HMA Surface Layer	Thickness (in)	4.9
	Effective Binder Content (%)	5.3
	Air Voids (%)	4.1
	Unit Weight (pcf)	143.9
	Cum. % Retained on ¾″ Sieve	0
	Cum. % Retained on 3/8″ Sieve	5
	Cum. % Retained on #4 Sieve	37
	% Passing #200 Sieve	7.6
	Asphalt Viscosity (10^6 poise)	12.86
Binder Course	Thickness (in)	5.0
	Effective Binder Content (%)	5.2
	Air Voids (%)	3.6
	Unit Weight (pcf)	144.2
	Cum. % Retained on ¾″ Sieve	0
	Cum. % Retained on 3/8″ Sieve	25
	Cum. % Retained on #4 Sieve	48
	% Passing #200 Sieve	6.6
	Asphalt Viscosity (10^6 poise)	21.95
Granular Base	Thickness (in)	5.4
	Plasticity Index	0
	Liquid Limit	0
	% Passing #200 Sieve	7.8
	% Passing #40 Sieve	23
	% Passing #4 Sieve	46
	Max Dry Unit Weight (pcf)	140
	Opt. Gravimetric Water Content (%)	5.0
Subgrade	Plasticity Index	0
	Liquid Limit	0
	% Passing #200 Sieve	13.1
	% Passing #40 Sieve	66
	% Passing #4 Sieve	97
	Max Dry Unit Weight (pcf)	113.5
	Opt. Gravimetric Water Content (%)	11.0

IRI and Service Life Predictions

Figure 39 shows the predicted IRI values in different age years of this section. The predicted IRI at the original pavement age of 21 years is about 112 in/mile, whereas the field observed IRI is 102 in/mile (as recorded in the LTPP database). The prediction indicates that the IRI of the original pavement reached the threshold of failure (i.e., 170

in/mile) at the age of 41 years. If a thin HMA overlay is placed in that year, it is predicted to bring the IRI down to a mean value of 120 in/mile in the first year.

Based on the predicted IRI mean and standard deviation values, the service life of this thin HMA overlay has a mean of 9.5 years and a standard deviation of 1.3 years. With 95% confidence, the service life falls between 7 to 12 years.

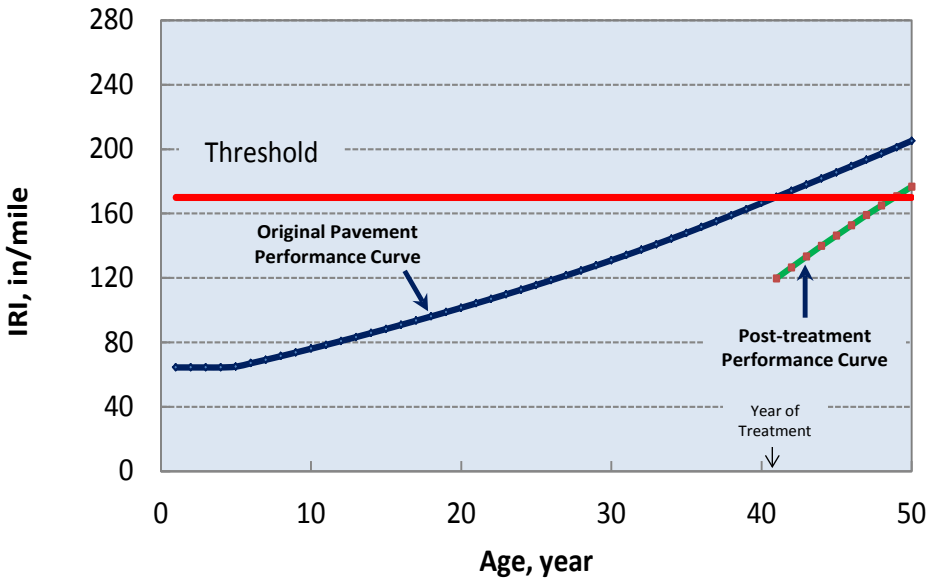

Figure 38 IRI predictions for Section 16-C310.

Pay Factor Curves

Similar to the previous case study, a lot size of 3,000 tons of overlay HMA mix was used, and each lot consisted of six sublots. Each sublot was sampled once and tested for each AQC. Thus, the sample size for each lot is six. The unit cost of HMA mix was assumed to be $60 per ton. An analysis period of 25 years was used in all the PRS simulations.

The target mean and standard deviation values for each AQC of the thin HMA overlay are presented in Table 22.

Table 22 Case Study #2: AQC Target Mean and Standard Deviation Values

AQC Targets	Thick (in)	PP8 (%)	PP200 (%)	AC (%)	AV (%)	IRI_0 (in/mile)
Mean	1.7	49.1	5.5	5.3	4.2	76.0
Std. Dev.	0.20	2.50	0.80	0.20	0.90	5.0

The simulations were performed on seven levels of each AQC's mean value and three levels of each AQC's standard deviation. A total of 21 combinations of mean and standard deviation values were simulated for each AQC, and the simulation results are shown in Figure 40.

In this case study, the PF curves show variations as the mean and standard deviation values of the AQCs change. Except for initial IRI (i.e., IRI_0), all other AQCs have a positive relationship between the PF and the mean AQC value within the given ranges (i.e., PF increases as the mean AQC value increases). As lower IRI is favorable, a lower PF value will be expected when the mean IRI_0 value is larger, as displayed in Figure 40.

The standard deviation of AQC values again has an impact on the lot PF. Similar to the first case study, the PF curves of the second case study have a consistent pattern: for any as-constructed mean value, as the standard deviation decreases, the pay factor increases.

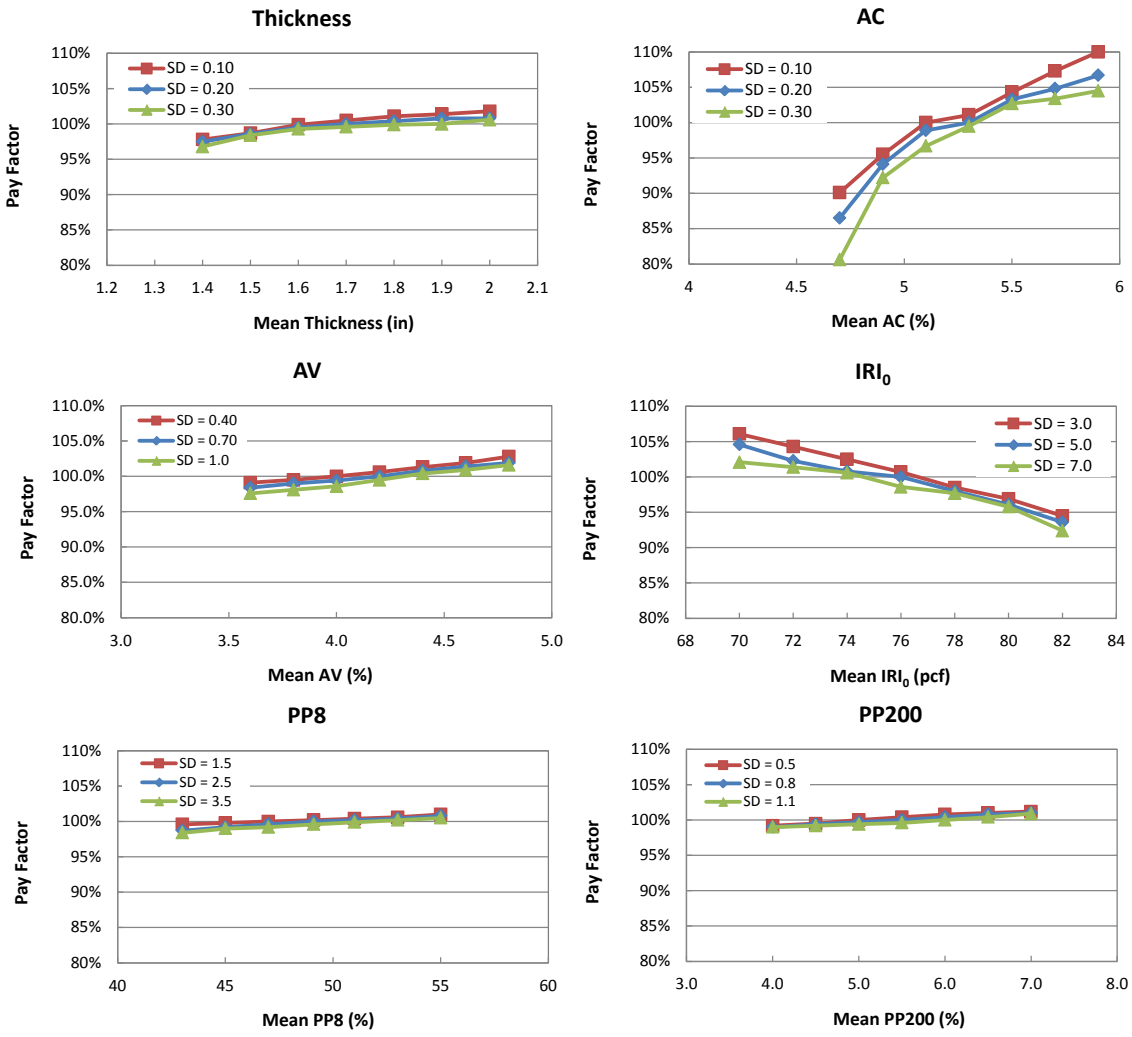

Figure 39 Pay factor curves for case study #2.

Figure 40 also shows that AC is the most influential AQC on the lot PF (i.e., the PF varies from 80% to 110% as the simulated AC varies from 4.7% to 5.9%), followed by IRI_0. The results also indicate that PP8 and PP200 have a negligible effect on the pay adjustment because the variations in these two variables can only result in a less than ±1.5% differentiation in the PF. Comparatively, overlay thickness and AV have an intermediate impact, among the AQCs, on the final PF.

CASE STUDY FOR PAVEMENT LAYOUT-3

Section Information

For cross-sectional layout-3, SPS-5 section 12-0505 was selected for applying the developed PRS methodology. This section is located on Highway US-1 in Martin County, Florida, with two lanes in each direction. The original pavement at this section was constructed in June 1971; and the thin HMA overlay treatment was applied on April 18, 1995. The granular base of this pavement was constructed using crushed gravel. The subbase was constructed using coarse soil-aggregate mixture, and poorly graded sand was used for the subgrade.

At this section, the annual air temperature is74.5 ^{o}F, the annual rainfall is 59.6 in, and the freezing index is 0 ^{o}F-days, on average. The initial AADTT was 242 trucks per day on each direction, with a 4.0% compound growth rate. A current view of this roadway section is displayed in Figure 41.

Figure 40 Current view of section 12-0505 in Martin County, Florida.

The pavement at this section consists of four layers: HMA surface layer, granular base, granular subbase, and subgrade. Table 23 summarizes the material and construction properties of existing pavement layers and the AQC values of the thin HMA overlay treatment at this roadway section.

Table 23 Pavement Characteristics of Section 12-0505

Layer	Attributes/AQC	Values
Thin HMA Overlay	Overlay Thickness (in)	1.9
	% Passing #8 Sieve	38
	% Passing #200 Sieve	2.1
	Asphalt Content (%)	6.5
	Air Voids (%)	3.7
	Initial IRI (in/mile)	60.2
Original HMA Surface Layer	Thickness (in)	2.9
	Effective Binder Content (%)	6.5
	Air Voids (%)	5.2
	Unit Weight (pcf)	136.8
	Cum. % Retained on ¾″ Sieve	0
	Cum. % Retained on 3/8″ Sieve	1
	Cum. % Retained on #4 Sieve	32
	% Passing #200 Sieve	4.9
	Asphalt Viscosity (10^6 poise)	13.03
Granular Subbase	Thickness (in)	8.8
	% Passing #200 Sieve	16.2
	% Passing #40 Sieve	34
	% Passing #4 Sieve	58
	Max Dry Unit Weight (pcf)	131
	Opt. Gravimetric Water Content (%)	8.5
Granular Base	Thickness (in)	11
	% Passing #200 Sieve	5.1
	% Passing #40 Sieve	65
	% Passing #4 Sieve	87
	Max Dry Unit Weight (pcf)	116
	Opt. Gravimetric Water Content (%)	9.5
Subgrade	% Passing #200 Sieve	1.5
	% Passing #40 Sieve	70
	% Passing #4 Sieve	100
	Max Dry Unit Weight (pcf)	107
	Opt. Gravimetric Water Content (%)	12

IRI and Service Life Predictions

Figure 42 shows the predicted IRI values in different age years at this section. The predicted IRI for the original pavement at the age of 24 years is about 144 in/mile,

which is not very far from the observed IRI of 122 in/mile (recorded in the LTPP database). The prediction indicates that the IRI of the original pavement reached the threshold of failure (i.e., 170 in/mile) at the age of 33 years. After the thin HMA overlay is applied, the IRI is predicted to be brought down to a mean value of 80 in/mile in the first year.

The predicted service life of the thin HMA overlay at this section has a mean of 12 years and a standard deviation of 1.5 years. With 95% confidence, the service life falls between 9 to 15 years.

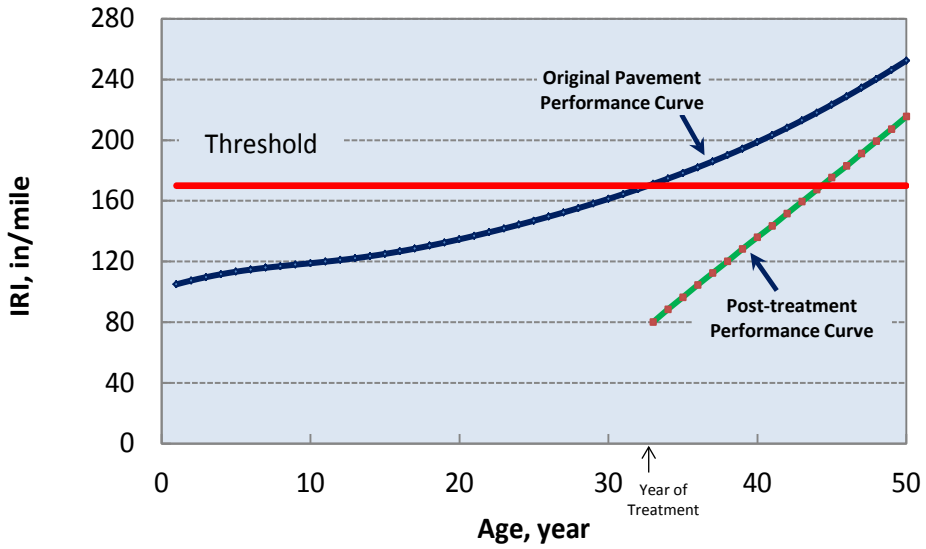

Figure 41 IRI predictions for Section 12-0505.

Pay Factor Curves

In this case study, the same analysis configuration as the previous case studies was used, except that a $50/ton unit cost was used for HMA mix and a 26 years analysis

period was used in the simulations. Table 24 presents the target mean and standard deviations of the thin HMA overlay AQCs.

Table 24 Case Study #3: AQC Target Mean and Standard Deviation Values

AQC Targets	Thick (in)	PP8 (%)	PP200 (%)	AC (%)	AV (%)	IRI_0 (in/mile)
Mean	1.9	38.0	2.1	6.5	3.7	60.2
Std. Dev.	0.20	2.50	0.80	0.20	0.90	5.0

Simulations were performed on seven levels of the mean value and three levels of the standard deviation for each AQC. The simulated PF curves are shown in Figure 43.

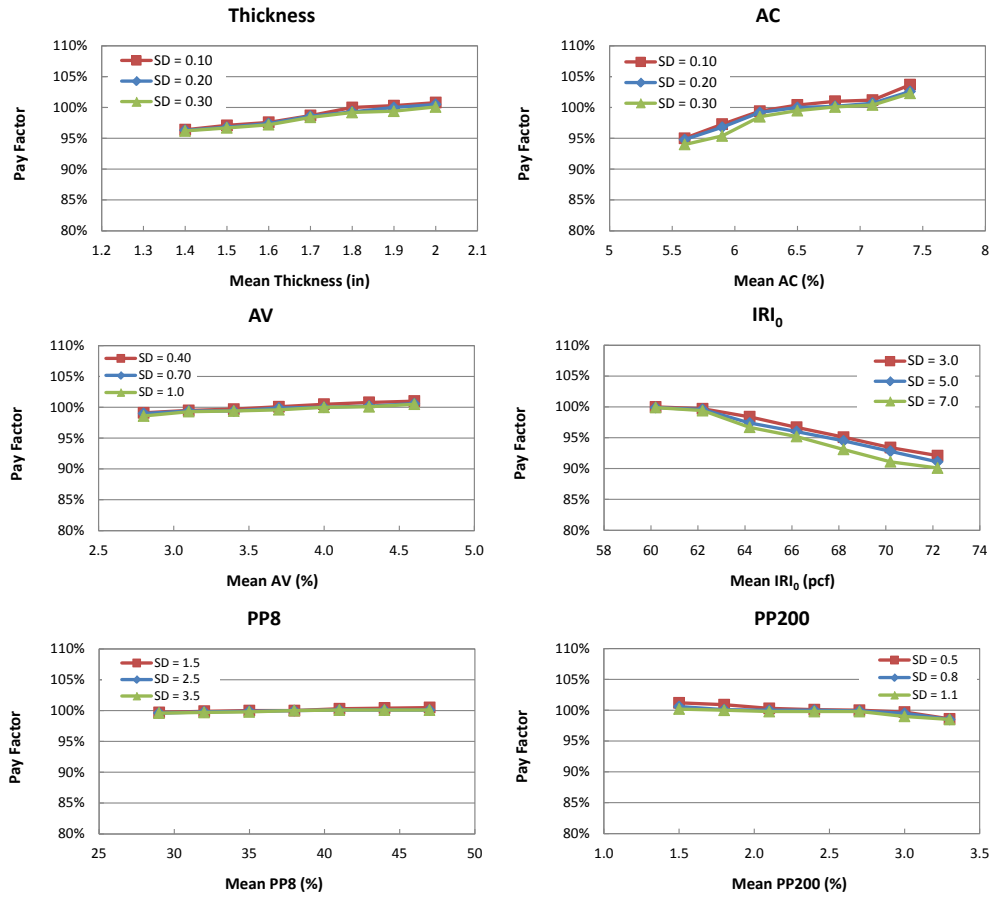

Figure 42 Pay factor curves for case study #3.

In this case study, AV and PP8 have very slight effect on the PF. The PF curves remain flat at 100% when the mean PP8 varies from 28% to 47%, regardless of the variation in the standard deviation. The PF curves also remain flat when the mean AV varies from 3.1% to 3.7%.

The PF curves in Figure 43 indicate that larger mean overlay Thickness, AC, AV, and lower mean IRI_0 and PP200 values (within the studied ranges) lead to a higher pay factor. The PF curves with respect to mean IRI_0 remain flat at lower IRI_0 values, and start to drop when the mean IRI_0 value exceed 64 in/mile (the target value is set at 60.2 in/mile).

Compared to case studies 1 and 2, the standard deviation impact on PF is less pronounced for most AQCs. The impact of standard deviation on PF is obvious only for IRI_0 and AC. This may be caused by the fact that the range of mean values appear to be too small to cause noticeable difference in the PF.

It can be seen that in this case study, the most influential factor is AC, which results in a variation from 93% to 103% in PF as the simulated AC level varies from 5.6% to 7.4%. IRI_0 can also result in approximately 10% variation in PF across different mean levels, and overlay thickness can result in about 5% variation in PF. In contrast, AV and PP8 each can result in less than ±1% differentiation in the lot PF.

CASE STUDY FOR PAVEMENT LAYOUT-4

Section Information

The LTTP GPS test section 34-1030 was used in this case study. This section is located on Highway 23 in Passaic County, New Jersey. It has two lanes in each

direction. The original pavement at this section was constructed in October, 1969; and the thin HMA overlay treatment was applied on September 18, 1997. Crushed gravel was used for constructing the granular base, sand for constructing the granular subbase, and poorly-graded sand with silt and gravel used for the subgrade.

This section has an annual air temperature of 50.8 ^{o}F, an annual rainfall of 48.4 in, and a freezing index of 275.2 ^{o}F-days, on average. The initial AADTT was 420 trucks per day on each direction, with a 1.5% compound growth rate. A current view of this roadway section is displayed in Figure 44.

Figure 43 Current view of section 34-1030 in Passaic County, New Jersey.

The pavement at this section consists of five layers: HMA surface layer, binder course, granular base, granular subbase, and subgrade. Table 25 summarizes the material and construction properties of existing pavement layers and the AQC values of thin HMA overlay treatment at this section.

Table 25 Pavement Characteristics of Section 34-1030

Layer	Attributes/AQC	Values
Thin HMA Overlay	Overlay Thickness (in)	1.8
	% Passing #8 Sieve	32
	% Passing #200 Sieve	7.1
	Asphalt Content (%)	5.6
	Air Voids (%)	6.1
	Initial IRI (in/mile)	110
Original HMA Surface Layer	Thickness (in)	1.8
	Effective Binder Content (%)	6.5
	Air Voids (%)	4.6
	Unit Weight (pcf)	148.6
	Cum. % Retained on ¾″ Sieve	0
	Cum. % Retained on 3/8″ Sieve	1
	Cum. % Retained on #4 Sieve	29
	% Passing #200 Sieve	5.7
	Asphalt Viscosity (10^6 poise)	13.03
Binder Course	Thickness (in)	4.2
	Effective Binder Content (%)	4.7
	Air Voids (%)	5.9
	Cum. % Retained on ¾″ Sieve	19
	Cum. % Retained on 3/8″ Sieve	46
	Cum. % Retained on #4 Sieve	58
	% Passing #200 Sieve	5.0
	Asphalt Viscosity (10^6 poise)	13.03
Granular Base	Thickness (in)	6.8
	Plasticity Index	0
	Liquid Limit	0
	% Passing #200 Sieve	0.5
	% Passing #40 Sieve	5
	% Passing #4 Sieve	16
	Max Dry Unit Weight (pcf)	137
	Opt. Gravimetric Water Content (%)	7.0
Granular Subbase	Thickness (in)	23.4
	Plasticity Index	0
	Liquid Limit	0
	% Passing #200 Sieve	5.9
	% Passing #40 Sieve	46
	% Passing #4 Sieve	67
	Max Dry Unit Weight (pcf)	132
	Opt. Gravimetric Water Content (%)	7.5
Subgrade	Plasticity Index	0
	Liquid Limit	0
	% Passing #200 Sieve	9.2
	% Passing #40 Sieve	31
	% Passing #4 Sieve	63
	Max Dry Unit Weight (pcf)	134
	Opt. Gravimetric Water Content (%)	10

IRI and Service Life Predictions

Figure 45 shows the predicted IRI values in different age years at this section. The predicted IRI at the original pavement age of 28 years is about 139 in/mile, which is lower than the 178 in/mile IRI value recorded in the database. The prediction indicates that the IRI on the original pavement reached the threshold of failure (i.e., 170 in/mile) at the age of 38 years. The thin HMA overlay treatment is predicted to bring the IRI down to a mean value of about 120 in/mile in the first year.

Based on the predicted IRI mean and standard deviation values, the service life of this thin HMA overlay has a mean of 8.5 years and a standard deviation of 1.3 years. With 95% confidence, the service life falls between 6 to 11 years.

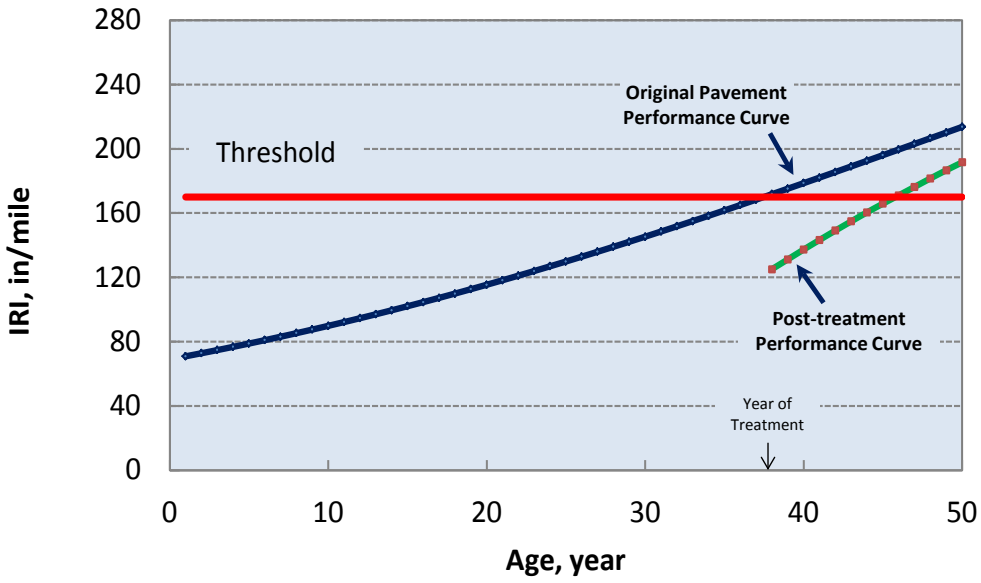

Figure 44 IRI predictions for Section 34-1030.

Pay Factor Curves

The same analysis configuration was conducted on this case study as the previous case studies, except for that an analysis period of 25 years was used here. The target mean and standard deviation values shown in Table 26 were used for the simulations.

Table 26 Case Study #4: AQC Target Mean and Standard Deviation Values

AQC Targets	Thick (in)	PP8 (%)	PP200 (%)	AC (%)	AV (%)	IRI_0 (in/mile)
Mean	1.8	32.0	7.1	5.6	6.1	110.0
Std. Dev.	0.20	2.50	0.80	0.20	0.90	5.0

Again, the PRS simulations were performed on seven levels of each AQC's mean value and three levels of each AQC's standard deviation value. A total of 21 combinations of mean and standard deviation levels were simulated for each AQC, and the simulation results are shown in Figure 46.

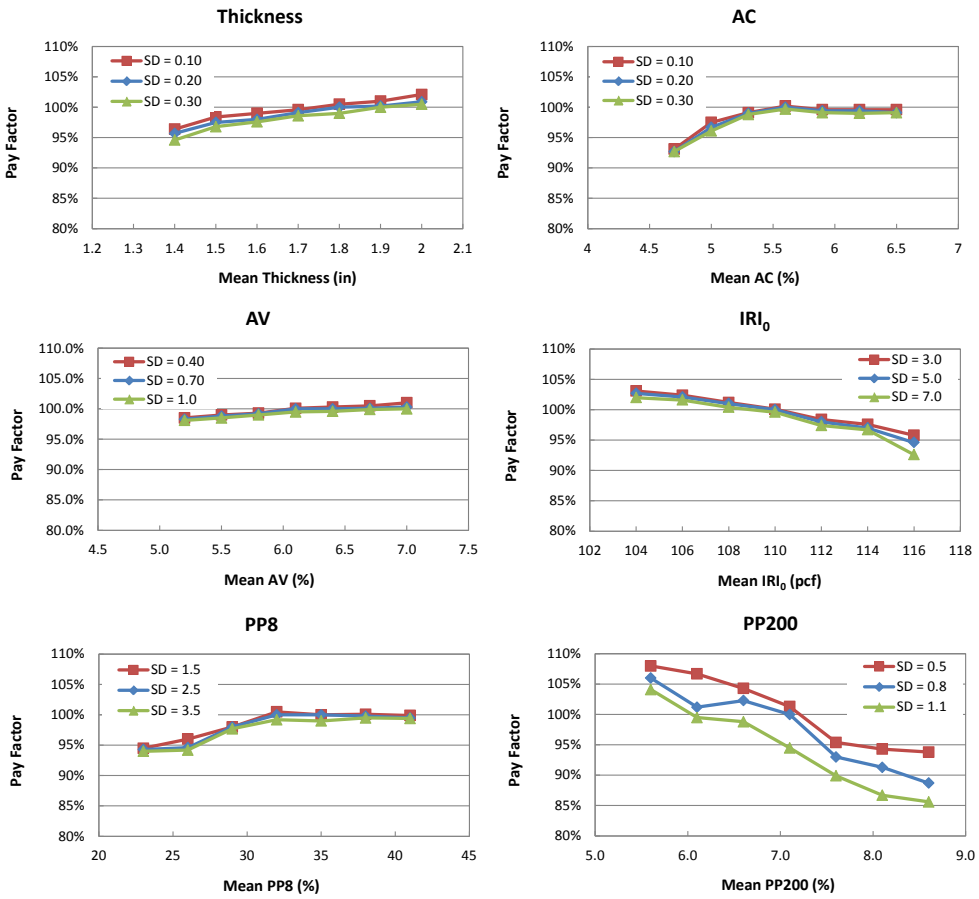

Figure 45 Pay factor curves for case study #4.

As shown in Figure 46, mean overlay Thickness and AV have a clear positive relationship with PF, within the studied ranges. In contrast, mean PP200 and IRI_0 have a clear negative relationship with PF. The PF curves with respect to mean AC have approximately concave down bell shape, indicating that the PF reaches maximum at the target AC level and decreases below 100% when the AC value deviates from the target level (i.e., 5.6%). With respect to PP8, the PF pattern is slightly different in that when PP8 is above 32%, the estimated PF becomes very stable around 100%. Therefore, in this particular case, lower PP200 and IRI_0 mean values lead to higher pay factors.

Similar to the other case studies, the PF curves of this case study have a consistent pattern: for any as-constructed mean value, as the standard deviation decreases, the pay factor increases.

Based on Figure 46, PP200 became the most influential factor on the lot PF, as the variation in PF can result in the PF varies from 85% to 108%. It was not consistent with what was observed in the previous three case studies. This might be due to the relatively higher range values of PP200 (i.e., 5.5% to 8.5%) in this case study, compared to the ranges of PP200 used in the previously case studies (2.4%-3.6%, 4%-7%, and 1.5%-3.4%, for case studies # 1, 2, and 3 respectively). Commonly required PP200 in HMA mix design is less than 7% (Cominsky 1994 and TxDOT 2004). In this case study, the PF corresponding to PP200 over 7% was lower than 100%, which was appropriate from the perspective of pavement engineering. The PF curves also show that AV has the lowest impact on the lot PF, and the other AQCs have a moderate impact on the final PF.

CONCLUDING REMARKS

To demonstrate and validate the applicability of the PRS methodology developed in this research, four case studies of thin HMA overlay on existing asphalt pavement were conducted. These case studies are LTPP test sections that represent different scenarios of existing pavement characteristics, site conditions, and thin HMA overlay quality.

Pay adjustment curves were developed to capture the variation of PF with respect to the variation in each AQC of the thin HMA overlay. These PF curves showed that the developed PRS methodology translates deviations from the target mean and target

standard deviation values into reasonable pay factors that represent the economic value of performance lost or gained due to differences between the treatment's target and as-constructed levels of quality.

With respect to mean overlay thickness and mean initial IRI, consistent patterns were found for all case studies: for overlay thickness, as the mean value increases, the PF increases; for initial IRI, as the mean value increases the PF decreases. With respect to asphalt content, air voids, percent passing #8 and #200 sieves, the patterns of PF versus mean AQC were not consistent among the case studies. This might be due to differences in the AQC range. For example, for air voids, a range of 5.7 to 6.3% was used in case study #1, whereas a range of 3.6 to 4.8% was used in case study #2. With respect to the effect of variability in the AQC (i.e., standard deviation) on the pay factor, a consistent pattern was found for all AQCs and all case studies: for any given as-constructed mean value, as the standard deviation increases, the pay factor decreases.

CHAPTER VII

SUMMARY, CONCLUSIONS, AND RECOMMENDATIONS

SUMMARY

During past decades, numerous endeavors have been made in the pavement community to develop performance-related specifications (PRS) for pavement constructions. Compared to traditional QC/QA specifications, PRS is more desirable because it employs objective mathematical relationships that correlate the initial quality of the pavement to its future performance. In this way, pay adjustment decisions can be made based on the performance lost or gained due to differences between the target and as-constructed levels of quality.

Although significant progress has been made for new pavement construction, the literature still lacks understanding of how PRS can be developed for and applied to pavement preservation treatments. This dissertation fills this gap in the literature and makes the following specific contributions:

- A systematic methodology for developing PRS for pavement preservation treatments was developed. To demonstrate the applicability of the developed PRS methodology, it was applied to thin HMA overlays (a commonly-used pavement preservation treatment).
- A novel modeling method was developed for predicting pavement post-treatment performance. The model consists of two tightly-coupled components: the first component is responsible for predicting the performance (e.g., IRI) of the existing pavement if no treatment was applied.

The second component is responsible for prediting the reduction in pavement deterioration due to the application of the preservation treatment.

- New models were developed using this approach for predicting the IRI of asphalt pavement treated with thin HMA overlay. Artificial neural networks (ANNs) were developed for predicting the IRI of the existing asphalt pavement and Bayesian regression models were developed for predicting the reduction in IRI due to applying the thin HMA overlay treatment.
- A novel approach for determining the probability distributions of service life and present-worth value (PWV) of pavement preservation treatments was developed. This approach allows for transforming the probabilistic distribution of pavement condition (predicted by the Bayesian model) into probability distributions for service life and PWV. Pay factors are then estimated based on the the difference between the as-constructed and target PWVs.
- Insights were obtained into the relationships between initial quality (measured in terms of both mean and standard deviation of key acceptance quality characteristics) and expected pay factors through analysis of real world case studies of pavements treated with thin HMA overlays.

CONCLUSIONS

The following concludions were made based on the results of this research:

- The developed ANNs for predicting IRI of asphalt pavement corrolate with the MEPDG IRI prediction model very closely. These ANNs have the

advantages of a) being independent (run as standalone algorithms), b) being rapid, and c) requiring fewer inputs.

- The Bayesian regression models developed to predict the reduction in IRI due to thin HMA overlay treatments have the advantages of considering seven key AQCs and high goodness of fit. The percent of outliers (i.e., data points falling within either 2.5% tail area of model predictions) were less than 5% for all the developed Bayesian models.
- The application of the PRS methodology to actual pavement sections showed that this methodology produces rational pay factor curves that account for both the mean and standard deviation of key AQCs.
- The following conclusions can be made based on the pay factor curves of the case studies:
    - With respect to mean overlay thickness and mean initial IRI, consistent patterns were found for all case studies: for overlay thickness, as the mean value increases, the PF increases; for initial IRI, as the mean value increases the PF decreases.
    - With respect to asphalt content, air voids, percent passing #8 and #200 sieves, the patterns of PF versus mean AQC were not consistent among the case studies. This might be due to differences in the AQC range. For example, for air voids, a range of 5.7 to 6.3% was used in case study #1, whereas a range of 3.6 to 4.8% was used in case study #2.

- With respect to the effect of variability in the AQC (i.e., standard deviation) on the pay factor, a consistent pattern was found for all AQCs and all case studies: for any given as-constructed mean value, as the standard deviation increases, the pay factor decreases.

- The impact of AQCs on the final PF vary between different pavement layouts. For example, different quality levels of percent air voids in HMA mix can result in a ±5% PF differentiation in Layout-1, whereas this effect is reduced to ±0.5% PF differentiation in Layout-3. The percent aggregate passing #200 sieve plays an important role in case study #4, whereas it is effective in the other three case studies. This might be due to the different ranges of AQC values that were used in these studies.
- Among the six AQCs of thin HMA overlay, asphalt content and initial IRI were found to be most influential for almost all four pavement layouts considered in this study. With exception of PP200 for layout-4, aggregate gradation (i.e., percent aggregate passing #200 sieve and # 8 sieve) has a minimal impact on the pay factor.

RECOMMENDATIONS

Studies are recommended in the future to enhance the developed PRS methodology and underlying models as follows:

- Extend the application of the developed methodology to other types of pavement preservation treatments. This study focuses on thin HMA overlays.

However, there are many types of pavement preservation treatments being widely used in the pavement industry.

- This study has focused on developing performance models for IRI only. Some other performance indicators, such as individual distress types, should also be considered in the future studies, if they are deemed to be adequate performance indicator for a particular preservation treatment type.
- The existing pavement structure is an important component in the developed PRS methodology. This research identified more than 15 different layer compositions from the LTPP database, but considered top four used layouts. Further studies can be conducted to consider other cross-sectional layouts of the existing pavement.
- Test the developed PRS methodology on additional case studies and field trials that represent broader climatic, traffic, and geographic conditions. A software user interface could be developed to integrate the components of the developed PRS components, take input values, perform PRS simulations, and report results in a user friendly manner.
- A mechanism for calibrating the developed ANNs for predicting the IRI of existing pavement was introduced in this dissertation. Future research efforts can also be focused on calibrating the ANNs using local pavement design and performance data.

REFERENCES

Aguiar-Moya, J. P. and Prozzi, J. A. (2011). *Development of Reliable Pavement Models*. Report No. SWUTC/11/161025-1, University of Texas at Austin, Austin, TX.

Aguiar-Moya, J. P., Banerjee, A., and Prozzi, J. A. (2009). *Sensitivity analysis of the M-EPDG using measured probability distributions of pavement layer thickness*. Compendium of CD-ROM Paper, Transportation Research Board, Washington D.C.

Ahn, S., Kandala, S., Uzan, J., and El-Basyouny, M.M. (2009). *Comparative analysis of input traffic data and MEPDG output of flexible pavements in State of Arizona*. Compendium of CD-ROM Paper, Transportation Research Board, Washington D.C.

Ali, H.A., and Tayabji, S.D. (1998). *Mechanistic Evaluation of Test Data from LTPP Flexible Pavement Test Sections*, Volume I. FHWA Report No. FHWA-RD-98-012, Federal Highway Administration: McLean, Virginia.

Alsugair, A. M., and Al-Qudrah, A. A. (1998). Artificial neural network approach for pavement maintenance. *Journal of Computing in Civil Engineering*, Vol. 12, No. 4, pp. 249-255.

Applied Research Associates (ARA). (2004). *Guide for Mechanistic-Empirical Design of New and Rehabilitated Pavement Structures* (Final Report), National Cooperative Highway Research Program, http://www.trb.org/mepdg/guide.htm.

Baus, R.L. and Stires, N.R. (2010). *Mechanistic-Empirical Pavement Design Guide Implementation*. FHWA/SCDOT Report No. FHWA-SC-10-01, University of South Carolina, June 2010.

Beale, M. H., Hagan, M. T., and Demuth, H. B. (2012). *Neural Network Toolbox User's Guide.* The MathWorks Inc., Natick, MA.

Brown, E. R., M. R. Hainin, A. Cooley, and G. Hurley. (2004). *Relationship of Air Voids, Lift Thickness, and Permeability in Hot Mix Asphalt Pavements.* NCHRP Report 531, National Cooperative Highway Research Program. Transportation Research Board. Washington, DC.

Chamberlin, W.P. (1995). *Performance-Related Specifications for Highway Construction and Rehabilitation.* NCHRP Synthesis of Highway Practice 212, Transportation Research Board, National Research Council, Washington, D.C.

Chen, C., and Zhang, J. (2011). Comparisons of IRI-Based Pavement Deterioration Prediction Models Using New Mexico Pavement Data. *Geo-Frontiers,* American Society of Civil Engineers, pp. 4594-4603.

Choi, J. H., Adams, T. M., and H. U., Bahia (2004). Pavement roughness modeling using back-propagation neural network. *Computer-Aided Civil and Infrastructure Engineering 19,* No. 4, pp. 295-303.

Cominsky, R. J., Huber, G. A., Kennedy, T. W., and Anderson, M. (1994). *The Superpave Mix Design Manual for New Construction and Overlays*, Report No. SHRP-A-407, Washington, DC: Strategic Highway Research Program.

Congdon, P. (2001). *Bayesian Statistical Modelling*. John Wiley & Sons, Ltd., New York.

Conover, W. (1980). *Practical Nonparametric Statistics*, 2nd ed. Wiley, New York.

Cuelho, E., Mokwa, R. and M., Akin (2006). *Preventive Maintenance Treatments of Flexible Pavements: A Synthesis of Highway Practice*. Publication No. FHWA/MT-06-009/8117-26, Montana Department of Transportation.

Darter, M. I., Hoerner, T. E., Smith, K. D., Okamoto, P. A., and Kopac, P. A. (1996). Development of prototype performance-related specification for concrete pavements. *Transportation Research Record: Journal of the Transportation Research Board*, No. 1544, pp. 81-90.

Elkins, G. E., Schmalzer, P., Thompson, T., Simpson, A, and Ostrom B. (2003). *Long-Term Pavement Performance Information Management System Pavement Performance Database User Reference Guide*. Publication No. FHWA-RD-03-088, Federal Highway Administration, Washington, D.C.

Eltahan A. A., Daleiden J. F., and Simpson A. L. (1999). Effectiveness of maintenance treatments of flexible pavements. *Transportation Research Record: Journal of the Transportaiton Research Board*, No. 1680, TRB, National Research Council, Washington D.C., pp. 18-25.

Epps J.A., Hand A, Seeds S., Schulz T., Alavi S., Monismith C.L., Deacon J.A., Harvey J.T., and Leahy R. (2002). *Recommended Performance-Related Specifications for Hot-Mix Asphalt Construction: Results of the Westrack Project,* NCHRP Report 455, Transportation Research Board of the National Academies, Washington, D.C., 2002.

Federal Highway Administration (FHWA). (1998). *Guide to Developing Performance-Related Specifications for PCC Pavements*, U.S. Department of Transportation, Federal Highway Administration, McLean, VA.

Federal Highway Administration (FHWA). (1999). *Pavement Preservation: A Road Map for the Future,* Publication No. FHWA-SA-99-015, Federal Highway Administration, Washington, D.C.

Federal Highway Administration (FHWA). (2005). *Pavement Preservation Definitions*, Memorandum, http://www.fhwa.dot.gov/pavement/preservation/091205.cfm.

Federal Highway Administration (FHWA). (2010). *Highway Statistics 2010*. Office of Highway Policy Information, Federal Highway Administration.

Fugro Consultants Inc., and Arizona State University (ASU). (2011). *A Performance-Related Specification for Hot-Mix Asphalt*, NCHRP Report 704, Transportation Research Board of the National Academies, Washington, D.C., 2011.

Funahashi, K. (1989). On the approximate realization of continuous mappings by neural networks. *Neural Networks*, Vol. 2, No. 3, pp. 183–192.

Garson, G. D. (1991). Interpreting neural-network connection weights. *AI Expert*, Vol. 6, No. 4, pp. 46-51.

Gelman, A., Meng, X. L., and Stern, H. (1996). Posterior predictive assessment of model fitness via realized discrepancies. *Statistica Sinica*, 6, pp. 733-759.

Geoffroy, D.N. (1996). *NCHRP Synthesis of Highway Practice 223: Cost-Effective Preventive Pavement Maintenance*, Project No. 20-5, FY 1993, Transportation Research Board, National Research Council, Washington, D.C.

Gravels, R.C. and Mahboub, K.C. (2006). Flexible pavement design: sensitivity of the NCHRP 1-37A pavement design guide, a global approach. *Airfield and Highway Pavements*, ASCE, pp. 224-235.

Guclu, A., Ceylan, H., Gopalakrishnan, K., and Kim, S. (2009). Sensitivity analysis of rigid pavement systems using the mechanistic-empirical design guide software. *Journal of Transportation Engineering*, American Society of Civil Engineers, pp. 555-562.

Guo, Z., and Uhrig, R. E. (1992). Sensitivity analysis and applications to nuclear power plant. *Neural Networks*, International Joint Conference on Neural Network, Vol. 2, pp. 453-458.

Haider, S. W., and Dwaikat, M. B. (2011). Estimating optimum timing for preventive maintenance treatment to mitigate pavement roughness. *Transportation Research Board: Journal of the Transportation Research Board*, No. 2235, Transportation Research Board of the National Academies, Washington, D.C.

Haykin, S. (2008). *Neural Networks and Learning Machines*, 3rd Edition. New York: Prentice Hall.

Hicks, R. G., Moulthrop, J. S., & Daleiden, J. (1999). Selecting a preventive maintenance treatment for flexible pavements. *Transportation Research Record: Journal of the Transportation Research Board*, No. 1680, Transportation Research Board of the National Academies, Washington, D.C.

Hoerner, T.E., and Darter, M.I. (1999). *Guide to Developing Performance-Related Specifications for PCC Pavements*, Volume I. FHWA Report FHWA-RD-98-155, Federal Highway Administration: McLean, Virginia.

Hoerner, T.E., Darter, M.I., Khazanovich, L., Titus-Glover, T., and Smith, K.L. (2000). *Improved Prediction Models for PCC Pavement Performance-Related Specifications*, Volume I, FHWA Report FHWA-RD-00-130, Federal Highway Administration: McLean, Virginia.

Hong, F., and Prozzi, J. A. (2006). Estimation of pavement performance deterioration using Bayesian approach. *Journal of infrastructure systems*, Vo. 12, No. 2, pp. 77-86.

Hornik, K., M. Stinchcombe, and H. White. (1989). Multilayer feedforward networks are universal approximators. *Neural Networks*, Vol. 2, No. 5, pp. 359–366.

Huang, Y.H. (2004). *Pavement Analysis and Design*, 2nd ed. University of Kentucky, Pearson Education, Inc.

Hughes, C. S. (1996). NCHRP Synthesis of Highway Practice 232: *Variability in Highway Pavement Construction*. Transportation Research Board, National Research Council, Washington, DC.

Hunter, A., Kennedy, L., Henry, J., and Ferguson, I. (2000). Application of neural networks and sensitivity analysis to improved prediction of trauma survival. *Computer Methods and Programs in Biomedicine*, Vol. 62, No. 1, pp. 11-19.

Iman, R.L., and Conover, W.J. (1982). A distribution-free approach to inducing rank correlation among input variables. *Communications in Statistics* B11, 311-334.

Indiana Department of Transportation (InDOT) (2013). *Indiana Design Manual*. Online version available at http://www.in.gov/indot/design_manual/files/Ch52_2013.pdf.

Jiménez, L. A., and Mrawira, D. (2011). Reliability-based initial pavement performance deterioration modelling. *International Journal of Pavement Engineering*, Vol. 12, No. 2, pp. 177-186.

Jiménez, L. A., and Mrawira, D. (2012). Bayesian regression in pavement deterioration modeling: revisiting the AASHO road test rut depth model. *Infraestructura Vial*, Vol. 14, No. 25.

Johnson, A.M. (2000). *Best Practices Handbook on Asphalt Pavement Maintenance*. Report No. 2000-04, Minnesota T2/LTAP Program, Center for Transportation Studies, University of Minnesota.

Kajner, L., Kurlanda, M., and Sparks, G. A. (1996). Development of Bayesian regression model to predict hot-mix asphalt concrete overlay roughness. Transportation Research Record: *Journal of the Transportation Research Board*, No. 1539, pp. 125-131.

Kim, S., Ceylan H., and Heitzman, M. (2005). Sensitivity analysis of design input parameters for two flexible pavement systems using the mechanistic-empirical pavement design guide, *Proceedings of the 2005 Mid-Continent Transportation Research Symposium*, Iowa State University, Ames, Iowa, August 2005.

Kleijnen, J. P. (1997). Sensitivity analysis and related analyses: a review of some statistical techniques. *Journal of Statistical Computation and Simulation*, Vol. 57, p.p. 111-142.

Kuźniar, K., and Waszczyszyn, Z. (2006). Neural networks and principal component analysis for identification of building natural periods. *Journal of Computing in Civil Engineering*, Vol. 20, No. 6, pp. 431-436.

La Torre, F., Domenichini, L., and Darter, M. I. (1998). Roughness prediction model based on the artificial neural network approach. *Proceedings of the 4th International Conference on Managing Pavements*, Transportation Research Board, Vol. 2.

Labi S., Mahmodi M.I., Fang C., and Nunoo C. (2007). *Cost-effectiveness of microsurfacing and thin HMA overlays: comparative analysis*, in the CD-ROM of the 86th Transportation Research Board Annual Meeting (No. 07-3265).

Lawrence, J., and Fredrickson, J. (1998). BrainMaker user's guide and reference manual. *California Scientific Software*, Nevada City, CA.

Link, W. A. and Barker, R. J. (2010). *Bayesian inference: with ecological applications*. Academic Press, London, UK.

Liu, L. and N.G. Gharaibeh. (2013). *Survival analysis of thin overlay and chip seal treatments using the long-term pavement performance data*, presented on the 92nd Annual Meeting of the Transportation Research Board, Washington, D.C.

Liu, L., M. Hossain, and R. Miller. (2010). Costs and benefit of thin surface treatments on bituminous pavements in Kansas, *Transportation Research Board: Journal of the Transportation Research Board*, No. 2150, Transportation Research Board of the National Academies, Washington, D.C., pp. 47-54.

Masad, S.A. and Little, D.N. (2004). *Sensitivity Analysis of Flexible Pavement Response and AASHTO 2002 Design Guide to Properties of Unbound Layers*. International Center for Aggregates Research (ICAR) Report 504-1, University of Texas at Austin.

McKay, M.D., Beckman, R. J. and Conover, W. J. (1979). A comparison of three methods of selecting values of input variables in the analysis of output from a computer code. *Technometrics* 21, pp. 239-245.

Michigan DOT. (2012). *Standard Specifications for Construction,* Item 505. Available at http://mdotwas1.mdot.state.mi.us/public/specbook/2012/

Molzer, C., Felsenstein, K., Litzka, J., and Shahm, M. (2001). Bayesian statistics for developing pavement performance models. In *Ponencia De La Fifth International Conference on Managing Pavements*, Ponencia (Vol. 39).

Morian, D. A., Gibson, S. D., and Epps, J. A. (1998). *Maintaining Flexible Pavements - The Long Term Pavement Performance Experiment SPS-3 5-Year Data Analysis*, FHWA-RD-97-102 Report, U.S. Department of Transportation.

Morian, D.A. (2011). *Cost Benefit Analysis of Including Microsurfacing in Pavement Treatment Strategies & Cycle Maintenance*. Report No. FHWA-PA-2011-001-080503, The Pennsylvania Department of Transportation, Harrisburg, PA, January 2011.

Mrawira, D., Welch, W. J., Schonlau, M., and Haas, R. (1999). Sensitivity analysis of computer models: World Bank HDM-III model. *Journal of Transportation Engineering*, Vol. 125, No. 5, pp. 421-428.

Najjar, Y. M., Basheer, I. A., and McReynolds, R. (1996). Neural modeling of Kansas soil swelling. *Transportation Research Record: Journal of the Transportation Research Board*, No. 1526, pp. 14-19.

National Cooperative Highway Research Program (NCHRP) (2011). *Performance-Related Specifications for Pavement Preservation Treatments*. NCHRP Project 10-82 Interim Report, Washington, D.C.

Neelon, B. H., O'Malley, A. J., and Normand, S. L. T. (2010). A Bayesian model for repeated measures zero-inflated count data with application to outpatient psychiatric service use. *Statistical Modeling*, 10(4), pp. 421-439.

Newcomb, D. E. (2009). *Thin Asphalt Overlays for Pavement Preservation*. NAPA Information Series 135, National Asphalt Pavement Association.

Nourani, V., and Sayyah Fard, M. (2012). Sensitivity analysis of the artificial neural network outputs in simulation of the evaporation process at different climatologic regimes. *Advances in Engineering Software*, Vol. 47, No. 1, pp. 127-146.

Orobio, A. and Zaniewski, J.P. (2011). Sampling-based sensitivity analysis of the mechanistic-empirical pavement design guide applied to material inputs, *Transportation Research Record: Journal of the Transportation Research Board*,

No. 2226, Transportation Research Board of the National Academies, Washington, D.C., pp. 85-93.

Owusu-Ababio, S. (1998). Effect of neural network topology on flexible pavement cracking prediction. *Computer-Aided Civil and Infrastructure Engineering*, Vol. 13, No. 5, pp. 349-355.

Papagiannakis, A.T. and Masad, E.A. (2008). *Pavement Design and Materials*. John Wiley & Sons, Inc., Hoboken, New Jersey.

Peshkin, D., Smith, K.L., Wolters, A., Krstulovich, J., Moulthrop, J. and Alvarado, C. (2011). *Guidelines for the Preservation of High-Traffic-Volume Roadways*. Strategic Highway Research Program (SHRP) 2 Report S-2-R26-RR-2, Transportation Research Board of the National Academies, Washington, D.C.

Peshkin, D.G., T.E. Hoerner, and K.A. Zimmerman. (2004). *Optimal Timing of Pavement Preventive Maintenance Treatment Applications*. NCHRP Report No 523. Transportation Research Board, National Research Council, Washington, D.C.

Reed, C.M. (1994). Seven-year performance evaluation of single pass, thin life bituminous concrete overlays. *Transportation Research Record: Journal of the Transportation Research Board*, No. 1454, Transportation Research Board of the National Academies, Washington, D.C.

Roberts, C. A., and Attoh-Okine, N. O. (1998). A comparative analysis of two artificial neural networks using pavement performance prediction. *Computer-Aided Civil and Infrastructure Engineering*, Vol. 13, No. 5, pp. 339-348.

Rooij, A. V., Johnson, R. P., and Jain, L. C. (1996). *Neural Network Training Using Genetic Algorithms*. World Scientific Publishing Co. Pte. Ltd., River Edge, New Jersey.

Sakhaeifar, M. S., Underwood, B. S., Kim, Y. R., Puccinelli, J., and Jackson, N. (2010). Development of artificial neural network predictive models for populating dynamic moduli of long-term pavement performance sections. Transportation Research Record: *Journal of the Transportation Research Board*, No. 2181, pp. 88-97.

SAS Institute Inc. SAS Online Doc, available at http://support.sas.com/onlinedoc/913/docMainpage.jsp, accessed 2013.

Sayers, M.W., Gillespie, T.D., and Queiroz, C.A.V. (1986). *The International Road Roughness Experiment.* World Bank Technical Paper 45, the World Bank, Washington, D.C.

Schwarts, C.W. and Carvalho, R.L. (2007). *Implementation of the NCHRP 1-37A Design Guide, Volume 2: Evaluation of Mechanistic-Empirical Design Procedure*. MDSHA No. SP0077B41, UMD FRS No. 430572, University of Maryland, February 2007.

Seeds, S. B., Basavaraju, R., Epps, J. A., and Weed, R. M. (1997). Development of performance-related specifications for hot-mix asphalt pavements through WesTrack. *Transportation Research Record: Journal of the Transportation Research Board*, No. 1575, Transportation Research Board of the National Academies, Washington, D.C., pp. 85-91.

Shafizadeh, K., and Mannering, F. (2003). Acceptability of pavement roughness on urban highways by driving public. Transportation Research Record: *Journal of the Transportation Research Board*, No. 1860, pp. 187-193.

Shekharan, A. R. (1999). Assessment of relative contribution of input variables to pavement performance prediction by artificial neural networks. *Transportation Research Record: Journal of the Transportation Research Board*, No. 1655, pp. 35-41.

Shi, J. J. (2000). Reducing prediction error by transforming input data for neural networks. *Journal of Computing in Civil Engineering*, Vol. 14, pp. 109-116.

Simpson, A. L., Rauhut, J. B., Jordahl, P. R., Owusu-Antwi, E., Darter, M. I., Ahmad, R., Pendleton, O. J., and Lee, Y. H. (1994). *Sensitivity Analyses for Selected Pavement Distresses*. SHRP Report No. SHRP-P-393, Strategic Highway Research Program, National Research Council, Washington, D.C.

Siraj, N., Mehta, Y.A., and Muriel, K.M. (2009). Verification of mechanistic-empirical pavement design guide for the State of New Jersey. *Proceedings of the 8th International Conference* (BCR2A'09), June 29 – July 2 2009, University of Illinois at Urban Champaign, Champaign, Illinois.

Smith, R., Freeman, T., and Pendleton, O. (1993). *Pavement Maintenance Effectiveness*. SHRP Report SHRP-H-358, National Research Council, Washington, D.C.

Smith, R.E. (2002). Integrating pavement preservation into a local agency pavement management system. *Transportation Research Record: Journal of the Transportation Research Board*, No. 1795, Transportation Research Board of the National Academies, Washington, D.C., pp. 27-32.

Spiegelhalter, D. J., Best, N. G., Carlin, B. P., and Van der Linde, A. (2002). Bayesian measures of model complexity and fit. *Journal of the Royal Statistical Society, Series B*, 64(4), pp. 583–616, with discussion.

Statisticat LLC. (2013). *Bayesian Inference*, online copy available at http://cran.r-project.org/web/packages/LaplacesDemon/vignettes/BayesianInference.pdf, accessed 2013.

Sumee, N. (2010). *Sensitivity of MEPDG Using Advanced Statistical Analyses*. Master's Thesis, University of New Mexico.

Tarefder, R.A., and Sumee, N. (2011). Evaluating sensitivity of pavement performance to mix design variables in MEPDG. *Geotechnical Special Publication*, No. 223, American Society of Civil Engineers, pp. 49-56.

Texas Department of Transportation (TxDOT). (2004). *Standard Specifications for Construction and Maintenance of Highways, Streets, and Bridges*, Item 341. Available at ftp://ftp.dot.state.tx.us/pub/txdot-info/des/spec/specbook.pdf

Train, K. (2001). A comparison of hierarchical Bayes and maximum simulated likelihood for mixed logit. *University of California, Berkeley*, pp. 1-13.

Transportation Research Board (TRB). (2009). *Glossary of Highway Quality Assurance Terms*. Electronic Circular E-C137, Transportation Research Board, 4th Update, Washington, DC.

Wade, M., R.l DeSombre, and D.G. Peshkin. (2001). *High Volume/High Speed Asphalt Roadway Preventive Maintenance Surface Treatments*. South Dakota Department of Transportation Report No. SD99-09.

Walls III, J., and Smith, M. R. (1998). *Life-Cycle Cost Analysis in Pavement Design-Interim Technical Bulletin*. FHWA-SA-98-079 Report, U.S. Department of Transportation

Weed, R. M. (2006). Mathematical modeling procedures for performance-related specifications. Transportation Research Record: *Journal of the Transportation Research Board*, No. 1946, pp. 63-70.0

Yang, J., Lu, J. J., Gunaratne, M., and Dietrich, B. (2006). Modeling crack deterioration of flexible pavements: comparison of recurrent Markov chains and artificial neural networks. *Transportation Research Record: Journal of the Transportation Research Board*, No. 1974, pp. 18-25.

Zhang, Z., Jaipuria, S., Murphy, M. R., Sims, T., and Garza, T. (2010). Pavement preservation: performance goal and its implications. *Transportation Research Record: Journal of the Transportation Research Board*, No. 2150, Transportation Research Board of the National Academies, Washington, D.C., pp. 28-35.

APPENDIX A

SUMMARY STATISTICS OF INPUT VARIABLES USED IN THE LHS PROCESS

Table A-1 Summary Statistics of Input Variables Used in the LHS Process

Category	Parameters	Layout 1 (600 Cases)			Layout 2 (700 Cases)			Layout 3 (700 Cases)			Layout 4 (1,000 Cases)		
		***a*[1]**	***b***	***PD*[2]**	***a***	***b***	***PD***	***a***	***b***	***PD***	***a***	***b***	***PD***
Site Factors	Initial AADTT, veh/day	100	3000	U	100	3000	U	100	3000	U	100	3000	U
	Comp. Growth Rate, %	0	10	U	0	10	U	0	10	U	0	10	U
HMA Surface Layer	Thickness, in	1	13	U	1	13	U	1	13	U	1	13	U
	Unit Weight, pcf	145.3	5.2	N	145.3	5.2	N	145.3	5.2	N	145.3	5.2	N
	Eff. Binder Content, %	5.5	0.8	N	5.5	0.8	N	5.5	0.8	N	5.5	0.8	N
	Air Voids, %	4.8	1.9	N	4.8	1.9	N	4.8	1.9	N	4.8	1.9	N
	% Retained on 3/4 Sieve	0	10	U	0	10	U	0	10	U	0	10	U
	% Retained on 3/8 Sieve	R34	40	U	R34	40	U	R34	40	U	R34	40	U
	% Retained on #4 Sieve	Max(R38,13)	60	U	Max(R38,13)	60	U	Max(R38,13)	60	U	Max(R38,13)	60	U
	% Passing #200 Sieve	5.7	1.6	N	5.7	1.6	N	5.7	1.6	N	5.7	1.6	N
Binder Course	Thickness, in				1	9	U				1	9	U
	Unit Weight, pcf				147.4	6.3	U				147.4	6.3	U
	Eff. Binder Content, %				4.9	0.8	N				4.9	0.8	N
	Air Voids, %				4.8	1.8	N				4.8	1.8	N
	% Retained on 3/4 Sieve				0	26	U				0	26	U
	% Retained on 3/8 Sieve				R34	50	U				R34	50	U
	% Retained on #4 Sieve				Max(R38,19)	65	U				Max(R38,19)	65	U
	% Retained on #200 Sieve				5.9	1.7	N				5.9	1.7	N
Granular Base	Thickness, in	1	30	U	1	30	U	1	30	U	1	30	U
	Plasticity Index	0	12	U	0	12	U	0	12	U	0	12	U
	Liquid Limit	PI	32	U	PI	32	U	PI	32	U	PI	32	U
	% Passing #200 Sieve	0	40	U	0	40	U	0	40	U	0	40	U
	% Passing #40 Sieve	Max(PP200,5)	70	U	Max(PP200,5)	70	U	Max(PP200,5)	70	U	Max(PP200,5)	70	U

[1] *a* and *b* are the LHS sampling parameters: 1) For uniform distributions, *a* and *b* are the minimum and maximum values, respectively; 2) For normal distributions, *a* and *b* are the mean and standard deviation, respectively.

[2] *PD* is the probability distribution of the corresponding variable, where *U* is uniform distribution and *N* is normal distribution.

Table A-1 Continued

Category	Parameters	Layout 1 (600 Cases)			Layout 2 (700 Cases)			Layout 3 (700 Cases)			Layout 4 (1,000 Cases)		
		a	***b***	***PD***	***a***	***b***	***PD***	***a***	***b***	***PD***	***a***	***b***	***PD***
	% Passing #10 Sieve	Max(PP40,13)	80	U	Max(PP40,13)	80	U	Max(PP40,13)	80	U	Max(PP40,13)	80	U
	% Passing #4 Sieve	Max(PP10,16)	90	U	Max(PP10,16)	90	U	Max(PP10,16)	90	U	Max(PP10,16)	90	U
	% Passing 1" Sieve	Max(PP4,40)	100	U	Max(PP4,40)	100	U	Max(PP4,40)	100	U	Max(PP4,40)	100	U
	Max Dry Unit Weight, pcf	135	7	N	135	7	N	135	7	N	135	7	N
	Opt. Moisture Content, %	7.4	2	N	7.4	2	N	7.4	2	N	7.4	2	N
Granular Subbase	Thickness, in							3	40	U	3	40	U
	Plasticity Index							0	11	U	0	11	U
	Liquid Limit							PI	32	U	PI	32	U
	% Passing #200 Sieve							3	35	U	3	35	U
	% Passing #40 Sieve							Max(PP200,8)	95	U	Max(PP200,8)	95	U
	% Passing #10 Sieve							Max(PP40,20)	100	U	Max(PP40,20)	100	U
	% Passing #4 Sieve							Max(PP10,30)	100	U	Max(PP10,30)	100	U
	% Passing 1" Sieve							Max(PP4,62)	100	U	Max(PP4,62)	100	U
	Max Dry Unit Weight, pcf							128.5	13	N	128.5	13	N
	Opt. Moisture Content, %							9.1	3	N	9.1	3	N
Subgrade	Plasticity Index	0	33	U	0	33	U	0	33	U	0	33	U
	Liquid Limit	PI	65	U	PI	65	U	PI	65	U	PI	65	U
	% Passing #200 Sieve	0	90	U	0	90	U	0	90	U	0	90	U
	% Passing #40 Sieve	Max(PP200,12)	100	U	Max(PP200,12)	100	U	Max(PP200,12)	100	U	Max(PP200,12)	100	U
	% Passing #10 Sieve	Max(PP40,20)	100	U	Max(PP40,20)	100	U	Max(PP40,20)	100	U	Max(PP40,20)	100	U
	% Passing #4 Sieve	Max(PP10,25)	100	U	Max(PP10,25)	100	U	Max(PP10,25)	100	U	Max(PP10,25)	100	U
	% Passing 1" Sieve	Max(PP4,63)	100	U	Max(PP4,63)	100	U	Max(PP4,63)	100	U	Max(PP4,63)	100	U
	Max Dry Unit Weight, pcf	116	10.3	N	116	10.3	N	116	10.3	N	116	10.3	N
	Opt. Moisture Content, %	12.8	3.8	N	12.8	3.8	N	12.8	3.8	N	12.8	3.8	N

APPENDIX B

FORMAT OF ANN AND ITS WEIGHT MATRIX

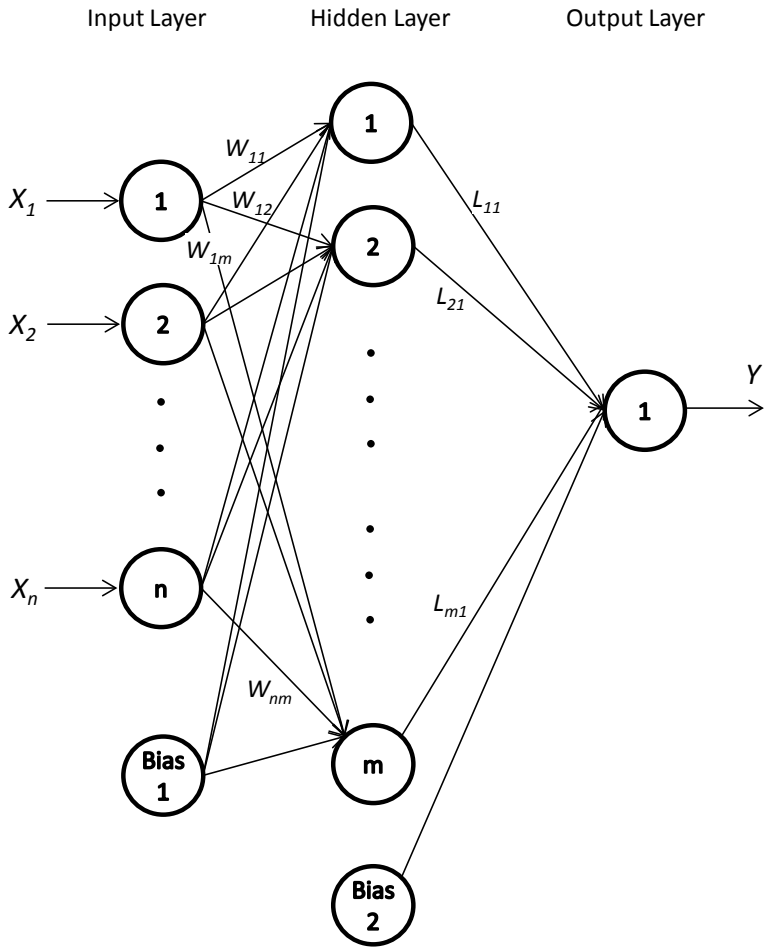

Figure B-1. Format of a typical ANN and connection weights.

APPENDIX C

WEIGHT MATRICES OF IRI ARTIFICIAL NEURAL NETWORKS

FOR PAVEMENT LAYOUTS 1 THROUGH 4

Table C-1 Connection Weights between Input and Hidden Layers for Layout-1

	w.1	w.2	w.3	w.4	w.5	w.6	w.7	w.8	w.9	w.10	w.11	w.12	w.13	w.14	w.15
W1.	1.23	-0.23	-1.39	-1.07	0.18	5.08	4.77	0.43	1.89	0.14	-0.28	-4.66	6.22	-1.82	3.56
W2.	0.37	-0.22	2.33	-0.23	-0.95	3.24	3.34	0.08	-0.47	0.07	-0.02	3.60	1.45	0.67	4.43
W3.	0.58	-0.54	-1.95	-0.10	4.52	5.15	2.72	0.17	0.64	0.17	-0.14	15.12	3.22	-2.48	-5.35
W4.	0.71	0.02	0.95	-0.21	-0.97	4.94	5.25	0.01	0.11	0.09	-0.60	16.84	-5.42	-2.14	-0.27
W5.	0.51	-0.26	-2.22	-0.19	0.65	9.05	0.85	-0.24	-1.50	0.09	-0.28	3.04	-16.10	-0.72	-8.10
W6.	-1.51	0.42	-0.65	1.15	-3.40	-4.17	-2.54	-0.26	0.01	-0.15	2.05	-5.78	4.55	0.69	15.92
W7.	-0.58	0.67	-7.14	0.87	-1.80	11.71	4.45	-0.33	0.70	-0.16	0.71	2.14	-1.98	-0.39	15.40
W8.	1.38	-0.64	6.26	-0.53	4.58	-2.86	3.75	0.08	0.17	0.13	-1.18	0.96	16.13	0.12	4.69
W9.	0.56	0.12	-2.68	0.33	-0.71	-2.78	0.21	-0.12	-0.17	0.03	-0.08	-2.18	-3.61	-0.14	0.08
W10.	0.14	-0.34	-0.58	-0.28	-1.79	-3.82	0.21	0.04	0.61	0.00	-0.05	-0.88	9.30	0.21	-4.50
W11.	0.21	0.21	2.91	-0.10	1.02	-1.21	3.26	0.03	-0.31	0.01	0.15	-4.77	-3.75	-1.51	-1.29
W12.	0.76	-0.29	1.11	0.40	-0.39	-1.36	-5.93	0.29	-0.68	0.16	-0.14	3.50	0.23	0.99	-11.56
W13.	-0.74	0.00	-0.12	-0.78	-6.76	-3.07	0.22	0.25	1.79	-0.03	-0.06	2.73	-8.15	-1.25	0.66
W14.	-1.06	0.03	1.24	0.96	-2.32	-5.87	-0.53	0.03	0.89	-0.07	0.30	-12.96	-0.88	-0.14	-1.07
W15.	0.45	0.15	-1.40	0.39	4.38	-3.34	-2.07	-0.02	0.60	0.06	0.08	2.52	-12.39	-0.25	0.76
W16.	0.06	-0.33	0.25	-0.64	2.30	1.77	-0.53	-0.04	-0.32	0.02	0.10	0.62	-10.55	0.14	-3.91
W17.	-0.38	0.20	2.64	0.28	0.42	-7.01	-0.32	0.08	0.06	-0.05	0.02	-0.90	0.40	1.01	-2.15
W18.	0.34	-0.68	1.25	0.14	1.28	-8.93	-3.04	-0.11	0.22	0.01	-0.39	-4.19	8.89	1.63	-0.24
W19.	0.39	-0.06	-7.69	0.18	-3.00	13.68	-2.37	-0.17	0.84	0.01	0.13	5.26	0.75	-1.22	-3.94
W20.	1.08	-0.02	0.66	-0.44	-7.13	-5.44	-1.61	0.25	-1.05	0.14	-0.17	-2.20	-7.26	-0.73	-1.44
W21.	1.35	0.91	4.94	0.95	0.98	11.34	-0.57	0.12	-1.18	0.05	0.08	0.81	11.30	-1.58	4.85
W22.	0.83	0.91	-0.74	1.43	6.41	6.21	-10.86	0.08	-1.82	0.10	0.40	13.11	5.10	0.64	-5.71
W23.	-0.41	-0.20	-3.27	0.06	2.74	12.88	0.87	-0.22	-1.28	0.02	0.05	-8.31	-5.67	-0.28	0.36
W24.	-0.21	-0.07	5.05	0.35	0.93	-10.85	-1.23	0.13	2.13	-0.05	-0.06	-8.11	0.88	-0.15	-2.20
W25.	0.51	-0.49	-0.43	0.13	1.13	1.42	-4.58	0.01	-0.18	0.09	-0.15	13.53	7.76	1.82	9.79
W26.	-0.16	-0.16	2.07	-0.15	6.49	1.40	-2.72	0.09	0.04	0.03	0.04	-8.25	0.74	1.06	1.94
W27.	0.66	0.61	-2.16	0.00	-3.06	-5.39	2.26	0.18	-0.92	0.07	0.02	12.96	-10.33	0.59	2.85
W28.	-0.31	-0.34	2.03	0.59	-1.58	-3.71	-7.94	-0.06	-1.03	-0.01	0.19	-3.42	1.08	1.96	3.58
W29.	-0.14	0.28	3.23	-0.11	-11.93	3.91	-9.49	0.08	-1.38	-0.06	-0.04	5.92	8.91	-1.41	0.28
W30.	-0.44	-0.10	0.57	0.03	-0.39	3.33	2.39	0.21	-0.05	-0.11	-0.70	0.13	0.47	0.01	-0.50

Table C-2 Connection Weights between Hidden and Output Layers for Layout-1

	L1.	L2.	L3.	L4.	L5.	L6.	L7.	L8.	L9.	L10.	L11.	L12.	L13.	L14.	L15.
L.1	0.233	-0.455	-0.102	0.230	0.120	0.094	0.068	0.866	-0.196	-3.021	-1.201	0.103	-0.090	-0.151	0.106

Table C-3 Biases for the Input and Hidden Neurons for Layout-1

B1	-1.53	-1.53	3.40	-0.39	11.92	-12.31	1.38	-0.01	0.73	-0.70	1.92	16.51	13.84	-2.70	-13.76
B2	-1.321														

Table C-4 Connection Weights between Input and Hidden Layers for Layout-2

	w.1	w.2	w.3	w.4	w.5	w.6	w.7	w.8	w.9	w.10	w.11	w.12	w.13	w.14	w.15
W1.	-0.63	5.00	11.41	5.81	6.98	0.69	-0.44	-0.05	0.73	-1.41	-17.40	-4.79	16.76	0.29	-0.35
W2.	-0.19	-6.50	7.75	10.81	1.94	0.05	-0.65	0.01	-2.38	0.64	6.11	0.65	7.57	-0.60	0.21
W3.	-1.10	2.42	-3.14	9.56	5.53	0.17	-0.29	0.10	-6.03	0.78	10.34	-5.25	6.73	0.01	0.10
W4.	-1.39	-1.54	0.04	7.32	-1.32	0.05	-0.12	0.07	2.78	1.40	-3.40	-0.80	-11.56	0.82	-0.07
W5.	-0.45	7.55	-1.28	2.86	1.69	-0.20	0.24	0.04	3.41	0.82	-6.45	0.39	0.52	1.68	0.34
W6.	5.66	4.42	-1.38	0.44	3.31	0.93	0.05	-0.14	8.83	0.49	-1.03	1.47	0.58	-1.18	1.25
W7.	0.30	-5.08	-8.37	-2.83	0.15	0.32	-0.14	0.03	-3.43	0.44	-4.91	2.52	1.21	0.61	-0.49
W8.	-0.14	8.00	-6.64	-2.75	-2.38	0.27	-0.24	0.04	-4.36	0.04	2.10	4.52	11.16	0.02	-0.16
W9.	-1.23	2.26	-3.09	-10.18	-2.41	-0.12	0.39	0.01	0.66	1.08	17.75	0.23	-12.53	0.53	0.05
W10.	-0.21	10.33	5.82	0.36	2.93	-0.02	0.16	0.01	3.75	0.34	-12.61	-3.05	-3.61	-0.39	-0.05
W11.	0.15	2.67	-0.49	3.45	-2.55	0.31	0.04	0.01	-7.08	0.61	8.91	1.62	-11.80	-0.11	-0.35
W12.	0.69	3.51	-6.87	-6.13	-1.69	0.56	-1.33	0.03	3.90	-0.55	-9.00	0.12	7.02	0.52	0.13
W13.	0.60	5.20	6.20	5.58	4.37	0.29	0.21	-0.01	0.26	0.56	5.55	0.15	8.58	-0.44	-0.17
W14.	-0.03	-4.00	-0.76	-3.02	-0.56	0.04	-0.25	-0.07	-2.54	-0.13	18.51	-3.33	11.32	0.12	0.16
W15.	2.68	4.48	-1.38	12.80	-0.60	0.37	-0.36	-0.10	-1.08	-0.35	7.63	2.47	-0.29	-0.75	0.48
W16.	0.45	-1.01	-4.66	-0.61	-1.98	0.72	-1.33	0.00	-0.45	-0.83	-3.46	4.08	-0.43	-0.18	0.44
W17.	-2.27	-3.13	3.41	1.80	3.06	-0.05	0.05	0.03	-3.47	-0.55	0.75	0.60	-9.01	0.44	-0.46
W18.	0.34	-0.48	-11.55	-7.62	-1.60	-0.21	0.65	0.04	0.55	-0.20	-5.20	4.00	-7.41	0.72	-0.28
W19.	0.00	-0.98	-12.70	4.25	-2.17	0.02	-0.22	0.02	-8.90	-0.72	1.12	0.69	-15.41	-0.22	-0.22
W20.	-0.45	-11.36	-1.77	-4.07	0.33	0.04	-0.17	0.00	-8.30	-0.48	-5.02	-0.27	3.04	-0.44	0.31
W21.	-0.44	-6.78	-8.64	4.53	0.57	-0.26	0.24	0.03	3.37	0.98	0.43	-1.39	13.51	0.01	-0.36
W22.	0.26	-2.17	6.47	-8.84	-3.48	0.17	-0.07	-0.01	-7.40	-0.11	3.24	2.28	-3.41	-0.08	0.28
W23.	0.20	-0.57	-4.31	0.57	-1.83	0.46	-0.48	-0.02	3.95	-0.32	-2.52	2.44	-11.05	0.01	0.06
W24.	0.83	-0.06	4.75	5.57	1.92	-0.77	0.95	-0.01	-2.94	-0.53	-5.46	-3.82	-3.53	0.19	-0.07
W25.	0.08	7.86	4.31	-2.10	2.59	-0.10	0.03	0.00	-1.33	0.12	3.17	-3.93	6.94	0.24	0.13
W26.	0.16	1.78	5.99	2.31	2.20	0.44	-0.62	-0.02	0.79	-0.36	-1.59	0.62	9.89	-0.05	0.11
W27.	-0.34	16.74	1.57	7.60	-1.08	-0.50	0.17	0.01	4.61	-0.65	3.62	-0.72	-12.57	0.25	0.04
W28.	-0.62	-7.05	6.24	-4.29	-2.14	0.35	-0.71	0.01	3.46	1.03	-2.53	2.27	7.57	-0.48	0.11
W29.	-0.13	2.30	-7.33	7.65	2.14	0.23	0.66	-0.05	-10.77	-0.91	3.82	0.45	-3.89	0.49	-0.09
W30.	0.37	-2.10	-6.24	-10.77	-1.86	0.54	-0.10	-0.03	-7.25	-0.34	10.09	-0.52	-17.25	0.45	-0.10
W31.	0.16	-0.38	-7.21	-18.96	-0.85	-0.05	0.07	0.03	2.83	-1.10	-0.48	5.98	-13.03	-0.86	-0.10
W32.	0.33	-8.40	-6.75	0.62	-1.23	-0.02	0.32	0.03	-6.53	0.08	-4.73	1.15	-8.00	0.36	0.03
W33.	0.12	0.44	-8.22	-8.95	-1.38	0.38	-0.10	0.00	3.64	0.32	1.03	0.99	-3.84	0.35	0.10
W34.	-0.74	-3.54	4.76	2.22	4.37	0.11	-0.24	0.09	-0.35	0.46	-10.43	1.88	2.37	0.26	-0.01
W35.	0.02	-1.27	-3.79	2.57	0.03	-0.63	0.74	-0.02	-1.11	0.08	1.02	-2.14	14.27	-0.15	0.13
W36.	-0.79	-1.45	-9.55	6.82	-1.57	-0.03	-0.76	0.01	8.56	-0.89	-12.41	-2.99	2.67	0.98	0.09
W37.	0.49	-2.18	-6.24	-13.49	-1.29	0.13	0.30	0.01	-0.38	-0.49	5.09	2.65	-6.02	0.01	-0.40
W38.	-0.63	-2.87	0.39	-8.89	-7.05	0.07	-0.33	-0.04	3.59	0.78	4.13	-0.19	-5.95	-0.29	0.02
W39.	-0.67	-1.81	1.02	-0.61	-0.16	-0.01	0.02	0.28	1.20	-0.30	0.97	0.25	-1.46	0.78	0.47

Table C-5 Connection Weights between Hidden and Output Layers for Layout-2

	L1.	L2.	L3.	L4.	L5.	L6.	L7.	L8.	L9.	L10.	L11.	L12.	L13.	L14.	L15.
L.1	-1.552	-0.033	0.036	0.044	-0.054	0.138	0.099	1.470	0.037	-0.077	0.039	-0.040	0.028	11.967	0.152

Table C-6 Biases for the Input and Hidden Neurons for Layout-2

B1	8.02	20.70	3.68	15.17	3.04	0.12	-0.69	-0.51	0.79	1.28	-3.06	1.28	5.41	-6.84	-2.05
B2	13.815														

Table C-7 Connection Weights between Input and Hidden Layers for Layout-3

	w.1	w.2	w.3	w.4	w.5	w.6	w.7	w.8	w.9	w.10	w.11	w.12	w.13	w.14	w.15
W1.	0.17	-15.26	-4.62	0.84	-5.09	-14.06	-0.36	-0.49	-5.85	-13.47	-1.28	-0.25	-0.95	3.03	5.95
W2.	0.14	14.46	1.42	-2.57	0.57	-4.34	-7.46	0.11	-2.76	10.61	-3.44	0.00	4.39	14.26	1.37
W3.	0.19	6.97	-3.86	0.83	-2.72	0.40	6.18	-0.12	-6.45	3.61	-8.80	-0.09	-0.21	1.65	5.52
W4.	0.70	19.23	5.54	1.22	0.05	13.82	-0.57	0.54	-1.68	10.75	5.57	-0.71	-1.65	-4.81	7.71
W5.	-0.04	5.78	3.01	0.19	-0.84	25.02	2.03	0.03	-1.83	2.53	-2.88	-0.45	0.42	8.96	4.73
W6.	-0.03	25.22	-1.67	-1.52	-0.63	12.89	-8.86	0.17	-0.76	-16.09	5.29	2.27	4.40	1.45	-4.91
W7.	-0.35	-6.71	-10.14	-2.97	-0.87	-0.29	0.79	-0.29	10.72	23.43	-4.35	0.42	3.05	5.96	6.23
W8.	0.03	0.93	-4.41	3.16	-4.39	14.70	3.17	0.15	10.11	-25.47	-11.02	-1.09	-2.43	1.39	-5.01
W9.	0.00	-8.21	0.86	2.78	-2.65	3.94	4.91	-0.08	-11.41	-13.09	-1.12	0.07	0.61	-13.81	-2.93
W10.	0.09	8.16	2.75	-2.22	1.56	1.27	1.26	0.13	-1.08	8.41	-0.19	-0.03	0.08	9.55	2.14
W11.	0.11	14.70	-1.69	-3.42	-3.13	-13.86	2.47	-0.19	1.34	-26.43	5.13	0.08	2.81	-3.13	0.86
W12.	-0.13	0.29	2.23	1.61	-2.23	-25.98	-0.40	-0.01	0.50	23.70	-3.48	-0.17	-1.39	-7.37	2.97
W13.	0.36	-28.30	4.68	-1.78	-7.09	3.17	1.69	0.06	-3.23	-11.35	4.27	-0.15	0.31	-1.20	-3.15
W14.	0.07	-0.97	-0.33	-4.47	0.20	-17.24	6.59	0.10	1.72	2.11	-0.08	0.04	0.41	3.50	-3.32
W15.	-0.09	13.65	2.72	-0.76	3.04	3.30	16.41	0.18	-5.14	2.25	-0.96	0.14	-3.72	-8.27	-1.11
W16.	0.16	10.75	-4.54	-0.70	-1.51	-12.57	3.23	0.03	-2.42	12.77	-10.94	-0.32	0.49	-0.73	10.06
W17.	-0.18	-7.88	4.20	3.16	4.52	-10.80	1.93	0.20	2.17	12.91	-2.84	0.16	-1.24	-1.71	-6.53
W18.	0.19	13.40	-4.90	-6.83	-0.86	-14.44	6.50	0.03	0.75	-30.71	-1.76	-0.19	0.15	-0.69	-10.41
W19.	0.00	-24.72	-1.06	2.70	-1.00	-0.78	-7.06	-0.12	-5.93	-17.39	2.87	0.06	0.29	-14.96	4.19
W20.	-0.12	-29.95	-4.77	3.05	3.57	-18.74	-14.17	-0.07	-5.79	-7.55	3.62	0.44	4.45	-22.61	4.00
W21.	0.10	2.80	-2.81	-2.45	0.27	-1.82	-0.19	-0.17	-0.61	-8.24	-1.45	0.10	2.31	11.23	2.29
W22.	0.08	-11.63	-3.70	-3.08	-4.16	9.49	-1.83	-0.05	-4.57	-13.91	-7.80	-0.24	3.27	7.35	-9.35
W23.	0.02	24.03	9.77	2.96	-3.33	8.29	-11.22	-0.08	-3.73	-7.25	-1.08	0.14	-4.85	1.23	-5.06
W24.	-0.37	-3.98	-3.11	-0.27	0.35	-7.26	-2.74	-0.03	0.59	-17.76	-3.82	-0.07	10.48	-9.07	0.95
W25.	0.21	2.57	-9.77	2.86	-1.92	15.24	-15.57	-0.06	14.09	5.39	-4.22	0.08	-3.40	2.80	3.49
W26.	-0.10	3.56	-7.12	0.14	0.10	7.23	4.54	0.00	-2.38	0.43	5.09	-0.03	4.26	-3.97	-13.06
W27.	-0.24	-8.23	-0.15	1.49	5.80	-14.22	13.22	-0.05	1.15	-13.04	1.87	-0.12	2.46	2.90	-6.66
W28.	0.13	-29.15	-0.29	-0.19	0.40	-1.16	5.65	0.17	2.90	6.72	1.20	-0.18	0.20	2.90	-1.44
W29.	0.02	29.70	-1.12	-0.97	7.03	2.46	-12.18	0.06	-1.38	-5.21	0.35	0.17	1.77	7.03	-1.48
W30.	0.18	10.59	1.29	-2.48	-4.48	-15.04	-0.85	0.09	4.29	-3.23	4.47	0.06	3.59	0.61	1.83
W31.	0.18	-5.20	-3.42	1.96	-1.05	3.59	-3.42	0.15	-5.44	-8.06	-8.22	0.05	1.17	-10.23	-1.78
W32.	0.40	-1.98	1.45	0.55	-0.52	2.20	1.48	-0.38	0.41	1.18	-2.72	-0.66	-0.03	-0.12	-2.03

Table C-8 Connection Weights between Hidden and Output Layers for Layout-3

	L1.	L2.	L3.	L4.	L5.	L6.	L7.	L8.	L9.	L10.	L11.	L12.	L13.	L14.	L15.
L.1	0.388	0.092	0.091	0.132	0.093	0.068	0.100	-0.477	0.093	0.108	-0.064	-1.186	0.097	-0.119	-0.081

Table C-9 Biases for the Input and Hidden Neurons for Layout-3

B1	0.32	28.61	-0.07	-3.36	-3.04	-5.15	6.60	-0.23	-0.63	7.56	-1.15	2.28	-8.75	-8.22	-1.15
B2	0.531														

Table C-10 Connection Weights between Input and Hidden Layers for Layout-4

	w.1	w.2	w.3	w.4	w.5	w.6	w.7	w.8	w.9	w.10	w.11	w.12	w.13	w.14	w.15
W1.	-0.06	0.24	2.70	2.59	-1.76	-1.76	-4.48	4.10	2.51	2.11	-8.24	-2.04	-6.43	-0.38	0.56
W2.	0.02	1.61	0.27	-0.12	4.03	-1.38	-2.98	-0.96	-0.05	-0.21	-0.44	-0.51	-0.86	-1.07	2.17
W3.	0.08	2.73	2.80	1.91	-0.67	-0.58	-2.56	5.49	2.12	1.58	-11.06	4.29	3.88	-0.87	2.76
W4.	0.06	-0.36	2.43	-0.20	2.07	1.41	-1.81	-4.31	-3.15	0.95	4.94	7.34	-2.48	0.65	1.64
W5.	0.04	1.30	0.59	-0.25	-1.34	-2.62	1.87	-2.28	0.29	-1.58	-3.65	2.83	-0.45	1.90	0.25
W6.	-0.10	3.31	-0.69	-0.04	4.26	-0.44	0.49	0.80	-1.41	-0.33	3.13	-1.18	-4.82	-8.10	0.10
W7.	0.03	3.46	1.14	-0.15	-8.81	-0.54	3.96	0.13	2.08	0.19	6.92	2.74	6.62	1.78	-0.75
W8.	0.03	0.55	-2.09	-0.08	4.96	0.11	-0.67	3.98	0.19	-1.58	1.72	3.55	1.15	0.22	4.77
W9.	0.01	-1.15	-3.90	-0.40	-0.35	-2.35	4.02	0.00	-2.07	0.74	-5.62	-7.27	-6.02	-0.70	2.16
W10.	0.00	1.47	3.08	-0.24	0.57	0.30	-0.60	4.14	-2.96	-0.14	-5.25	-1.45	1.50	0.04	2.92
W11.	-0.01	5.46	-0.28	0.05	2.50	-3.08	-0.12	4.73	-1.35	1.10	4.89	-0.61	-4.94	1.18	4.17
W12.	0.01	-4.95	-3.60	0.19	-1.74	-2.73	-1.69	5.51	-0.48	-1.43	1.61	0.97	-0.30	-0.28	0.84
W13.	-0.01	2.82	-0.28	-0.25	-2.78	3.39	5.18	4.37	0.51	1.77	-2.06	-5.31	-1.26	-0.23	-2.58
W14.	-0.03	0.71	-0.58	-0.02	-0.60	-3.27	3.75	5.12	1.12	-0.82	0.00	-0.43	-4.21	0.04	-1.20
W15.	-0.07	5.21	1.75	0.26	-0.06	5.82	0.27	0.42	1.77	0.16	-6.11	0.27	-3.16	-3.96	-0.69
W16.	0.01	0.65	1.48	0.02	1.84	-0.52	7.95	2.73	0.77	0.03	-5.58	-1.17	8.00	0.04	5.19
W17.	0.01	-3.97	-1.35	0.07	-1.29	-2.62	2.38	3.89	-0.83	3.00	0.40	-1.67	0.26	3.21	1.96
W18.	0.01	0.87	-1.11	0.25	-3.28	1.45	1.67	6.31	3.39	0.63	0.44	-2.39	5.28	-0.14	0.33
W19.	0.00	2.26	-1.21	0.19	-3.48	-0.89	-0.84	4.24	1.38	-0.43	4.84	-0.07	2.97	-0.10	-0.64
W20.	0.01	-2.12	-0.41	0.07	5.18	-0.60	-2.19	-0.79	0.46	-0.66	0.33	2.81	3.12	-0.88	2.34
W21.	0.00	-0.72	0.46	-0.21	1.55	-1.54	1.29	4.62	-3.62	1.21	2.14	-1.46	2.70	-0.79	3.09
W22.	0.00	-1.24	-2.63	-0.06	-1.86	-1.04	3.02	2.53	-0.13	1.63	1.23	-1.06	3.41	0.25	-2.14
W23.	-0.02	-3.11	-0.25	-0.17	1.66	3.75	-1.06	1.09	1.19	-0.37	-3.47	-1.70	0.18	-0.71	-1.85
W24.	0.00	1.02	1.28	0.11	6.66	-5.38	0.90	7.72	4.21	0.10	4.96	-1.75	-8.26	-0.55	6.88
W25.	0.00	-0.02	-0.81	0.12	3.38	0.58	0.78	2.49	-0.76	1.81	-1.47	-0.98	2.11	0.36	5.02
W26.	-0.01	1.70	2.70	-0.48	-0.01	4.17	-1.68	1.95	-1.72	-1.18	-3.43	1.30	-1.87	-0.28	1.47
W27.	0.00	-1.97	0.62	0.18	-2.45	-0.25	-1.64	-1.38	-1.91	1.51	2.40	-1.31	2.75	1.14	-1.83
W28.	0.00	-3.68	0.61	-0.45	-5.29	3.70	4.02	1.11	0.20	-0.54	-4.90	-0.64	4.01	0.94	-3.78
W29.	-0.03	-0.67	-4.69	-0.16	10.17	0.37	-1.84	3.01	-1.83	-0.77	3.83	-4.09	0.31	-0.62	2.95
W30.	0.04	-4.14	1.22	-0.15	-0.95	-8.25	5.99	3.76	1.64	0.52	-0.09	-1.73	-0.10	1.01	2.96
W31.	0.03	1.34	0.18	0.16	-1.98	-8.58	5.98	1.01	3.65	2.82	0.53	-2.38	1.22	0.15	-1.66
W32.	0.01	2.80	0.87	0.15	7.39	-1.92	0.75	0.02	1.24	1.42	2.38	-2.14	-5.08	-0.20	6.46
W33.	0.00	0.68	0.17	-0.15	-0.65	3.90	0.49	-4.39	-1.14	2.72	3.79	-3.48	3.03	0.82	-1.13
W34.	0.00	3.81	0.60	0.21	-1.05	0.18	-1.40	-1.47	-1.26	-0.58	-1.38	-0.29	1.12	-0.92	1.95
W35.	-0.01	1.19	0.21	-0.10	0.94	5.19	-0.13	-1.93	0.41	1.50	1.06	1.25	-1.10	0.03	-1.12
W36.	-0.01	-2.16	-3.33	0.27	-2.26	-3.93	5.72	0.32	-2.80	2.88	0.75	-0.36	1.51	0.29	-4.16
W37.	0.02	-1.41	0.85	-0.32	9.17	2.22	-1.52	-6.58	0.94	1.62	-2.30	-4.97	-6.91	-0.07	6.99
W38.	-0.02	-3.11	0.54	-0.40	-0.44	3.05	-0.52	3.45	-0.06	-0.24	-1.71	-1.15	0.53	-0.39	0.33
W39.	-0.01	2.63	4.72	-0.57	0.87	-0.11	2.12	-2.48	-0.03	-0.60	1.72	-2.05	-5.54	-0.74	1.97
W40.	0.05	1.44	-1.37	0.05	-3.74	1.93	-1.61	0.40	4.14	-0.68	4.29	4.24	0.19	0.50	-0.38
W41.	0.00	0.65	-0.94	0.53	-2.95	0.37	-3.08	5.95	1.25	-1.99	-5.02	-2.16	2.53	0.60	2.23
W42.	0.05	1.49	2.26	-0.35	0.42	3.75	-3.79	4.37	2.93	-1.70	-2.43	-1.20	-4.07	-0.16	3.86

Table C-11 Connection Weights between Hidden and Output Layers for Layout-4

	L1.	L2.	L3.	L4.	L5.	L6.	L7.	L8.	L9.	L10.	L11.	L12.	L13.	L14.	L15.
L.1	1.694	-0.050	0.044	0.096	0.038	0.052	0.048	0.032	-0.047	-0.054	0.036	-0.045	-0.037	7.067	-0.056

Table C-12 Biases for the Input and Hidden Neurons for Layout-4

B1	-0.70	12.76	11.53	1.71	-8.73	-0.02	-1.64	0.72	1.27	-0.31	-3.73	2.10	-6.14	-12.66	-8.81
B2	7.349														

APPENDIX D

COMPUTER PROGRAMMING CODES WRITTEN IN THIS STUDY

LHS CODES USED FOR GENERATING MEPDG SIMULATION DATA

The following Matlab codes were written for generating the MEPDG simulation datasets for pavement design layouts 1 through 4:

```
function [X S_Class] = genFinalData(n,layout)
%Generate final data sets for different pavement structural layouts.
%   n = sample size of the data set to be generated.
%   layout: 1 for OSL-GB-SS, 2 for OSL-BC-GB-SS, 3 for OSL-GB-SB-SS, and 4 for
OSL-BC-GB-SB-SS.
%   X = output for generated LHS sample data with a sample size of n.
%   S_Class = soil classifications for data in X, in columns for
base/subbase/subgrade layers depending on the layout.

if layout~=1 && layout~=2 && layout~=3 && layout~=4
    disp('please input a valid layout value, from 1, 2, 3, and 4.')
    X=[];S_Class={};
else
    disp('generating simulation data...')

RandStream('mt19937ar','Seed',12);

if layout == 1  % layout #1 AC-GB-SS
    X=zeros();
    X(1:n,:)=1:n;
    S_Class={};

    % site condition and traffic
    X(:,2:3)=lhs_empirco(coordinate,n);
    X(:,4)=lhsu(3,15,n);  % watertable depth, ft
    X(:,5)=lhsu(5,3000,n); % AADTT
    X(:,6)=lhsu(0,10,n); % growth rate (%)

    % original surface layer
    X(:,7)=lhsu(1,13,n);  % thickness, in.
    X(:,8)=floor(lhsu(1,12,n));  % binder type
    X(:,9:12)=genGradation(n,1); % generate surface layer aggregate gradation
    X(:,13)=latin_hs(145.3,5.2,n,1); % unit weight, pcf
    X(:,14)=latin_hs(5.5,0.8,n,1); % asphalt content
    X(:,15)=lhs_empir(OSL_av,n); % air voids
    for i=1:n
        S_Class{i,3}=checkBinderType(X(i,8));  % OSL layer binder type
    end

    % base layer
    X(:,21:27)=genGradation(n,3); % generate base aggregate gradation and PI/LL
    for i=1:n
        while (strcmp(checkSoilClass(X(i,21:27)),'A-4')~= 0) |
(strcmp(checkSoilClass(X(i,21:27)),'A-6')~= 0) % for those 'A-4' or 'A-6' cases,
the soil gradation needs to be regenerated.
            X(i,21:27)=genGradation(1,3);
        end
    end
    %X(:,16)={};   % base material type, will be filled from S_Class{:,1}
    X(:,17)=lhsu(1,30,n);  % thickness
    X(:,19)=latin_hs(135,7,n,1);  % max dry density, pcf
```

```
    X(:,20)=latin_hs(7.4,2,n,1);  % optimum moist content
    for i=1:n
        while X(i,20)./(62.4./X(i,19)-1/2.7)>=100   % regenerate data if the
calculated degree of saturation >= 100%
            X(i,19)=latin_hs(135,7,1,1);
            X(i,20)=latin_hs(7.4,2,1,1);
        end
    end
    for i=1:n
        S_Class{i,1}=checkSoilClass(X(i,21:27));  % define checkSoilClass
    end
    for i=1:n
        switch S_Class{i,1}
            case 'A-1-a'
                X(i,18)=lhsu(16000,42000,1);
            case 'A-1-b'
                X(i,18)=lhsu(16000,40000,1);
            case 'A-2-4'
                X(i,18)=lhsu(14000,37500,1);
            case 'A-2-5'
                X(i,18)=lhsu(14000,33000,1);
            case 'A-2-6'
                X(i,18)=lhsu(14000,31000,1);
            case 'A-2-7'
                X(i,18)=lhsu(14000,28000,1);
            case 'A-3'
                X(i,18)=lhsu(14000,35500,1);
            case 'A-4'
                X(i,18)=lhsu(13000,29000,1);
            case 'A-5'
                X(i,18)=lhsu(6000,25500,1);
            case 'A-6'
                X(i,18)=lhsu(12000,24000,1);
            case 'A-7-5'
                X(i,18)=lhsu(8000,17500,1);
            case 'A-7-6'
                X(i,18)=lhsu(5000,13500,1);
        end
    end

    % subgrade
    %X(:,28)=()  % subgrade material type, will be filled from S_Class{:,2}
    X(:,30)=latin_hs(116,10.3,n,1);  % max dry density, pcf
    X(:,31)=latin_hs(12.8,3.8,n,1);  % optimum moist content
    for i=1:n
        while X(i,31)./(62.4./X(i,30)-1/2.7)>=100   % regenerate data if the
calculated degree of saturation >= 100%
            X(i,30)=latin_hs(116,10.3,1,1);
            X(i,31)=latin_hs(12.8,3.8,1,1);
        end
    end
    X(:,32:38)=genGradation(n,5);    % generate subgrade gradation and PI/LL
    for i=1:n
        S_Class{i,2}=checkSoilClass(X(i,32:38));
    end
    for i=1:n
        switch S_Class{i,2}
            case 'A-1-a'
                X(i,29)=lhsu(16000,42000,1);
            case 'A-1-b'
```

```
                X(i,29)=lhsu(16000,40000,1);
            case 'A-2-4'
                X(i,29)=lhsu(14000,37500,1);
            case 'A-2-5'
                X(i,29)=lhsu(14000,33000,1);
            case 'A-2-6'
                X(i,29)=lhsu(14000,31000,1);
            case 'A-2-7'
                X(i,29)=lhsu(14000,28000,1);
            case 'A-3'
                X(i,29)=lhsu(14000,35500,1);
            case 'A-4'
                X(i,29)=lhsu(13000,29000,1);
            case 'A-5'
                X(i,29)=lhsu(6000,25500,1);
            case 'A-6'
                X(i,29)=lhsu(12000,24000,1);
            case 'A-7-5'
                X(i,29)=lhsu(8000,17500,1);
            case 'A-7-6'
                X(i,29)=lhsu(5000,13500,1);
        end
    end

elseif layout==2  % layout #2  AC-AC-GB-SS
    X=zeros();
    X(1:n,:)=1:n;
    S_Class={}; % column 1 = base matl type; column 2 = subgrade matl type;
column 3 = OSL asphalt type; column 4 = Binder asphalt type

    % site condition and traffic
    X(:,2:3)=lhs_empirco(coordinate,n);
    X(:,4)=lhsu(3,15,n);  % watertable depth, ft
    X(:,5)=lhsu(5,3000,n); % AADTT
    X(:,6)=lhsu(0,10,n); % growth rate (%)

    % original surface layer
    X(:,7)=lhsu(1,13,n);  % thickness, in.
    X(:,8)=floor(lhsu(1,12,n));  % binder type
    X(:,9:12)=genGradation(n,1); % generate surface layer aggregate gradation
    X(:,13)=latin_hs(145.3,5.2,n,1); % unit weight, pcf
    X(:,14)=latin_hs(5.5,0.8,n,1); % asphalt content
    X(:,15)=lhs_empir(OSL_av,n); % air voids
    for i=1:n
        S_Class{i,3}=checkBinderType(X(i,8));  % OSL layer binder type
    end

    % binder course layer
    X(:,16)=lhsu(1,9,n);  % thickness, in.
    X(:,17)=floor(lhsu(1,12,n));  % binder type
    X(:,18:21)=genGradation(n,2); % generate surface layer aggregate gradation
    X(:,22)=latin_hs(147.4,6.3,n,1); % unit weight, pcf
    X(:,23)=latin_hs(4.9,0.8,n,1); % asphalt content
    X(:,24)=lhs_empir(BC_av,n); % air voids
    for i=1:n
        S_Class{i,4}=checkBinderType(X(i,17));  % Binder course layer binder
type
    end

    % base layer
```

```
    X(:,30:36)=genGradation(n,3); % generate base aggregate gradation and PI/LL
    for i=1:n
        while (strcmp(checkSoilClass(X(i,30:36)),'A-4')~= 0) |
(strcmp(checkSoilClass(X(i,30:36)),'A-6')~= 0) % for those 'A-4' or 'A-6' cases,
the soil gradation needs to be regenerated..
            X(i,30:36)=genGradation(1,3);
        end
    end
    %X(:,25)={};   % base material type, will be filled from S_Class{:,1}
    X(:,26)=lhsu(1,30,n);  % thickness
    X(:,28)=latin_hs(135,7,n,1);  % max dry density, pcf
    X(:,29)=latin_hs(7.4,2,n,1);  % optimum moist content
    for i=1:n
        while X(i,29)./(62.4./X(i,28)-1/2.7)>=100   % regenerate data if the
calculated degree of saturation >= 100%
            X(i,28)=latin_hs(135,7,1,1);
            X(i,29)=latin_hs(7.4,2,1,1);
        end
    end
    for i=1:n
        S_Class{i,1}=checkSoilClass(X(i,30:36));  % define checkSoilClass
    end
    for i=1:n
        switch S_Class{i,1}
            case 'A-1-a'
                X(i,27)=lhsu(16000,42000,1);
            case 'A-1-b'
                X(i,27)=lhsu(16000,40000,1);
            case 'A-2-4'
                X(i,27)=lhsu(14000,37500,1);
            case 'A-2-5'
                X(i,27)=lhsu(14000,33000,1);
            case 'A-2-6'
                X(i,27)=lhsu(14000,31000,1);
            case 'A-2-7'
                X(i,27)=lhsu(14000,28000,1);
            case 'A-3'
                X(i,27)=lhsu(14000,35500,1);
            case 'A-4'
                X(i,27)=lhsu(13000,29000,1);
            case 'A-5'
                X(i,27)=lhsu(6000,25500,1);
            case 'A-6'
                X(i,27)=lhsu(12000,24000,1);
            case 'A-7-5'
                X(i,27)=lhsu(8000,17500,1);
            case 'A-7-6'
                X(i,27)=lhsu(5000,13500,1);
        end
    end

    % subgrade
    %X(:,37)=()  % subgrade material type, will be filled from S_Class{:,2}
    X(:,39)=latin_hs(116,10.3,n,1);  % max dry density, pcf
    X(:,40)=latin_hs(12.8,3.8,n,1);  % optimum moist content
    for i=1:n
        while X(i,40)./(62.4./X(i,39)-1/2.7)>=100   % regenerate data if the
calculated degree of saturation >= 100%
            X(i,39)=latin_hs(116,10.3,1,1);
            X(i,40)=latin_hs(12.8,3.8,1,1);
```

```
        end
    end
    X(:,41:47)=genGradation(n,5);    % generate subgrade gradation and PI/LL
    for i=1:n
        S_Class{i,2}=checkSoilClass(X(i,41:47));
    end
    for i=1:n
        switch S_Class{i,2}
            case 'A-1-a'
                X(i,38)=lhsu(16000,42000,1);
            case 'A-1-b'
                X(i,38)=lhsu(16000,40000,1);
            case 'A-2-4'
                X(i,38)=lhsu(14000,37500,1);
            case 'A-2-5'
                X(i,38)=lhsu(14000,33000,1);
            case 'A-2-6'
                X(i,38)=lhsu(14000,31000,1);
            case 'A-2-7'
                X(i,38)=lhsu(14000,28000,1);
            case 'A-3'
                X(i,38)=lhsu(14000,35500,1);
            case 'A-4'
                X(i,38)=lhsu(13000,29000,1);
            case 'A-5'
                X(i,38)=lhsu(6000,25500,1);
            case 'A-6'
                X(i,38)=lhsu(12000,24000,1);
            case 'A-7-5'
                X(i,38)=lhsu(8000,17500,1);
            case 'A-7-6'
                X(i,38)=lhsu(5000,13500,1);
        end
    end

elseif layout==3  % layout #3 AC-GB-GS-SS
    X=zeros();
    X(1:n,:)=1:n;
    S_Class={};

    % site condition and traffic
    X(:,2:3)=lhs_empirco(coordinate,n);
    X(:,4)=lhsu(3,15,n);  % watertable depth, ft
    X(:,5)=lhsu(5,3000,n); % AADTT
    X(:,6)=lhsu(0,10,n); % growth rate (%)

    % original surface layer
    X(:,7)=lhsu(1,13,n);  % thickness, in.
    X(:,8)=floor(lhsu(1,12,n));  % binder type
    X(:,9:12)=genGradation(n,1); % generate surface layer aggregate gradation
    X(:,13)=latin_hs(145.3,5.2,n,1); % unit weight, pcf
    X(:,14)=latin_hs(5.5,0.8,n,1); % asphalt content
    X(:,15)=lhs_empir(OSL_av,n); % air voids
    for i=1:n
        S_Class{i,4}=checkBinderType(X(i,8));  % OSL layer binder type
    end

    % base layer
    X(:,21:27)=genGradation(n,3); % generate base aggregate gradation and PI/LL
    for i=1:n
```

```
        while (strcmp(checkSoilClass(X(i,21:27)),'A-4')~= 0) |
(strcmp(checkSoilClass(X(i,21:27)),'A-6')~= 0) % for those 'A-4' or 'A-6' cases,
the soil gradation needs to be regenerated..
            X(i,21:27)=genGradation(1,3);
        end
    end
    %X(:,16)={};   % base material type, will be filled from S_Class{:,1}
    X(:,17)=lhsu(1,30,n);  % thickness
    X(:,19)=latin_hs(135,7,n,1);  % max dry density, pcf
    X(:,20)=latin_hs(7.4,2,n,1);  % optimum moist content
    for i=1:n
        while X(i,20)./(62.4./X(i,19)-1/2.7)>=100   % regenerate data if the
calculated degree of saturation >= 100%
            X(i,19)=latin_hs(135,7,1,1);
            X(i,20)=latin_hs(7.4,2,1,1);
        end
    end
    for i=1:n
        S_Class{i,1}=checkSoilClass(X(i,21:27));  % define checkSoilClass
    end
    for i=1:n
        switch S_Class{i,1}
            case 'A-1-a'
                X(i,18)=lhsu(16000,42000,1);
            case 'A-1-b'
                X(i,18)=lhsu(16000,40000,1);
            case 'A-2-4'
                X(i,18)=lhsu(14000,37500,1);
            case 'A-2-5'
                X(i,18)=lhsu(14000,33000,1);
            case 'A-2-6'
                X(i,18)=lhsu(14000,31000,1);
            case 'A-2-7'
                X(i,18)=lhsu(14000,28000,1);
            case 'A-3'
                X(i,18)=lhsu(14000,35500,1);
            case 'A-4'
                X(i,18)=lhsu(13000,29000,1);
            case 'A-5'
                X(i,18)=lhsu(6000,25500,1);
            case 'A-6'
                X(i,18)=lhsu(12000,24000,1);
            case 'A-7-5'
                X(i,18)=lhsu(8000,17500,1);
            case 'A-7-6'
                X(i,18)=lhsu(5000,13500,1);
        end
    end

    % Subbase layer
    X(:,33:39)=genGradation(n,4); % generate base aggregate gradation and PI/LL
    for i=1:n
        while (strcmp(checkSoilClass(X(i,33:39)),'A-4')~= 0) |
(strcmp(checkSoilClass(X(i,33:39)),'A-6')~= 0) % for those 'A-4' or 'A-6' cases,
the soil gradation needs to be regenerated..
            X(i,33:39)=genGradation(1,4);
        end
    end
    %X(:,16)={};   % base material type, will be filled from S_Class{:,1}
    X(:,29)=lhsu(3,40,n);  % thickness
```

```
    X(:,31)=latin_hs(128.5,13,n,1);  % max dry density, pcf
    X(:,32)=latin_hs(9.1,3,n,1);  % optimum moist content
    for i=1:n
        while X(i,32)./(62.4./X(i,31)-1/2.7)>=100   % regenerate data if the
calculated degree of saturation >= 100%
            X(i,31)=latin_hs(128.5,13,1,1);
            X(i,32)=latin_hs(9.1,3,1,1);
        end
    end
    for i=1:n
        S_Class{i,2}=checkSoilClass(X(i,33:39));  % define checkSoilClass
    end
    for i=1:n
        switch S_Class{i,2}
            case 'A-1-a'
                X(i,30)=lhsu(16000,42000,1);
            case 'A-1-b'
                X(i,30)=lhsu(16000,40000,1);
            case 'A-2-4'
                X(i,30)=lhsu(14000,37500,1);
            case 'A-2-5'
                X(i,30)=lhsu(14000,33000,1);
            case 'A-2-6'
                X(i,30)=lhsu(14000,31000,1);
            case 'A-2-7'
                X(i,30)=lhsu(14000,28000,1);
            case 'A-3'
                X(i,30)=lhsu(14000,35500,1);
            case 'A-4'
                X(i,30)=lhsu(13000,29000,1);
            case 'A-5'
                X(i,30)=lhsu(6000,25500,1);
            case 'A-6'
                X(i,30)=lhsu(12000,24000,1);
            case 'A-7-5'
                X(i,30)=lhsu(8000,17500,1);
            case 'A-7-6'
                X(i,30)=lhsu(5000,13500,1);
        end
    end

    % subgrade
    %X(:,28)=()  % subgrade material type, will be filled from S_Class{:,2}
    X(:,42)=latin_hs(116,10.3,n,1);  % max dry density, pcf
    X(:,43)=latin_hs(12.8,3.8,n,1);  % optimum moist content
    for i=1:n
        while X(i,43)./(62.4./X(i,42)-1/2.7)>=100   % regenerate data if the
calculated degree of saturation >= 100%
            X(i,42)=latin_hs(116,10.3,1,1);
            X(i,43)=latin_hs(12.8,3.8,1,1);
        end
    end
    X(:,44:50)=genGradation(n,5);    % generate subgrade gradation and PI/LL
    for i=1:n
        S_Class{i,3}=checkSoilClass(X(i,44:50));
    end
    for i=1:n
        switch S_Class{i,3}
            case 'A-1-a'
                X(i,41)=lhsu(16000,42000,1);
```

```
            case 'A-1-b'
                X(i,41)=lhsu(16000,40000,1);
            case 'A-2-4'
                X(i,41)=lhsu(14000,37500,1);
            case 'A-2-5'
                X(i,41)=lhsu(14000,33000,1);
            case 'A-2-6'
                X(i,41)=lhsu(14000,31000,1);
            case 'A-2-7'
                X(i,41)=lhsu(14000,28000,1);
            case 'A-3'
                X(i,41)=lhsu(14000,35500,1);
            case 'A-4'
                X(i,41)=lhsu(13000,29000,1);
            case 'A-5'
                X(i,41)=lhsu(6000,25500,1);
            case 'A-6'
                X(i,41)=lhsu(12000,24000,1);
            case 'A-7-5'
                X(i,41)=lhsu(8000,17500,1);
            case 'A-7-6'
                X(i,41)=lhsu(5000,13500,1);
        end
    end

elseif layout==4  %layout #4  AC-AC-GB-SB-SS
    X=zeros();
    X(1:n,:)=1:n;
    S_Class={};

    % site condition and traffic
    X(:,2:3)=lhs_empirco(coordinate,n);
    X(:,4)=lhsu(3,15,n);  % watertable depth, ft
    X(:,5)=lhsu(5,3000,n); % AADTT
    X(:,6)=lhsu(0,10,n); % growth rate (%)

    % original surface layer
    X(:,7)=lhsu(1,13,n);  % thickness, in.
    X(:,8)=floor(lhsu(1,12,n));  % binder type
    X(:,9:12)=genGradation(n,1); % generate surface layer aggregate gradation
    X(:,13)=latin_hs(145.3,5.2,n,1); % unit weight, pcf
    X(:,14)=latin_hs(5.5,0.8,n,1); % asphalt content
    X(:,15)=lhs_empir(OSL_av,n); % air voids
    for i=1:n
        S_Class{i,4}=checkBinderType(X(i,8));  % OSL layer binder type
    end
    % binder course layer
    X(:,16)=lhsu(1,9,n);  % thickness, in.
    X(:,17)=floor(lhsu(1,12,n));  % binder type
    X(:,18:21)=genGradation(n,2); % generate surface layer aggregate gradation
    X(:,22)=latin_hs(147.4,6.3,n,1); % unit weight, pcf
    X(:,23)=latin_hs(4.9,0.8,n,1); % asphalt content
    X(:,24)=lhs_empir(BC_av,n); % air voids
    for i=1:n
        S_Class{i,5}=checkBinderType(X(i,17));  % Binder course layer binder
type
    end
    % base layer
    X(:,30:36)=genGradation(n,3); % generate base aggregate gradation and PI/LL
    for i=1:n
```

```
        while (strcmp(checkSoilClass(X(i,30:36)),'A-4')~= 0) |
(strcmp(checkSoilClass(X(i,30:36)),'A-6')~= 0) % for those 'A-4' or 'A-6' cases,
the soil gradation needs to be regenerated..
            X(i,30:36)=genGradation(1,3);
        end
    end
    %X(:,16)={};   % base material type, will be filled from S_Class{:,1}
    X(:,26)=lhsu(1,30,n);  % thickness
    X(:,28)=latin_hs(135,7,n,1);  % max dry density, pcf
    X(:,29)=latin_hs(7.4,2,n,1);  % optimum moist content
    for i=1:n
        while X(i,29)./(62.4./X(i,28)-1/2.7)>=100   % regenerate data if the
calculated degree of saturation >= 100%
            X(i,28)=latin_hs(135,7,1,1);
            X(i,29)=latin_hs(7.4,2,1,1);
        end
    end
    for i=1:n
        S_Class{i,1}=checkSoilClass(X(i,30:36));  % define checkSoilClass
    end
    for i=1:n
        switch S_Class{i,1}
            case 'A-1-a'
                X(i,27)=lhsu(16000,42000,1);
            case 'A-1-b'
                X(i,27)=lhsu(16000,40000,1);
            case 'A-2-4'
                X(i,27)=lhsu(14000,37500,1);
            case 'A-2-5'
                X(i,27)=lhsu(14000,33000,1);
            case 'A-2-6'
                X(i,27)=lhsu(14000,31000,1);
            case 'A-2-7'
                X(i,27)=lhsu(14000,28000,1);
            case 'A-3'
                X(i,27)=lhsu(14000,35500,1);
            case 'A-4'
                X(i,27)=lhsu(13000,29000,1);
            case 'A-5'
                X(i,27)=lhsu(6000,25500,1);
            case 'A-6'
                X(i,27)=lhsu(12000,24000,1);
            case 'A-7-5'
                X(i,27)=lhsu(8000,17500,1);
            case 'A-7-6'
                X(i,27)=lhsu(5000,13500,1);
        end
    end
    % Subbase layer
    X(:,42:48)=genGradation(n,4); % generate base aggregate gradation and PI/LL
     for i=1:n
        while (strcmp(checkSoilClass(X(i,42:48)),'A-4')~= 0) |
(strcmp(checkSoilClass(X(i,42:48)),'A-6')~= 0) % for those 'A-4' or 'A-6' cases,
the soil gradation needs to be regenerated..
            X(i,42:48)=genGradation(1,4);
        end
    end
    %X(:,16)={};   % base material type, will be filled from S_Class{:,1}
    X(:,38)=lhsu(3,40,n);  % thickness
    X(:,40)=latin_hs(128.5,13,n,1);  % max dry density, pcf
```

```
    X(:,41)=latin_hs(9.1,3,n,1);  % optimum moist content
    for i=1:n
        while X(i,41)./(62.4./X(i,40)-1/2.7)>=100   % regenerate data if the
calculated degree of saturation >= 100%
            X(i,40)=latin_hs(128.5,13,1,1);
            X(i,41)=latin_hs(9.1,3,1,1);
        end
    end
    for i=1:n
        S_Class{i,2}=checkSoilClass(X(i,42:48));  % need to define
checkSoilClass
    end
    for i=1:n
        switch S_Class{i,2}
            case 'A-1-a'
                X(i,39)=lhsu(16000,42000,1);
            case 'A-1-b'
                X(i,39)=lhsu(16000,40000,1);
            case 'A-2-4'
                X(i,39)=lhsu(14000,37500,1);
            case 'A-2-5'
                X(i,39)=lhsu(14000,33000,1);
            case 'A-2-6'
                X(i,39)=lhsu(14000,31000,1);
            case 'A-2-7'
                X(i,39)=lhsu(14000,28000,1);
            case 'A-3'
                X(i,39)=lhsu(14000,35500,1);
            case 'A-4'
                X(i,39)=lhsu(13000,29000,1);
            case 'A-5'
                X(i,39)=lhsu(6000,25500,1);
            case 'A-6'
                X(i,39)=lhsu(12000,24000,1);
            case 'A-7-5'
                X(i,39)=lhsu(8000,17500,1);
            case 'A-7-6'
                X(i,39)=lhsu(5000,13500,1);
        end
    end
    % subgrade
    %X(:,28)=()  % subgrade material type, will be filled from S_Class{:,2}
    X(:,51)=latin_hs(116,10.3,n,1);  % max dry density, pcf
    X(:,52)=latin_hs(12.8,3.8,n,1);  % optimum moist content
    for i=1:n
        while X(i,52)./(62.4./X(i,51)-1/2.7)>=100   % regenerate data if the
calculated degree of saturation >= 100%
            X(i,51)=latin_hs(116,10.3,1,1);
            X(i,52)=latin_hs(12.8,3.8,1,1);
        end
    end
    X(:,53:59)=genGradation(n,5);    % generate subgrade gradation and PI/LL
    for i=1:n
        S_Class{i,3}=checkSoilClass(X(i,53:59));
    end
    for i=1:n
        switch S_Class{i,3}
            case 'A-1-a'
                X(i,50)=lhsu(16000,42000,1);
            case 'A-1-b'
```

```
                X(i,50)=lhsu(16000,40000,1);
            case 'A-2-4'
                X(i,50)=lhsu(14000,37500,1);
            case 'A-2-5'
                X(i,50)=lhsu(14000,33000,1);
            case 'A-2-6'
                X(i,50)=lhsu(14000,31000,1);
            case 'A-2-7'
                X(i,50)=lhsu(14000,28000,1);
            case 'A-3'
                X(i,50)=lhsu(14000,35500,1);
            case 'A-4'
                X(i,50)=lhsu(13000,29000,1);
            case 'A-5'
                X(i,50)=lhsu(6000,25500,1);
            case 'A-6'
                X(i,50)=lhsu(12000,24000,1);
            case 'A-7-5'
                X(i,50)=lhsu(8000,17500,1);
            case 'A-7-6'
                X(i,50)=lhsu(5000,13500,1);
        end
    end

end
end
disp('Data generation completed!')
```

SAMPLE AUTOIT CODES FOR INPUTTING MEPDG SIMULATION DATA

The following codes were used in AutoIt for inputting MEPDG simulation data for pavement design layout #1:

```
#ce ----------------------------------------------------------------------------
#include <Excel.au3>
#include <GUIConstantsEx.au3>
#include <TreeViewConstants.au3>
#include <WindowsConstants.au3>

Func _Au3RecordSetup()
Opt('WinWaitDelay',100)
Opt('WinDetectHiddenText',1)
Opt('MouseCoordMode',0)
EndFunc

Func _WinWaitActivate($title,$text,$timeout=0)
    WinWait($title,$text,$timeout)
    If Not WinActive($title,$text) Then WinActivate($title,$text)
    WinWaitActive($title,$text,$timeout)
EndFunc

_Au3RecordSetup()
;#endregion --- Internal functions Au3Recorder End ---

$filePath = "C:\Simulation\Layout1-"
$sExcelFilePath="C:\Simulation\layout1.xls"
$oExcel=_ExcelBookOpen($sExcelFilePath,1)

$i=1

For $i=1 TO 600
    ; load site and traffic conditions
    Local $Latitude = Round(_ExcelReadCell($oExcel, $i+2, 2),3)
    Local $Longitude = Round(_ExcelReadCell($oExcel, $i+2, 3),3)
    Local $WaterTable = Round(_ExcelReadCell($oExcel, $i+2, 4),1)
    Local $AADTT = Int(_ExcelReadCell($oExcel, $i+2,5))
    Local $GrowthRate = Round(_ExcelReadCell($oExcel, $i+2, 6),1)

    ; load original surface layer properties
    Local $OSLThick = Round(_ExcelReadCell($oExcel, $i+2, 7),1)
    Local $OSLBinder = _ExcelReadCell($oExcel, $i+2, 8)
    Local $OSLR34 = Round(_ExcelReadCell($oExcel, $i+2, 9),1)
    Local $OSLR38 = Round(_ExcelReadCell($oExcel, $i+2, 10),1)
    Local $OSLR4 = Round(_ExcelReadCell($oExcel, $i+2, 11),1)
    Local $OSLPP200 =Round( _ExcelReadCell($oExcel, $i+2, 12),1)
    Local $OSLUW = Round(_ExcelReadCell($oExcel, $i+2, 13),1)
    Local $OSLAC = Round(_ExcelReadCell($oExcel, $i+2, 14),1)
    Local $OSLAV = Round(_ExcelReadCell($oExcel, $i+2, 15),1)

    ; load base layer properties
    Local $BaseMaterial = _ExcelReadCell($oExcel, $i+2, 16)
    Local $BaseThick = Round(_ExcelReadCell($oExcel, $i+2, 17),1)
    Local $BaseResMod = Int(_ExcelReadCell($oExcel, $i+2, 18))
```

```
    Local $BaseDensity = Round(_ExcelReadCell($oExcel, $i+2, 19),1)
    Local $BaseMoist = Round(_ExcelReadCell($oExcel, $i+2, 20),1)
    Local $BasePP200 = Round(_ExcelReadCell($oExcel, $i+2, 21),1)
    Local $BasePP40 = Round(_ExcelReadCell($oExcel, $i+2, 22),1)
    Local $BasePP10 = Round(_ExcelReadCell($oExcel, $i+2, 23),1)
    Local $BasePP4 = Round(_ExcelReadCell($oExcel, $i+2, 24),1)
    Local $BasePP1 =Round(_ExcelReadCell($oExcel, $i+2, 25),1)
    Local $BasePI = Int(_ExcelReadCell($oExcel, $i+2, 26))
    Local $BaseLL = Int(_ExcelReadCell($oExcel, $i+2, 27))

    Local $SubgradeMaterial = _ExcelReadCell($oExcel, $i+2, 28)
    Local $SubgradeResMod = Int(_ExcelReadCell($oExcel, $i+2, 29))
    Local $SubgradeDensity = Round(_ExcelReadCell($oExcel, $i+2, 30),1)
    Local $SubgradeMoist = Round(_ExcelReadCell($oExcel, $i+2, 31),1)
    Local $SubgradePP200 = Round(_ExcelReadCell($oExcel, $i+2, 32),1)
    Local $SubgradePP40 =Round(_ExcelReadCell($oExcel, $i+2, 33),1)
    Local $SubgradePP10 = Round(_ExcelReadCell($oExcel, $i+2, 34),1)
    Local $SubgradePP4 = Round(_ExcelReadCell($oExcel, $i+2, 35),1)
    Local $SubgradePP1 = Round(_ExcelReadCell($oExcel, $i+2, 36),1)
    Local $SubgradePI = Int(_ExcelReadCell($oExcel, $i+2, 37))
    Local $SubgradeLL = Int(_ExcelReadCell($oExcel, $i+2, 38))

Run('C:\DG2002\Dg2k2.exe')
_WinWaitActivate("Untitled - Mechanistic Empirical Pavement Design Guide","")
Send("{ALTDOWN}{ALTUP}fn")
_WinWaitActivate("Create New Project","")
Send("{ENTER}")
_WinWaitActivate("Untitled - Mechanistic Empirical Pavement Design Guide","")
MouseClick("left",110,105,2)
_WinWaitActivate("General Information","")
Send("30{TAB}{SHIFTDOWN}j{SHIFTUP}uly{TAB}1978{TAB}{SHIFTDOWN}a{SHIFTUP}ugust{T
AB}1978{TAB}{TAB}{SHIFTDOWN}{TAB}{TAB}{TAB}{TAB}{TAB}{TAB}{TAB}{SHIFTUP}1978{SH
IFTDOWN}{TAB}{SHIFTUP}{SHIFTDOWN}a{SHIFTUP}pril")
MouseClick("left",72,288,1)
Send("{Enter}")
MouseClick("left",110,125,2)
_WinWaitActivate("Site/Project Identification","")
MouseMove(170,340)
MouseDown("left")
MouseMove(169,340)
MouseUp("left")
_WinWaitActivate("Untitled - Mechanistic Empirical Pavement Design Guide","")
;MouseClick("left",72,138,2)
;_WinWaitActivate("Analysis Parameters","")
;MouseClick("left",223,486,1)
;_WinWaitActivate("Untitled - Mechanistic Empirical Pavement Design Guide","")
Send("{CTRLDOWN}s{CTRLUP}")
_WinWaitActivate("Save As","")
Send("{DEL}")
Sleep(1000)
Send($filePath & $i & "{ENTER 2}") ;
_WinWaitActivate("Layout1-"& $i &".dgp - Mechanistic Empirical Pavement Design
Guide","")

;Input Module
;Traffic
MouseClick("left",53,265,2)
_WinWaitActivate("Traffic","")
Send($AADTT)
```

```
MouseClick("left",248,423,1)
IF $AADTT<100 Then WinWaitActive("Traffic - Warning","")
If WinActive("Traffic - Warning","") Then
    ControlClick("Traffic - Warning","","[Class:Button;ID:1]","left",1)
EndIf
_WinWaitActivate("Traffic Volume Adjustment Factors","")
MouseClick("left",457,288,1)
Send("{BACKSPACE}" & $GrowthRate)
MouseClick("left",353,38,1)
MouseClick("left",242,36,1)
MouseClick("left",65,36,1)
MouseClick("left",229,473,1)
_WinWaitActivate("Traffic","")
MouseClick("left",207,317,1)
IF $AADTT<100 Then WinWaitActive("Traffic - Warning","")
If WinActive("Traffic - Warning","") Then
    ControlClick("Traffic - Warning","","[Class:Button;Instance:1;ID:1]","",1)
EndIf
_WinWaitActivate("Traffic Volume Adjustment Factors","")
MouseClick("left",229,480,1)
_WinWaitActivate("Traffic","")
MouseClick("left",211,350,1)
_WinWaitActivate("Axle Load Distribution Factors","")
MouseClick("left",269,412,1)
_WinWaitActivate("Traffic","")
MouseClick("left",207,377,1)
_WinWaitActivate("General Traffic Inputs","")
MouseClick("left",212,189,1)
MouseMove(312,188)
MouseDown("left")
MouseMove(313,188)
MouseUp("left")
MouseMove(201,456)
MouseDown("left")
MouseMove(202,456)
MouseUp("left")
_WinWaitActivate("Traffic","")
MouseMove(175,477)
MouseDown("left")
MouseMove(176,477)
MouseUp("left")
IF $AADTT<100 Then WinWaitActive("Traffic - Warning","")
If WinActive("Traffic - Warning","") Then
    ControlClick("Traffic - Warning","","[Class:Button;ID:1]","left",1)
EndIf
_WinWaitActivate("Layout1-"& $i &".dgp - Mechanistic Empirical Pavement Design
Guide","")

;Climate
MouseClick("left",69,464,2)
_WinWaitActivate("Environment/Climatic","")
MouseClick("left",76,128,1)
MouseClick("left",50,126,1)
MouseClick("left",439,55,1)
Send($Latitude & "{TAB}" & $Longitude & "{TAB}500")
MouseClick("left",548,178,1)
Send($WaterTable)
;_ChooseClimate($i)
MouseClick("left",134,298,1)
```

```
MouseClick("left",134,321,1)
MouseClick("left",134,344,1)
MouseClick("left",134,367,1)
MouseClick("left",134,390,1)
MouseClick("left",134,413,1)
MouseClick("left",58,468,1)
;_CheckClimate($i);
_WinWaitActivate("Save generated climatic data file.","")
Sleep(1000)
Send("Layout1-"& $i &".icm{ENTER}")


;Pavement Structural Properties
_WinWaitActivate("Layout1-"& $i &".dgp - Mechanistic Empirical Pavement Design
Guide","")
MouseClick("left",59,480,2)
_WinWaitActivate("Structure","")
MouseMove(596,302)
MouseDown("left")
MouseMove(597,302)
MouseUp("left")

; 1. Original HMA Surface
_WinWaitActivate("Asphalt Material Properties","")
MouseClick("left",315,84,1)
Send("{BACKSPACE}{BACKSPACE}" & $OSLThick)
_ACLayerBinderType($OSLBinder) ; input the asphalt binder types used in the OSL
layer.
MouseClick("left",61,145,1)
Send($OSLR34 & "{TAB}" & $OSLR38 & "{TAB}" & $OSLR4 & "{TAB}" & $OSLPP200)
MouseClick("left",295,149,1)
MouseClick("left",228,403,1)
Send("{BACKSPACE}{BACKSPACE}{BACKSPACE}{BACKSPACE}" & $OSLAC & "{TAB}" & $OSLAV
& "{TAB}" & $OSLUW & "{ENTER}")
If $OSLThick<1 Then WinWaitActive("Asphalt Material Properties - Error","")
If WinActive("Asphalt Material Properties - Error","") Then
    ControlClick("Asphalt Material Properties -
Error","","[Class:Button;ID:2]","",1)
    Send("{BACKSPACE 5}" & (1+$OSLThick) & "{Enter}")
EndIf
_WinWaitActivate("Dg2k2","")
Send("{ENTER}")
_WinWaitActivate("Structure","")
MouseClick("left",74,311,1)
_WinWaitActivate("Insert Layer After","")

; 2. Granular Base
_InputBaseMaterial($BaseMaterial)  ; call function _InputBaseMaterial to select
Base material type
MouseClick("left",175,184,1) ; select "Thickness (in)"
Send($BaseThick) ; send Base thickness
MouseClick("left",129,234,1)
_WinWaitActivate("Structure","")
MouseClick("left",616,313,1) ; select "Edit" to modify Base layer properties
_WinWaitActivate("Unbound Layer - Layer #2","")
MouseClick("left",452,397,1)
Send("{BACKSPACE}{BACKSPACE}{BACKSPACE}{BACKSPACE}{BACKSPACE}{BACKSPACE}" &
$BaseResMod)
MouseClick("left",178,72,1)
```

```
MouseClick("left",180,140,1)
Send("{DEL}")
MouseClick("left",157,205,1)
Send($BasePP200 & "{DOWN}{DOWN}{DOWN}{DOWN}{DOWN}" & $BasePP40 &
"{DOWN}{DOWN}{DOWN}{DOWN}" & $BasePP10 & "{DOWN}{DOWN}" & $BasePP4 &
"{DOWN}{DOWN}{DOWN}{DOWN}" & $BasePP1)
MouseClick("left",482,140,1)
Send($BasePI & "{DOWN}" & $BaseLL)
MouseClick("left",438,376,1)
MouseClick("left",434,419,1)
MouseClick("left",486,376,1)
Send($BaseDensity)
MouseMove(489,421)
MouseDown("left")
MouseMove(490,421)
MouseUp("left")
Send($BaseMoist)
MouseClick("left",451,102,1)
If WinActive("Change Material Warning","Changing the unbound material") Then
ControlClick("Change Material Warning","Changing the unbound
material","[Class:Button;ID:2]","left",1)
Send("{ENTER}")
If WinActive("Dg2k2","The input sieve") Then ControlClick("Dg2k2","The input
sieve","[Class:Button;ID:7]","left",1) ; if the input gradation and PI values
don't agree with the pre-selected Material type, a message will pop up; here we
just choose "No" to close it.
;Send("{ENTER}")
_WinWaitActivate("Structure","")

; 3. Subgrade
MouseClick("left",83,307,1)
_WinWaitActivate("Insert Layer After","")
_InputSubgradeMaterial($SubgradeMaterial) ; call _InputSubgradeMaterial
function to select Subgrade material type.
MouseClick("left",216,187,1)
MouseClick("left",129,240,1)
_WinWaitActivate("Structure","")
MouseClick("left",602,313,1)
_WinWaitActivate("Unbound Layer - Layer #3","")
MouseClick("left",419,398,2)
Send($SubgradeResMod)
MouseClick("left",174,82,1)
MouseClick("left",158,136,1)
Send("{DEL}")
MouseClick("left",150,208,1)
Send($SubgradePP200 & "{DOWN}{DOWN}{DOWN}{DOWN}{DOWN}" & $SubgradePP40 &
"{DOWN}{DOWN}{DOWN}{DOWN}" & $SubgradePP10 & "{DOWN}{DOWN}" & $SubgradePP4 &
"{DOWN}{DOWN}{DOWN}{DOWN}" & $SubgradePP1)
MouseClick("left",485,142,1)
Send($SubgradePI & "{DOWN}" & $SubgradeLL)
MouseClick("left",437,376,1)
MouseClick("left",490,371,1)
Send($SubgradeDensity)
MouseClick("left",435,421,1)
MouseClick("left",482,421,1)
Send($SubgradeMoist)
MouseClick("left",462,106,1)
```

```
IF WinActive("Dg2k2","") Then MouseClick("left",401,221,1)  ; if the input
gradation and PI values don't agree with the pre-selected Material type, a
message will pop up; here we just choose "No" to close it.
Send("{Enter}")
If WinExists("Change Material Warning","") Then
    ControlClick("Change Material Warning","","[Class:Button;ID:2]","left",1)
    Send("{Enter}")
    If WinExists("Dg2k2","The input sieve and index propeties") Then
ControlClick("Dg2k2","The input sieve and index
propeties","[Class:Button;ID:7]","left",1)
EndIf
;MouseClick("left",214,587,1)
_WinWaitActivate("Structure","")
MouseClick("left",520,370,1)
_WinWaitActivate("Layout1-"& $i &".dgp - Mechanistic Empirical Pavement Design
Guide","")
MouseClick("left",101,500,2)
_WinWaitActivate("HMA Design Properties","")
MouseClick("left",166,343,1)
_WinWaitActivate("Layout1-"& $i &".dgp - Mechanistic Empirical Pavement Design
Guide","")
MouseClick("left",114,591,2)
_WinWaitActivate("Thermal Cracking","")
MouseClick("left",189,483,1)
_WinWaitActivate("Layout1-"& $i &".dgp - Mechanistic Empirical Pavement Design
Guide","")
Send("{CTRLDOWN}s{CTRLUP}")
Send("{ALTDOWN}{ALTUP}fx")

Run('cmd.exe')
_WinWaitActivate("C:\Windows\system32\cmd.exe","")
Sleep(1000)
Send("taskkill /f /im Excel.exe /t {Enter}")
Sleep(1000)
Send("exit{Enter}")

Sleep(4000)
$oExcel=_ExcelBookOpen($sExcelFilePath,0)
;_ExcelBookClose($oExcel,0)
Sleep(3000)
Next



Func _ACLayerBinderType($x)
Switch $x
    Case "AC-2.5"
        MouseClick("left",212,207,1)
        MouseClick("left",244,304,1)
    Case "AC-5"
        MouseClick("left",212,207,1)
        MouseClick("left",244,319,1)
    Case "AC-10"
        MouseClick("left",212,207,1)
        MouseClick("left",244,338,1)
    Case "AC-20"
        MouseClick("left",212,207,1)
        MouseClick("left",244,359,1)
```

```
    Case "AC-30"
        MouseClick("left",212,207,1)
        MouseClick("left",244,377,1)
    Case "AC-40"
        MouseClick("left",212,207,1)
        MouseClick("left",244,392,1)
    Case "PEN 40-50"
        MouseClick("left",211,233,1)
        MouseClick("left",226,300,1)
    Case "PEN 60-70"
        MouseClick("left",211,233,1)
        MouseClick("left",227,318,1)
    Case "PEN 85-100"
        MouseClick("left",211,233,1)
        MouseClick("left",233,340,1)
    Case "PEN 120-150"
        MouseClick("left",211,233,1)
        MouseClick("left",236,360,1)
    Case "PEN 200-300"
        MouseClick("left",211,233,1)
        MouseClick("left",236,378,1)
    Case Else
        MsgBox(0,"Error","Asphalt binder type needs to be specified...")
EndSwitch
EndFunc

Func _InputBaseMaterial($y)
    Switch $y
        Case "A-1-a"
            MouseClick("left",331,93,1)  ; select "Material Type"
            MouseClick("left",139,139,1) ; select "Granular Base"
            MouseClick("left",330,126,1) ; select "Material"
            MouseClick("left",131,219,1) ; select "A-1-a"
        Case "A-1-b"
            MouseClick("left",331,93,1)
            MouseClick("left",139,139,1)
            MouseClick("left",330,126,1)
            MouseClick("left",131,233,1)
        Case "A-2-4"
            MouseClick("left",331,93,1)
            MouseClick("left",139,139,1)
            MouseClick("left",330,126,1)
            MouseClick("left",131,247,1)
        Case "A-2-5"
            MouseClick("left",331,93,1)
            MouseClick("left",139,139,1)
            MouseClick("left",330,126,1)
            MouseClick("left",131,261,1)
        Case "A-2-6"
            MouseClick("left",331,93,1)
            MouseClick("left",139,139,1)
            MouseClick("left",330,126,1)
            MouseClick("left",131,275,1)
        Case "A-2-7"
            MouseClick("left",331,93,1)
            MouseClick("left",139,139,1)
            MouseClick("left",330,126,1)
            MouseClick("left",131,289,1)
        Case "A-3"
```

```
            MouseClick("left",331,93,1)
            MouseClick("left",139,139,1)
            MouseClick("left",330,126,1)
            MouseClick("left",131,303,1)
        Case Else
            MsgBox(0,"Error","Base material type needs to be specified...")
    EndSwitch
EndFunc

Func _InputSubgradeMaterial($z)
    Switch $z
        Case "A-1-a"
            MouseClick("left",333,90,1) ; select "Material Type"
            MouseClick("left",160,152,1) ; select "Subgrade"
            MouseClick("left",333,124,1) ; select "Material"
            MouseClick("left",236,140,1) ;A-1-a
        Case "A-1-b"
            MouseClick("left",333,90,1)
            MouseClick("left",160,152,1)
            MouseClick("left",333,124,1)
            MouseClick("left",261,154,1)
        Case "A-2-4"
            MouseClick("left",333,90,1)
            MouseClick("left",160,152,1)
            MouseClick("left",333,124,1)
            MouseClick("left",195,168,1)
        Case "A-2-5"
            MouseClick("left",333,90,1)
            MouseClick("left",160,152,1)
            MouseClick("left",333,124,1)
            MouseClick("left",165,182,1)
        Case "A-2-6"
            MouseClick("left",333,90,1)
            MouseClick("left",160,152,1)
            MouseClick("left",333,124,1)
            MouseClick("left",149,196,1)
        Case "A-2-7"
            MouseClick("left",333,90,1)
            MouseClick("left",160,152,1)
            MouseClick("left",333,124,1)
            MouseClick("left",145,210,1)
        Case "A-3"
            MouseClick("left",333,90,1)
            MouseClick("left",160,152,1)
            MouseClick("left",333,124,1)
            MouseClick("left",129,224,1)
        Case "A-4"
            MouseClick("left",333,90,1)
            MouseClick("left",160,152,1)
            MouseClick("left",333,124,1)
            MouseClick("left",139,238,1)
        Case "A-5"
            MouseClick("left",333,90,1)
            MouseClick("left",160,152,1)
            MouseClick("left",333,124,1)
            MouseClick("left",139,252,1)
        Case "A-6"
            MouseClick("left",333,90,1)
            MouseClick("left",160,152,1)
```

```
            MouseClick("left",333,124,1)
            MouseClick("left",141,265,1)
        Case "A-7-5"
            MouseClick("left",333,90,1)
            MouseClick("left",160,152,1)
            MouseClick("left",333,124,1)
            MouseClick("left",131,278,1)
        Case "A-7-6"
            MouseClick("left",333,90,1)
            MouseClick("left",160,152,1)
            MouseClick("left",333,124,1)
            MouseClick("left",140,291,1)
        Case Else
            MsgBox(0,"error","Subgrade material needs to be specified...")
    EndSwitch
EndFunc
```

MATLAB CODES USED FOR EXTRACTING MEPDG SIMULATION RESULTS

The following Matlab codes were used for reading MEPDG simulation results, which were stored in separate Excel spreadsheets. Using Matlab, the output can then be aggregated into one summary spreadsheet.

```
function [x y] = readMEPDGdata(layout)
% Read MEPDG simulation results into matrix 'x' and array 'y'.
% x contains numbers and y contains text.
% layout = layout type:
%                 1 for SS-GB-OSL
%                 2 for SS-GB-BC-OSL
%                 3 for SS-SB-GB-OSL
%                 4 for SS-SB-GB-BC-OSL
% MEPDG generated performance data are also extracted into 'x'.

x=[];
y={};
if layout == 1
    disp('Layout = 1. Please wait for data to be read from the spreadsheets. It
may take a few hours to complete!');
        % y is an array containing the names of each column.
    y{1,1} = 'Avg_Annual_Air_Temp'; y{1,2} = 'Avg_Annual_Rainfall'; y{1,3} =
'Freeze_Index'; y{1,4} = 'Water_Table_Depth'; y{1,5} = 'AADTT'; y{1,6} =
'Growth_Rate'; y{1,7} = 'OSL_Thick'; y{1,8} = 'Eff_Binder_Content'; y{1,9} =
'Air_Voids'; y{1,10} = 'Unit_Weight'; y{1,11} = 'R34'; y{1,12} = 'R38';
y{1,13} = 'R4'; y{1,14} = 'PP200'; y{1,15} = 'A'; y{1,16} = 'VTS';
y{1,17} = 'Avg_Tensile_Strength'; y{1,18} = 'Mix_VMA'; y{1,19} = 'Base_Thick';
y{1,20} = 'Base_Res_Modulus'; y{1,21} = 'Base_PI'; y{1,22} = 'Base_LL'; y{1,23}
= 'Base_PP200'; y{1,24} = 'Base_PP40'; y{1,25} = 'Base_PP4'; y{1,26} =
'Base_D60'; y{1,27} = 'Base_Max_Dry_Unit_Weight'; y{1,28} =
'Base_Opt_Grav_Water_Content'; y{1,29} = 'Sugrade_Res_Modulus'; y{1,30} =
'Subgrade_PI'; y{1,31} = 'Subgrade_LL'; y{1,32} = 'Subgrade_PP200';
y{1,33} = 'Sugrade_PP40'; y{1,34} = 'Subgrade_PP4'; y{1,35} = 'Sugrade_D60';
y{1,36} = 'Subgrade_Max_Dry_Unit_Weight'; y{1,37} =
'Subgrade_Opt_Grav_Water_Content'; y{1,38} = 'Age'; y{1,39} =
'Longitudinal_Crack'; y{1,40} = 'Alligator_Crack'; y{1,41} = 'Transverse_Crack';
y{1,42} = 'Total_Rutting'; y{1,43} = 'IRI'; y{1,44} = 'IRI_Std'; y{1,45} =
'Subtotal_AC_Rutting';

    for i = [1:93 95:98 103:177 210:527 534:572 598:600]
        tic;
        filePath = ['C:\MEPDG Simulation\Layout', int2str(layout),'\Layout',
int2str(layout), '-', int2str(i), '.xls'];
        % reading climatic data
        x(((i-1)*30+1):i*30,1) = checkTemp(filePath);  % mean annual air temp,
F
        x(((i-1)*30+1):i*30,2) = checkRain(filePath);  % mean annual rainfall,
in.
        x(((i-1)*30+1):i*30,3) = checkFreeze(filePath);  % freezing index, F-
days
```

```
        [a, b]=xlsread(filePath,'Input Summary','B13:O328'); % read numeric
data in 'Input Summary' sheets into 'a' and text data into 'b'
        x(((i-1)*30+1):i*30,4) = a(1382); % depth of water table, ft

        % reading traffic data
        x(((i-1)*30+1):i*30,5) = a(1601);  % AADTT, veh/day
        x(((i-1)*30+1):i*30,6) = a(383);  % Growth rate

        % reading OSL layer data
        x(((i-1)*30+1):i*30,7) = a(1395); % thickness, in.
        x(((i-1)*30+1):i*30,8) = a(1402); % effective binder content, %
        x(((i-1)*30+1):i*30,9) = a(1403); % air voids, %
        x(((i-1)*30+1):i*30,10) = a(1404); % total unit weight, pcf
        x(((i-1)*30+1):i*30,11) = a(1413); % R34
        x(((i-1)*30+1):i*30,12) = a(1414); % R38
        x(((i-1)*30+1):i*30,13) = a(1415); % R4
        x(((i-1)*30+1):i*30,14) = a(1416); % PP200
        A = b(2058); x(((i-1)*30+1):i*30,15) = str2num(A{1,1}(1:8));     % A
(for calculating binder viscosity)
        VTS = b(2059); x(((i-1)*30+1):i*30,16) = str2num(VTS{1,1}(1:6)); % VTS
(for calculating binder viscosity)
        x(((i-1)*30+1):i*30,17) = a(1740); % avg tensile strength at 14F, psi
        x(((i-1)*30+1):i*30,18) = a(1741); % mixture VMA (%)

        % reading base data
        x(((i-1)*30+1):i*30,19) = a(1442); % base thickness, in.
        x(((i-1)*30+1):i*30,20) = a(1449); % base res modulus, psi
        x(((i-1)*30+1):i*30,21) = a(1768); % plasticity index
        x(((i-1)*30+1):i*30,22) = a(1769); % liquid limit
        x(((i-1)*30+1):i*30,23) = a(1771); % PP200 (%)
        x(((i-1)*30+1):i*30,24) = a(1772); % PP40 (%)
        x(((i-1)*30+1):i*30,25) = a(1773); % PP4 (%)
        x(((i-1)*30+1):i*30,26) = a(1777); % D60, mm
        b_uw = b(2447); x(((i-1)*30+1):i*30,27) = str2num(b_uw{1,1}(1:5)); %
max dry unit weight, pcf
        b_wc = b(2450); x(((i-1)*30+1):i*30,28) = str2num(b_wc{1,1}(1:4)); %
opt. gravimetric water content (%)

        % reading subgrade data
        x(((i-1)*30+1):i*30,29) = a(1518); % subgrade res modulus, psi
        x(((i-1)*30+1):i*30,30) = a(1837); % plasticity index
        x(((i-1)*30+1):i*30,31) = a(1838); % liquid limit
        x(((i-1)*30+1):i*30,32) = a(1840); % PP200 (%)
        x(((i-1)*30+1):i*30,33) = a(1841); % PP40 (%)
        x(((i-1)*30+1):i*30,34) = a(1842); % PP4 (%)
        x(((i-1)*30+1):i*30,35) = a(1846); % D60, mm
        ss_uw = b(2516); x(((i-1)*30+1):i*30,36) = str2num(ss_uw{1,1}(1:5)); %
max dry unit weight, pcf
        ss_wc = b(2519); x(((i-1)*30+1):i*30,37) = str2num(ss_wc{1,1}(1:4)); %
opt. gravimetric water content (%)

        % age
        x(((i-1)*30+1):i*30,38) = 1:30; % age, years

        % reading distress/performance values
        [c, d] = xlsread(filePath,'Distress Summary','B2:N364'); % read
distress summary into 'a'.
```

```
        for j=1:30
            x((i-1)*30+j,39) = c(find(c(:,2)==j),4);  % longitudinal cracking
            x((i-1)*30+j,40) = c(find(c(:,2)==j),5);  % alligator cracking
            x((i-1)*30+j,41) = c(find(c(:,2)==j),8);  % transverse cracking
            x((i-1)*30+j,42) = c(find(c(:,2)==j),10); % total rutting
            x((i-1)*30+j,43) = c(find(c(:,2)==j),11); % IRI
            x((i-1)*30+j,44) = (c(find(c(:,2)==j),13)-
c(find(c(:,2)==j),11))/1.6449; % IRI standard deviation
            x((i-1)*30+j,45) = c(find(c(:,2)==j),9);  % subtotal AC rutting
(may not be used as a performance indicator, just in case!!!
        end
        %!taskkill /f /im Excel.exe /t
        t(i) = toc;
        disp(['Case #', int2str(i), ' was done. It consumed ', num2str(t(i)/60),
' minutes for this case!']);
    end
        disp(['Data extraction process is done. It took ',
num2str(round(sum(t)/60)),' minutes for this whole process!!!']);

elseif layout == 2
    disp('Layout = 2. Please wait for data to be read from the spreadsheets. It
may take a few hours to complete!');
        % y is an array containing the names of each column.
        y{1,1} = 'Avg_Annual_Air_Temp'; y{1,2} = 'Avg_Annual_Rainfall'; y{1,3}
= 'Freeze_Index'; y{1,4} = 'Water_Table_Depth';
        y{1,5} = 'AADTT'; y{1,6} = 'Growth_Rate'; y{1,7} = 'OSL_Thick'; y{1,8}
= 'OSL_Eff_Binder_Content';
        y{1,9} = 'OSL_Air_Voids'; y{1,10} = 'OSL_Unit_Weight'; y{1,11} =
'OSL_R34'; y{1,12} = 'OSL_R38';
        y{1,13} = 'OSL_R4'; y{1,14} = 'OSL_PP200'; y{1,15} = 'OSL_A'; y{1,16} =
'OSL_VTS';
        y{1,17} = 'OSL_Avg_Tensile_Strength'; y{1,18} = 'OSL_Mix_VMA'; y{1,19}
= 'BC_Thick'; y{1,20} = 'BC_Eff_Binder_Content';
        y{1,21} = 'BC_Air_Voids'; y{1,22} = 'BC_Unit_Weight'; y{1,23} =
'BC_R34'; y{1,24} = 'BC_R38';
        y{1,25} = 'BC_R4'; y{1,26} = 'BC_PP200'; y{1,27} = 'BC_A'; y{1,28} =
'BC_VTS';
        y{1,29} = 'Base_Thick'; y{1,30} = 'Base_Res_Modulus';
        y{1,31} = 'Base_PI'; y{1,32} = 'Base_LL'; y{1,33} = 'Base_PP200';
y{1,34} = 'Base_PP40';
        y{1,35} = 'Base_PP4'; y{1,36} = 'Base_D60'; y{1,37} =
'Base_Max_Dry_Unit_Weight'; y{1,38} = 'Base_Opt_Grav_Water_Content';
        y{1,39} = 'Sugrade_Res_Modulus'; y{1,40} = 'Subgrade_PI'; y{1,41} =
'Subgrade_LL'; y{1,42} = 'Subgrade_PP200';
        y{1,43} = 'Sugrade_PP40'; y{1,44} = 'Subgrade_PP4'; y{1,45} =
'Sugrade_D60'; y{1,46} = 'Subgrade_Max_Dry_Unit_Weight';
        y{1,47} = 'Subgrade_Opt_Grav_Water_Content'; y{1,48} = 'Age'; y{1,49} =
'Longitudinal_Crack'; y{1,50} = 'Alligator_Crack';
        y{1,51} = 'Transverse_Crack'; y{1,52} = 'Total_Rutting'; y{1,53} =
'IRI'; y{1,54} = 'Subtotal_AC_Rutting';

    for i = [1:69 71:75 77:118 120:299 301:320 322:354 356:359 362:378 381:398
400:435 437:652 654:700]
        tic;
        filePath = ['C:\MEPDG Simulation\Layout', int2str(layout),'\Layout',
int2str(layout), '-', int2str(i), '.xls'];
        % reading climatic data
        x(((i-1)*30+1):i*30,1) = checkTemp(filePath);  % mean annual air temp,
F
```

```
        x(((i-1)*30+1):i*30,2) = checkRain(filePath);  % mean annual rainfall,
in.
        x(((i-1)*30+1):i*30,3) = checkFreeze(filePath);  % freezing index, F-
days

        [a, b]=xlsread(filePath,'Input Summary','B13:O435'); % read numeric
data in 'Input Summary' sheets into 'a' and text data into 'b'
        x(((i-1)*30+1):i*30,4) = a(1810); % depth of water table, ft

        % reading traffic data
        x(((i-1)*30+1):i*30,5) = a(2136);  % AADTT, veh/day
        x(((i-1)*30+1):i*30,6) = a(490);  % Growth rate

        % reading OSL layer data
        x(((i-1)*30+1):i*30,7) = a(1823); % thickness, in.
        x(((i-1)*30+1):i*30,8) = a(1830); % effective binder content, %
        x(((i-1)*30+1):i*30,9) = a(1831); % air voids, %
        x(((i-1)*30+1):i*30,10) = a(1832); % total unit weight, pcf
        x(((i-1)*30+1):i*30,11) = a(1841); % R34
        x(((i-1)*30+1):i*30,12) = a(1842); % R38
        x(((i-1)*30+1):i*30,13) = a(1843); % R4
        x(((i-1)*30+1):i*30,14) = a(1844); % PP200
        A = b(2700); x(((i-1)*30+1):i*30,15) = str2num(A{1,1}(1:8));     % A
(for calculating binder viscosity)
        VTS = b(2701); x(((i-1)*30+1):i*30,16) = str2num(VTS{1,1}(1:6)); % VTS
(for calculating binder viscosity)
        x(((i-1)*30+1):i*30,17) = a(2275); % avg tensile strength at 14F, psi
        x(((i-1)*30+1):i*30,18) = a(2276); % mixture VMA (%)

        % reading BC layer data
        x(((i-1)*30+1):i*30,19) = a(1870); % thickness, in.
        x(((i-1)*30+1):i*30,20) = a(1877); % effective binder content, %
        x(((i-1)*30+1):i*30,21) = a(1878); % air voids, %
        x(((i-1)*30+1):i*30,22) = a(1879); % total unit weight, pcf
        x(((i-1)*30+1):i*30,23) = a(1888); % R34
        x(((i-1)*30+1):i*30,24) = a(1889); % R38
        x(((i-1)*30+1):i*30,25) = a(1890); % R4
        x(((i-1)*30+1):i*30,26) = a(1891); % PP200
        A = b(2747); x(((i-1)*30+1):i*30,27) = str2num(A{1,1}(1:8));     % A
(for calculating binder viscosity)
        VTS = b(2748); x(((i-1)*30+1):i*30,28) = str2num(VTS{1,1}(1:6)); % VTS
(for calculating binder viscosity)

        % reading base data
        x(((i-1)*30+1):i*30,29) = a(1902); % base thickness, in.
        x(((i-1)*30+1):i*30,30) = a(1909); % base res modulus, psi
        x(((i-1)*30+1):i*30,31) = a(2335); % plasticity index
        x(((i-1)*30+1):i*30,32) = a(2336); % liquid limit
        x(((i-1)*30+1):i*30,33) = a(2338); % PP200 (%)
        x(((i-1)*30+1):i*30,34) = a(2339); % PP40 (%)
        x(((i-1)*30+1):i*30,35) = a(2340); % PP4 (%)
        x(((i-1)*30+1):i*30,36) = a(2344); % D60, mm
        b_uw = b(3228); x(((i-1)*30+1):i*30,37) = str2num(b_uw{1,1}(1:5)); %
max dry unit weight, pcf
        b_wc = b(3231); x(((i-1)*30+1):i*30,38) = str2num(b_wc{1,1}(1:4)); %
opt. gravimetric water content (%)

        % reading subgrade data
```

```
        x(((i-1)*30+1):i*30,39) = a(1978); % subgrade res modulus, psi
        x(((i-1)*30+1):i*30,40) = a(2404); % plasticity index
        x(((i-1)*30+1):i*30,41) = a(2405); % liquid limit
        x(((i-1)*30+1):i*30,42) = a(2407); % PP200 (%)
        x(((i-1)*30+1):i*30,43) = a(2408); % PP40 (%)
        x(((i-1)*30+1):i*30,44) = a(2409); % PP4 (%)
        x(((i-1)*30+1):i*30,45) = a(2413); % D60, mm
        ss_uw = b(3297); x(((i-1)*30+1):i*30,46) = str2num(ss_uw{1,1}(1:5)); %
max dry unit weight, pcf
        ss_wc = b(3300); x(((i-1)*30+1):i*30,47) = str2num(ss_wc{1,1}(1:4)); %
opt. gravimetric water content (%)

        % age
        x(((i-1)*30+1):i*30,48) = 1:30; % age, years

        % reading distress/performance values
        [c, d] = xlsread(filePath,'Distress Summary','B2:N364'); % read
distress summary into 'a'.
        for j=1:30
            x((i-1)*30+j,49) = c(find(c(:,2)==j),4);  % longitudinal cracking
            x((i-1)*30+j,50) = c(find(c(:,2)==j),5);  % alligator cracking
            x((i-1)*30+j,51) = c(find(c(:,2)==j),8);  % transverse cracking
            x((i-1)*30+j,52) = c(find(c(:,2)==j),10); % total rutting
            x((i-1)*30+j,53) = c(find(c(:,2)==j),11); % IRI
            x((i-1)*30+j,54) = c(find(c(:,2)==j),9);  % subtotal AC rutting
(may not be used as a performance indicator, just in case!!!
        end
        %!taskkill /f /im Excel.exe /t
        t(i) = toc;
        disp(['Case #', int2str(i), ' was done. It consumed ', num2str(t(i)/60),
' minutes for this case!']);
    end
        disp(['Data extraction process is done. It took ',
num2str(round(sum(t)/60)),' minutes for this whole process!!!']);

elseif layout == 3
    disp('Layout = 3. Please wait for data to be read from the spreadsheets. It
may take a few hours to complete!');
        % y is an array containing the names of each column.
        y{1,1} = 'Avg_Annual_Air_Temp'; y{1,2} = 'Avg_Annual_Rainfall'; y{1,3}
= 'Freeze_Index'; y{1,4} = 'Water_Table_Depth';
        y{1,5} = 'AADTT'; y{1,6} = 'Growth_Rate'; y{1,7} = 'OSL_Thick'; y{1,8}
= 'OSL_Eff_Binder_Content';
        y{1,9} = 'OSL_Air_Voids'; y{1,10} = 'OSL_Unit_Weight'; y{1,11} =
'OSL_R34'; y{1,12} = 'OSL_R38';
        y{1,13} = 'OSL_R4'; y{1,14} = 'OSL_PP200'; y{1,15} = 'OSL_A'; y{1,16} =
'OSL_VTS';
        y{1,17} = 'OSL_Avg_Tensile_Strength'; y{1,18} = 'OSL_Mix_VMA'; y{1,19}
= 'Base_Thick'; y{1,20} = 'Base_Res_Modulus';
        y{1,21} = 'Base_PI'; y{1,22} = 'Base_LL'; y{1,23} = 'Base_PP200';
y{1,24} = 'Base_PP40';
        y{1,25} = 'Base_PP4'; y{1,26} = 'Base_D60'; y{1,27} =
'Base_Max_Dry_Unit_Weight'; y{1,28} = 'Base_Opt_Grav_Water_Content';
        y{1,29} = 'Subbase_Thick'; y{1,30} = 'Subbase_Res_Modulus';
        y{1,31} = 'Subbase_PI'; y{1,32} = 'Subbase_LL'; y{1,33} =
'Subbase_PP200'; y{1,34} = 'Subbase_PP40';
        y{1,35} = 'Subbase_PP4'; y{1,36} = 'Subbase_D60'; y{1,37} =
'Subbase_Max_Dry_Unit_Weight'; y{1,38} = 'Subbase_Opt_Grav_Water_Content';
```

```
        y{1,39} = 'Sugrade_Res_Modulus'; y{1,40} = 'Subgrade_PI'; y{1,41} =
'Subgrade_LL'; y{1,42} = 'Subgrade_PP200';
        y{1,43} = 'Sugrade_PP40'; y{1,44} = 'Subgrade_PP4'; y{1,45} =
'Sugrade_D60'; y{1,46} = 'Subgrade_Max_Dry_Unit_Weight';
        y{1,47} = 'Subgrade_Opt_Grav_Water_Content'; y{1,48} = 'Age'; y{1,49} =
'Longitudinal_Crack'; y{1,50} = 'Alligator_Crack';
        y{1,51} = 'Transverse_Crack'; y{1,52} = 'Total_Rutting'; y{1,53} =
'IRI'; y{1,54} = 'Subtotal_AC_Rutting';

    for i = [1:119 121:171 173:183 185:187 189:208 210:264 266:280 283:359
361:365 367:436 438:615 617:625 627:700]
        tic;
        filePath = ['C:\MEPDG Simulation\Layout', int2str(layout),'\Layout',
int2str(layout), '-', int2str(i), '.xls'];
        % reading climatic data
        x(((i-1)*30+1):i*30,1) = checkTemp(filePath);  % mean annual air temp,
F
        x(((i-1)*30+1):i*30,2) = checkRain(filePath);  % mean annual rainfall,
in.
        x(((i-1)*30+1):i*30,3) = checkFreeze(filePath);  % freezing index, F-
days

        [a, b]=xlsread(filePath,'Input Summary','B13:O472'); % read numeric
data in 'Input Summary' sheets into 'a' and text data into 'b'
        x(((i-1)*30+1):i*30,4) = a(1958); % depth of water table, ft

        % reading traffic data
        x(((i-1)*30+1):i*30,5) = a(2321);  % AADTT, veh/day
        x(((i-1)*30+1):i*30,6) = a(527);  % Growth rate

        % reading OSL layer data
        x(((i-1)*30+1):i*30,7) = a(1971); % thickness, in.
        x(((i-1)*30+1):i*30,8) = a(1978); % effective binder content, %
        x(((i-1)*30+1):i*30,9) = a(1979); % air voids, %
        x(((i-1)*30+1):i*30,10) = a(1980); % total unit weight, pcf
        x(((i-1)*30+1):i*30,11) = a(1989); % R34
        x(((i-1)*30+1):i*30,12) = a(1990); % R38
        x(((i-1)*30+1):i*30,13) = a(1991); % R4
        x(((i-1)*30+1):i*30,14) = a(1992); % PP200
        A = b(2922); x(((i-1)*30+1):i*30,15) = str2num(A{1,1}(1:8));     % A
(for calculating binder viscosity)
        VTS = b(2923); x(((i-1)*30+1):i*30,16) = str2num(VTS{1,1}(1:6)); % VTS
(for calculating binder viscosity)
        x(((i-1)*30+1):i*30,17) = a(2460); % avg tensile strength at 14F, psi
        x(((i-1)*30+1):i*30,18) = a(2461); % mixture VMA (%)

        % reading base data
        x(((i-1)*30+1):i*30,19) = a(2018); % base thickness, in.
        x(((i-1)*30+1):i*30,20) = a(2025); % base res modulus, psi
        x(((i-1)*30+1):i*30,21) = a(2488); % plasticity index
        x(((i-1)*30+1):i*30,22) = a(2489); % liquid limit
        x(((i-1)*30+1):i*30,23) = a(2491); % PP200 (%)
        x(((i-1)*30+1):i*30,24) = a(2492); % PP40 (%)
        x(((i-1)*30+1):i*30,25) = a(2493); % PP4 (%)
        x(((i-1)*30+1):i*30,26) = a(2497); % D60, mm
        b_uw = b(3455); x(((i-1)*30+1):i*30,27) = str2num(b_uw{1,1}(1:5)); %
max dry unit weight, pcf
```

```
        b_wc = b(3458); x(((i-1)*30+1):i*30,28) = str2num(b_wc{1,1}(1:4)); %
opt. gravimetric water content (%)

        % reading subbase data
        x(((i-1)*30+1):i*30,29) = a(2087); % base thickness, in.
        x(((i-1)*30+1):i*30,30) = a(2094); % base res modulus, psi
        x(((i-1)*30+1):i*30,31) = a(2557); % plasticity index
        x(((i-1)*30+1):i*30,32) = a(2558); % liquid limit
        x(((i-1)*30+1):i*30,33) = a(2560); % PP200 (%)
        x(((i-1)*30+1):i*30,34) = a(2561); % PP40 (%)
        x(((i-1)*30+1):i*30,35) = a(2562); % PP4 (%)
        x(((i-1)*30+1):i*30,36) = a(2566); % D60, mm
        b_uw = b(3524); x(((i-1)*30+1):i*30,37) = str2num(b_uw{1,1}(1:5)); %
max dry unit weight, pcf
        b_wc = b(3527); x(((i-1)*30+1):i*30,38) = str2num(b_wc{1,1}(1:4)); %
opt. gravimetric water content (%)

        % reading subgrade data
        x(((i-1)*30+1):i*30,39) = a(2163); % subgrade res modulus, psi
        x(((i-1)*30+1):i*30,40) = a(2626); % plasticity index
        x(((i-1)*30+1):i*30,41) = a(2627); % liquid limit
        x(((i-1)*30+1):i*30,42) = a(2629); % PP200 (%)
        x(((i-1)*30+1):i*30,43) = a(2630); % PP40 (%)
        x(((i-1)*30+1):i*30,44) = a(2631); % PP4 (%)
        x(((i-1)*30+1):i*30,45) = a(2635); % D60, mm
        ss_uw = b(3593); x(((i-1)*30+1):i*30,46) = str2num(ss_uw{1,1}(1:5)); %
max dry unit weight, pcf
        ss_wc = b(3596); x(((i-1)*30+1):i*30,47) = str2num(ss_wc{1,1}(1:4)); %
opt. gravimetric water content (%)

        % age
        x(((i-1)*30+1):i*30,48) = 1:30; % age, years

        % reading distress/performance values
        [c, d] = xlsread(filePath,'Distress Summary','B2:N364'); % read
distress summary into 'a'.
        for j=1:30
            x((i-1)*30+j,49) = c(find(c(:,2)==j),4);  % longitudinal cracking
            x((i-1)*30+j,50) = c(find(c(:,2)==j),5);  % alligator cracking
            x((i-1)*30+j,51) = c(find(c(:,2)==j),8);  % transverse cracking
            x((i-1)*30+j,52) = c(find(c(:,2)==j),10); % total rutting
            x((i-1)*30+j,53) = c(find(c(:,2)==j),11); % IRI
            x((i-1)*30+j,54) = c(find(c(:,2)==j),9);  % subtotal AC rutting
(may not be used as a performance indicator, just in case!!!
        end
        %!taskkill /f /im Excel.exe /t
        t(i) = toc;
        disp(['Case #', int2str(i), ' was done. It consumed ', num2str(t(i)/60),
' minutes for this case!']);
    end
        disp(['Data extraction process is done. It took ',
num2str(round(sum(t)/60)),' minutes for this whole process!!!']);

elseif layout == 4
    disp('Layout = 4. Please wait for data to be read from the spreadsheets. It
may take a few hours to complete!');
        % y is an array containing the names of each column.
```

```
        y{1,1} = 'Avg_Annual_Air_Temp'; y{1,2} = 'Avg_Annual_Rainfall'; y{1,3}
= 'Freeze_Index'; y{1,4} = 'Water_Table_Depth';
        y{1,5} = 'AADTT'; y{1,6} = 'Growth_Rate'; y{1,7} = 'OSL_Thick'; y{1,8}
= 'OSL_Eff_Binder_Content';
        y{1,9} = 'OSL_Air_Voids'; y{1,10} = 'OSL_Unit_Weight'; y{1,11} =
'OSL_R34'; y{1,12} = 'OSL_R38';
        y{1,13} = 'OSL_R4'; y{1,14} = 'OSL_PP200'; y{1,15} = 'OSL_A'; y{1,16} =
'OSL_VTS';
        y{1,17} = 'OSL_Avg_Tensile_Strength'; y{1,18} = 'OSL_Mix_VMA'; y{1,19}
= 'BC_Thick'; y{1,20} = 'BC_Eff_Binder_Content';
        y{1,21} = 'BC_Air_Voids'; y{1,22} = 'BC_Unit_Weight'; y{1,23} =
'BC_R34'; y{1,24} = 'BC_R38';
        y{1,25} = 'BC_R4'; y{1,26} = 'BC_PP200'; y{1,27} = 'BC_A'; y{1,28} =
'BC_VTS';
        y{1,29} = 'Base_Thick'; y{1,30} = 'Base_Res_Modulus';
        y{1,31} = 'Base_PI'; y{1,32} = 'Base_LL'; y{1,33} = 'Base_PP200';
y{1,34} = 'Base_PP40';
        y{1,35} = 'Base_PP4'; y{1,36} = 'Base_D60'; y{1,37} =
'Base_Max_Dry_Unit_Weight'; y{1,38} = 'Base_Opt_Grav_Water_Content';
        y{1,39} = 'Subbase_Thick'; y{1,40} = 'Subbase_Res_Modulus';
        y{1,41} = 'Subbase_PI'; y{1,42} = 'Subbase_LL'; y{1,43} =
'Subbase_PP200'; y{1,44} = 'Subbase_PP40';
        y{1,45} = 'Subbase_PP4'; y{1,46} = 'Subbase_D60'; y{1,47} =
'Subbase_Max_Dry_Unit_Weight'; y{1,48} = 'Subbase_Opt_Grav_Water_Content';
        y{1,49} = 'Sugrade_Res_Modulus'; y{1,50} = 'Subgrade_PI'; y{1,51} =
'Subgrade_LL'; y{1,52} = 'Subgrade_PP200';
        y{1,53} = 'Sugrade_PP40'; y{1,54} = 'Subgrade_PP4'; y{1,55} =
'Sugrade_D60'; y{1,56} = 'Subgrade_Max_Dry_Unit_Weight';
        y{1,57} = 'Subgrade_Opt_Grav_Water_Content'; y{1,58} = 'Age'; y{1,59} =
'Longitudinal_Crack'; y{1,60} = 'Alligator_Crack';
        y{1,61} = 'Transverse_Crack'; y{1,62} = 'Total_Rutting'; y{1,63} =
'IRI'; y{1,64} = 'Subtotal_AC_Rutting';

    for i = [1:1000]
        tic;
        filePath = ['C:\MEPDG Simulation\Layout', int2str(layout),'\Layout',
int2str(layout), '-', int2str(i), '.xls'];
        % reading climatic data
        x(((i-1)*30+1):i*30,1) = checkTemp(filePath);  % mean annual air temp,
F
        x(((i-1)*30+1):i*30,2) = checkRain(filePath);  % mean annual rainfall,
in.
        x(((i-1)*30+1):i*30,3) = checkFreeze(filePath);  % freezing index, F-
days

        [a, b]=xlsread(filePath,'Input Summary','B13:O504'); % read numeric
data in 'Input Summary' sheets into 'a' and text data into 'b'
        x(((i-1)*30+1):i*30,4) = a(2086); % depth of water table, ft

        % reading traffic data
        x(((i-1)*30+1):i*30,5) = a(2481);  % AADTT, veh/day
        x(((i-1)*30+1):i*30,6) = a(559);  % Growth rate

        % reading OSL layer data
        x(((i-1)*30+1):i*30,7) = a(2099); % thickness, in.
        x(((i-1)*30+1):i*30,8) = a(2106); % effective binder content, %
        x(((i-1)*30+1):i*30,9) = a(2107); % air voids, %
        x(((i-1)*30+1):i*30,10) = a(2108); % total unit weight, pcf
        x(((i-1)*30+1):i*30,11) = a(2117); % R34
```

```
        x(((i-1)*30+1):i*30,12) = a(2118); % R38
        x(((i-1)*30+1):i*30,13) = a(2119); % R4
        x(((i-1)*30+1):i*30,14) = a(2120); % PP200
        A = b(3114); x(((i-1)*30+1):i*30,15) = str2num(A{1,1}(1:8));     % A
(for calculating binder viscosity)
        VTS = b(3115); x(((i-1)*30+1):i*30,16) = str2num(VTS{1,1}(1:6)); % VTS
(for calculating binder viscosity)
        x(((i-1)*30+1):i*30,17) = a(2620); % avg tensile strength at 14F, psi
        x(((i-1)*30+1):i*30,18) = a(2621); % mixture VMA (%)

        % reading BC layer data
        x(((i-1)*30+1):i*30,19) = a(2146); % thickness, in.
        x(((i-1)*30+1):i*30,20) = a(2153); % effective binder content, %
        x(((i-1)*30+1):i*30,21) = a(2154); % air voids, %
        x(((i-1)*30+1):i*30,22) = a(2155); % total unit weight, pcf
        x(((i-1)*30+1):i*30,23) = a(2164); % R34
        x(((i-1)*30+1):i*30,24) = a(2165); % R38
        x(((i-1)*30+1):i*30,25) = a(2166); % R4
        x(((i-1)*30+1):i*30,26) = a(2167); % PP200
        A = b(3161); x(((i-1)*30+1):i*30,27) = str2num(A{1,1}(1:8));     % A
(for calculating binder viscosity)
        VTS = b(3162); x(((i-1)*30+1):i*30,28) = str2num(VTS{1,1}(1:6)); % VTS
(for calculating binder viscosity)

        % reading base data
        x(((i-1)*30+1):i*30,29) = a(2178); % base thickness, in.
        x(((i-1)*30+1):i*30,30) = a(2185); % base res modulus, psi
        x(((i-1)*30+1):i*30,31) = a(2680); % plasticity index
        x(((i-1)*30+1):i*30,32) = a(2681); % liquid limit
        x(((i-1)*30+1):i*30,33) = a(2683); % PP200 (%)
        x(((i-1)*30+1):i*30,34) = a(2684); % PP40 (%)
        x(((i-1)*30+1):i*30,35) = a(2685); % PP4 (%)
        x(((i-1)*30+1):i*30,36) = a(2689); % D60, mm
        b_uw = b(3711); x(((i-1)*30+1):i*30,37) = str2num(b_uw{1,1}(1:5)); %
max dry unit weight, pcf
        b_wc = b(3714); x(((i-1)*30+1):i*30,38) = str2num(b_wc{1,1}(1:4)); %
opt. gravimetric water content (%)

        % reading subbase data
        x(((i-1)*30+1):i*30,39) = a(2247); % base thickness, in.
        x(((i-1)*30+1):i*30,40) = a(2254); % base res modulus, psi
        x(((i-1)*30+1):i*30,41) = a(2749); % plasticity index
        x(((i-1)*30+1):i*30,42) = a(2750); % liquid limit
        x(((i-1)*30+1):i*30,43) = a(2752); % PP200 (%)
        x(((i-1)*30+1):i*30,44) = a(2753); % PP40 (%)
        x(((i-1)*30+1):i*30,45) = a(2754); % PP4 (%)
        x(((i-1)*30+1):i*30,46) = a(2758); % D60, mm
        b_uw = b(3780); x(((i-1)*30+1):i*30,47) = str2num(b_uw{1,1}(1:5)); %
max dry unit weight, pcf
        b_wc = b(3783); x(((i-1)*30+1):i*30,48) = str2num(b_wc{1,1}(1:4)); %
opt. gravimetric water content (%)

        % reading subgrade data
        x(((i-1)*30+1):i*30,49) = a(2323); % subgrade res modulus, psi
        x(((i-1)*30+1):i*30,50) = a(2818); % plasticity index
        x(((i-1)*30+1):i*30,51) = a(2819); % liquid limit
        x(((i-1)*30+1):i*30,52) = a(2821); % PP200 (%)
        x(((i-1)*30+1):i*30,53) = a(2822); % PP40 (%)
        x(((i-1)*30+1):i*30,54) = a(2823); % PP4 (%)
```

```
        x(((i-1)*30+1):i*30,55) = a(2827); % D60, mm
        ss_uw = b(3849); x(((i-1)*30+1):i*30,56) = str2num(ss_uw{1,1}(1:5)); %
max dry unit weight, pcf
        ss_wc = b(3852); x(((i-1)*30+1):i*30,57) = str2num(ss_wc{1,1}(1:4)); %
opt. gravimetric water content (%)

        % age
        x(((i-1)*30+1):i*30,58) = 1:30; % age, years

        % reading distress/performance values
        [c, d] = xlsread(filePath,'Distress Summary','B2:N364'); % read
distress summary into 'a'.
        for j=1:30
            x((i-1)*30+j,59) = c(find(c(:,2)==j),4);  % longitudinal cracking
            x((i-1)*30+j,60) = c(find(c(:,2)==j),5);  % alligator cracking
            x((i-1)*30+j,61) = c(find(c(:,2)==j),8);  % transverse cracking
            x((i-1)*30+j,62) = c(find(c(:,2)==j),10); % total rutting
            x((i-1)*30+j,63) = c(find(c(:,2)==j),11); % IRI
            x((i-1)*30+j,64) = c(find(c(:,2)==j),9);  % subtotal AC rutting
(may not be used as a performance indicator, just in case!!!
        end
        %!taskkill /f /im Excel.exe /t
        t(i) = toc;
        disp(['Case #', int2str(i), ' was done. It consumed ', num2str(t(i)/60),
' minutes for this case!']);
    end
        disp(['Data extraction process is done. It took ',
num2str(round(sum(t)/60)),' minutes for this whole process!!!']);
else
    disp('Other layout types have not been developed!!!');
end
```

SAMPLE MATLAB CODES USED FOR DEVELOPING ANNS

The following is the Matlab codes used for developing the ANNs for predicting IRI in existing pavement that has Layout-1 pavement design:

```
% The ANNs has the architecture of 30-15-1.
% Work directory = “c:\ANNs\Layout1”
Layout1_Input =
xlsread('c:\ANNs\Layout1\Layout1.xls','Layout1_IRI','A2:AD18001');
Layout1_IRI =
xlsread('c:\ANNs\Layout1\Layout1.xls','Layout1_IRI','AE2:AE18001');

net = feedforwardnet(15);
net.layers{1}.transferFcn = 'tansig';
net.layers{2}.transferFcn = 'satlins';

[net_L1_30_15_1 tr_L1_30_15_1] = train(net, Layout1_Input', Layout1_IRI');
iri_pred = net_L1_30_15_1(Layout1_Input');

% plot ANNs prediction against MEPDG prediction for the three sub-datasets
figure(1); plotregression(Layout1_IRI(tr_L1_30_15_1.trainInd)',
iri_pred(tr_L1_30_15_1.trainInd), 'Training')
figure(2); plotregression(Layout1_IRI(tr_L1_30_15_1.valInd)',
iri_pred(tr_L1_30_15_1.valInd), 'Validation')
figure(3); plotregression(Layout1_IRI(tr_L1_30_15_1.testInd)',
iri_pred(tr_L1_30_15_1.testInd), 'Testing')
```

SAMPLE SAS CODES FOR DEVELOPING BAYESIAN LINEAR MODEL

The following SAS codes were written to develop Bayesian linear models for pavement design layout #1:

```
libname Bayesian 'C:\Modeling\Bayesian regression\SAS modeling\library';

PROC IMPORT OUT= WORK.Layout1
            DATAFILE= "C:\Modeling\Bayesian regression \Layout1.xlsx"
            DBMS=EXCEL REPLACE;
     RANGE="Layout1";
     GETNAMES=YES;
     MIXED=NO;
     SCANTEXT=YES;
     USEDATE=YES;
     SCANTIME=YES;
RUN;

data Bayesian.Layout1;
       set work.Layout1;
       logIRI = log(Delta_IRI);
run;

proc reg data=Bayesian.Layout1;
       model logIRI = Rain FI AADTT Thick PP8 PP200 UW AC AV IRI0 Age;
       model logIRI = Rain FI AADTT Thick PP8 PP200 UW AC AC2 AV AV2 IRI0 Age;
       model logIRI = Rain FI AADTT PP200 UW AC AC2 AV AV2 Thick_UW Rain_AC
FI_AC IRI0 Age;
       model logIRI = Rain AADTT PP8 PP200 UW AC AC2 AV AV2 Thick_UW Rain_AC
FI_AC FI_AV IRI0 Age;
       model logIRI = Rain FI AADTT Thick PP8 PP200 AC AC2 AV AV2 Thick_UW
Rain_AC FI_AC FI_AV IRI0 Age;
       model logIRI = Rain FI AADTT Thick PP8 PP200 UW AC AC2 AV AV2 Thick_UW
Rain_AC FI_AC FI_AV IRI0 Age;
       model logIRI = Temp Rain FI AADTT Thick PP8 PP200 UW AC AC2 AV AV2
Thick_UW Rain_AC FI_AC FI_AV IRI0 Age;
       model logIRI = Temp Rain FI AADTT Thick PP8 PP200 UW AC AC2 AV AV2 AC_AV
Thick_UW Rain_AC FI_AC FI_AV IRI0 Age;
       model logIRI = Temp Rain FI AADTT Thick PP8 PP200 UW AC AC2 AV AV2 AC_AV
Thick_UW Rain_AC FI_AC FI_AV IRI0 Age / selection = stepwise;
run;

title 'Bayesian Regression Modeling for Layout-1';
ods graphics on;
proc genmod data=Bayesian.Layout1;
       model logIRI = Rain FI AADTT Thick PP8 PP200 UW AC AV IRI0 Age;
       model logIRI = Rain FI AADTT Thick PP8 PP200 UW AC AC2 AV AV2 IRI0 Age;
       model logIRI = Rain FI AADTT PP200 UW AC AC2 AV AV2 Thick_UW Rain_AC
FI_AC IRI0 Age;
       model logIRI = Rain AADTT PP8 PP200 UW AC AC2 AV AV2 Thick_UW Rain_AC
FI_AC FI_AV IRI0 Age;
       model logIRI = Rain FI AADTT Thick PP8 PP200 AC AC2 AV AV2 Thick_UW
Rain_AC FI_AC FI_AV IRI0 Age;
       model logIRI = Rain FI AADTT Thick PP8 PP200 UW AC AC2 AV AV2 Thick_UW
Rain_AC FI_AC FI_AV IRI0 Age;
```

```
      model logIRI = Temp Rain FI AADTT Thick PP8 PP200 UW AC AC2 AV AV2
Thick_UW Rain_AC FI_AC FI_AV IRI0 Age;
      model logIRI = Temp Rain FI AADTT Thick PP8 PP200 UW AC AC2 AV AV2 AC_AV
Thick_UW Rain_AC FI_AC FI_AV IRI0 Age;
      bayes seed=1 OutPost=Bayesian.BayesInfo_Layout1;
run;
ods graphics off;

PROC EXPORT DATA= BAYESIAN.Bayesinfo_layout1
            OUTFILE= "C:\Modeling\Bayesian regression\SAS
modeling\MCMC_weights.xlsx"
            DBMS=EXCEL REPLACE;
     SHEET="Layout1";
RUN;
```

SAMPLE EXCEL VBA CODES FOR DEVELOPING THE PRS FRAMEWORK

The following are some sample Excel VBA codes used for developing the PRS framework:

```
'Predicting the IRI of Pre-Treatment Pavement using the ANNs
Sub Layout1_IRI_Pred_V1()
If (Worksheets("DemoLayout1").Range("U1").Value <> "Layout-1") Then
MsgBox ("Please check your pavement design.")
GoTo Ende
Else
    Worksheets("NN-inExcel").Cells(21, 2) = Worksheets("DemoLayout1").Cells(3,
7)   'air temp
    Worksheets("NN-inExcel").Cells(22, 2) = Worksheets("DemoLayout1").Cells(4,
7)   'rainfall
    Worksheets("NN-inExcel").Cells(23, 2) = Worksheets("DemoLayout1").Cells(5,
7)   'freeze index
    Worksheets("NN-inExcel").Cells(24, 2) = Worksheets("DemoLayout1").Cells(8,
7)   'AADTT
    Worksheets("NN-inExcel").Cells(25, 2) = Worksheets("DemoLayout1").Cells(9,
7) / 100 'growth rate
    Worksheets("NN-inExcel").Cells(26, 2) = Worksheets("DemoLayout1").Cells(14,
7)  'OSL thick
    Worksheets("NN-inExcel").Cells(27, 2) = Worksheets("DemoLayout1").Cells(15,
7)  'eff AC%
    Worksheets("NN-inExcel").Cells(28, 2) = Worksheets("DemoLayout1").Cells(16,
7)  'AV%
    Worksheets("NN-inExcel").Cells(29, 2) = Worksheets("DemoLayout1").Cells(17,
7) 'unit weight
    Worksheets("NN-inExcel").Cells(30, 2) = Worksheets("DemoLayout1").Cells(18,
7) 'R34
    Worksheets("NN-inExcel").Cells(31, 2) = Worksheets("DemoLayout1").Cells(19,
7) 'R38
    Worksheets("NN-inExcel").Cells(32, 2) = Worksheets("DemoLayout1").Cells(20,
7) 'R4
    Worksheets("NN-inExcel").Cells(33, 2) = Worksheets("DemoLayout1").Cells(21,
7) 'PP200
    Worksheets("NN-inExcel").Cells(34, 2) = Worksheets("DemoLayout1").Cells(25,
7) 'Viscosity
    Worksheets("NN-inExcel").Cells(35, 2) = Worksheets("DemoLayout1").Cells(42,
7) 'Base thick
    Worksheets("NN-inExcel").Cells(36, 2) = Worksheets("DemoLayout1").Cells(43,
7) 'PI
    Worksheets("NN-inExcel").Cells(37, 2) = Worksheets("DemoLayout1").Cells(44,
7) 'LL
    Worksheets("NN-inExcel").Cells(38, 2) = Worksheets("DemoLayout1").Cells(45,
7) 'PP200
    Worksheets("NN-inExcel").Cells(39, 2) = Worksheets("DemoLayout1").Cells(46,
7) 'PP40
    Worksheets("NN-inExcel").Cells(40, 2) = Worksheets("DemoLayout1").Cells(47,
7) 'PP4
    Worksheets("NN-inExcel").Cells(41, 2) = Worksheets("DemoLayout1").Cells(48,
7) 'max dry unit weight
    Worksheets("NN-inExcel").Cells(42, 2) = Worksheets("DemoLayout1").Cells(49,
7) 'opt grav. water content
```

```
    Worksheets("NN-inExcel").Cells(43, 2) = Worksheets("DemoLayout1").Cells(62,
7) 'subgrade PI
    Worksheets("NN-inExcel").Cells(44, 2) = Worksheets("DemoLayout1").Cells(63,
7)  'LL
    Worksheets("NN-inExcel").Cells(45, 2) = Worksheets("DemoLayout1").Cells(64,
7)  'PP200
    Worksheets("NN-inExcel").Cells(46, 2) = Worksheets("DemoLayout1").Cells(65,
7)  'PP40
    Worksheets("NN-inExcel").Cells(47, 2) = Worksheets("DemoLayout1").Cells(66,
7) 'PP4
    Worksheets("NN-inExcel").Cells(48, 2) = Worksheets("DemoLayout1").Cells(67,
7) 'max dry unit weight
    Worksheets("NN-inExcel").Cells(49, 2) = Worksheets("DemoLayout1").Cells(68,
7) 'opt grav water content

    For i = 1 To Worksheets("DemoLayout1").Cells(3, 10)
        Worksheets("DemoLayout1").Cells(i + 12, 9) = i
        Worksheets("NN-inExcel").Cells(50, 2) = i
        Worksheets("DemoLayout1").Cells(i + 12, 10) = Worksheets("NN-
inExcel").Cells(60, 2)
        With Worksheets("DemoLayout1")
        If .Cells(i + 12, 10) > .Cells(8, 10) Then
            .Cells(i + 12, 10).Interior.ColorIndex = 3
            .Cells(i + 12, 9).Interior.ColorIndex = 3
        End If
        End With
    Next i
End If
Ende:
End Sub


'Predicting IRI reduction using the Bayesian model
Sub Bayes_Layout1_Pred()
If (Worksheets("DemoLayout1").Range("U1").Value <> "Layout-1") Then
MsgBox ("Please check your pavement design.")
GoTo Ende
Else
    Worksheets("DemoLayout1").Range("K13:O62").Interior.ColorIndex = 2
    Worksheets("DemoLayout1").Range("K13:O62") = ""
    Worksheets("DemoLayout1").Cells(5, 17) = ""
    Worksheets("DemoLayout1").Cells(5, 18) = ""
    age = Worksheets("DemoLayout1").Cells(5, 10)
    RL = Worksheets("DemoLayout1").Cells(3, 17)
    For i = 1 To (Worksheets("DemoLayout1").Cells(3, 10) - age + 1)
        Worksheets("Layout1").Cells(4, 17) = i
        Worksheets("DemoLayout1").Cells(11 + age + i, 11) = i
        Worksheets("DemoLayout1").Cells(11 + age + i, 12) =
Worksheets("Layout1").Cells(7, 19)
        Worksheets("DemoLayout1").Cells(11 + age + i, 13) =
Worksheets("Layout1").Cells(8, 19)
        Worksheets("DemoLayout1").Cells(11 + age + i, 14) =
Worksheets("DemoLayout1").Cells(11 + age + i, 10) -
Worksheets("DemoLayout1").Cells(11 + age + i, 12)
        Worksheets("DemoLayout1").Cells(11 + age + i, 15) =
WorksheetFunction.Norm_Dist(Worksheets("DemoLayout1").Cells(8, 10),
Worksheets("DemoLayout1").Cells(11 + age + i, 14),
Worksheets("DemoLayout1").Cells(11 + age + i, 13), True)
```

```
        With Worksheets("DemoLayout1")
        If .Cells(11 + age + i, 15) <= RL Then
            .Cells(11 + age + i, 15).Interior.ColorIndex = 3
            .Cells(11 + age + i, 11).Interior.ColorIndex = 3
        End If
        If .Cells(11 + age + i, 15) < (1 - RL) Then
            .Cells(11 + age + i, 15).Interior.ColorIndex = 2
            .Cells(11 + age + i, 11).Interior.ColorIndex = 2
        End If
        End With
    Next i
    For i = 1 To 50
        With Worksheets("DemoLayout1")
        If .Cells(11 + age + i, 15) <= RL Then
            .Cells(5, 17) = .Cells(11 + age + i, 11)
            Exit For
        End If
        End With
    Next i
    For i = 1 To 50
        With Worksheets("DemoLayout1")
        If .Cells(11 + age + i, 15) < (1 - RL) Then
            .Cells(5, 18) = .Cells(10 + age + i, 11)
            Exit For
        End If
        End With
    Next i
End If

Ende:
End Sub
```